CHEMICAL CONSEQUENCES OF AIR QUALITY STANDARDS AND OF CONTROL IMPLEMENTATION PROGRAMS: ROLES OF HYDROCARBONS, OXIDES OF NITROGEN, AND AGED SMOG IN THE PRODUCTION OF PHOTOCHEMICAL OXIDANT

Contract No. 4-214
California Air Resources Board
Final Report
May 1976

Principal Investigator

Dr. James N. Pitts, Jr.

Program Manager

Dr. Arthur M. Winer

Program Research Staff

Dr. Karen R. Darnall
Dr. George J. Doyle
Dr. John M. McAfee

Technical Support Staff

Mr. Frank R. Burleson
Ms. Sharron L. Harris
Mr. William D. Long

Contributing Research Staff

Dr. William P. Carter
Dr. William C. Kuby
Dr. Alan C. Lloyd
Ms. Minn P. Poe
Dr. Edgar R. Stephens
Dr. Jerome P. Smith

STATEWIDE AIR POLLUTION RESEARCH CENTER
UNIVERSITY OF CALIFORNIA
RIVERSIDE, CALIFORNIA 92521

ABSTRACT

The environmental chamber facility established at the Statewide Air Pollution Research Center, University of California, Riverside, under a joint Air Resources Board--University of California (Project Clean Air) program has been employed to generate an experimental data base:

- For evaluating the effectiveness of various technical approaches to oxidant control in the California South Coast Air Basin, and
- For assessing the impact of incremental control strategies, such as new car emission controls, vehicle inspection, maintenance programs, etc.

The previously validated "surrogate" mixture of hydrocarbons (HC) and oxides of nitrogen (NO_x) has been irradiated, using a wide range of initial concentrations and irradiation times, with particular emphasis on long-term irradiations ($\geq$ 9 hours) and the effect of added aldehydes. These experiments provide data applicable to assessments of:

- Effects on oxidant production in the South Coast Air Basin that might have resulted from full implementation of the 1974-75 NO_x retrofit program for 1966-70 light duty motor vehicles.
- The degree of HC and NO_x control required to meet air quality standards for oxidant for downwind areas of the South Coast Air Basin, and
- Effects of aged smog on oxidant production.

Preliminary work has also been carried out concerning the design of dynamic chamber experiments which would attempt to more realistically simulate air parcel transport. Thus, a diffusion model has beem employed to investigate the rates of dilution and fresh pollutant addition occurring during characteristic air parcel histories in the South Coast Air Basin.

As a result of the disclosure, in June 1974, of differences in ozone concentrations measured by different potassium iodide (KI) calibration procedures, and because accurate ozone measurements are critical in this research program, we undertook an investigation of the stoichiometry of the 2% neutral buffered potassium iodide (NBKI) method for ozone ambient concentrations using long-path infrared spectroscopy. Results of this investigation and their implications for the existing oxidant air monitoring data base in the South Coast Air Basin are presented here.

This report was submitted in fulfillment of contract No. 4-214 by the Statewide Air Pollution Research Center, University of California, Riverside, under the partial sponsorship of the California Air Resources Board. Work was completed as of June 30, 1975.

TABLE OF CONTENTS

LIST OF FIGURES

LIST OF FIGURES (continued)

LIST OF FIGURES (continued)

LIST OF FIGURES (continued)

LIST OF TABLES

LIST OF TABLES

EXECUTIVE SUMMARY

In order to provide an experimental data base relating to major unresolved issues of photochemical smog formation, the SAPRC environmental chamber facility was designed and constructed with support from the California Air Resources Board beginning in 1970. Upon completion of the facility in early 1973, an experimental program was undertaken to generate a detailed data base for establishing the quantitative relationships between initial hydrocarbon (HC) and oxides of nitrogen (NO_x) precursor levels and production of photochemical oxidants, ozone in particular. A unique smog "surrogate" was developed (see Table 1) to simulate the HC-NO_x primary pollutant mix in the South Coast Air Basin which results from all major sources, including natural gas leaks, evaporative and geogenic emissions, as well as auto exhaust. The data obtained from irradiation of this mixture in the SAPRC all-glass chamber under simulated atmospheric conditions, when compared with ambient air monitoring data and the results of irradiations of ambient air in the all-glass chamber, indicated that a reasonable simulation of the atmospheric situation could be achieved.

In 1973, a systematic study of the effect on production of ozone resulting from across-the-board reductions in nonmethane hydrocarbons (NMHC), methane and carbon monoxide (CO) levels was begun. Experiments have been carried out for 5 levels of surrogate hydrocarbons (NMHC ≃ 2.6, 2.1, 1.3, 0.69 and 0.46 ppmC) and with several NO_x concentrations below 0.6 ppm. Extensive data including the <u>specific</u> determination of ozone, nitrogen dioxide, and peroxyacetyl nitrate, as well as measurement of nitric oxide, CO and formaldehyde, and detailed analysis for C_1-C_9 hydrocarbons including oxygenates and aromatics were obtained for more than 60 surrogate experiments in 1973-74. Continuation of this study in the current year has more than doubled the surrogate data base and the composite data set has been applied to:

(a) an assessment of the potential effect on ambient ozone levels in the South Coast Air Basin resulting from an "incremental" control strategy, i.e., the California NO_x retrofit program for 1966-70 light-duty motor vehicles;

Table 1. Surrogate Mixture for Simulation of 6-9 AM Ambient Air Pollutant Burden in Los Angeles

Pollutant group	Initial concentration	Individual components, nominal concentration
Aromatics	440 ppbC	Toluene, 115 ppbC m-Xylene, 325 ppbC
Saturates	1400 ppbC	n-Butane, 785 ppbC 2,3-Dimethylbutane, 615 ppbC
Fuel olefins	130 ppbC	cis-2-Butene, 60 ppbC 2-Methyl-2-butene, 70 ppbC
Cracking products	220 ppbC	Ethylene, 84 ppbC Propene, 35 ppbC Acetylene, 101 ppbC
Oxygenates	65 ppbC	Formaldehyde, 54 ppbC Acetaldehyde, 5 ppbC Acetone, 6 ppbC
Natural gas components	3000 ppbC	Ethane, 160 ppbC Propane, 40 ppbC Methane, 2800 ppbC
Carbon monoxide	7000 ppb	
Nitrogen oxides	300 ppb	NO, 270 ppb NO_2, 30 ppb

(b) an evaluation of ozone production in downwind portions of the South Coast Air Basin based on extrapolation of the 6-hour HC-NO_x-O_3 data base (the majority of the surrogate experiments) to 9 hours with validation provided by about twenty 9-hour (or longer) runs carried out in the current year;

(c) a study of the "aged smog" phenomenon using added aldehyde as a typical aged smog component.

The design of smog chamber experiments which will more accurately simulate full-day irradiation and air parcel transport effects has been initiated using transport and diffusion models in conjunction with meteorological and ambient air monitoring data to analyze characteristic air parcel trajectories.

As a result of the revelation in June 1974 of serious differences in existing calibration methods for ozone, we investigated the 2% neutral buffered potassium iodide (NBKI) method which had been employed in the SAPRC chamber program with the following results:

(a) the first determination of the absolute absorptivity of the 9.6 μ infrared band of ozone;

(b) determination of the stoichiometry of the NBKI method as a function of the relative humidity of the sample;

(c) establishment of the consistency of the infrared method of measuring ozone with the uv absorption method in a collaborative study with W. B. DeMore;

(d) generation of an internally consistent set of oxidant air quality data for the California South Coast Air Basin.

Results from the studies cited above are summarized here and are described in more complete detail in Sections III-A through III-F.

NO_x Retrofit Program. One approach to achieving conditions which will ultimately meet the Federal ambient air quality standard for oxidant is to implement a series of emission control programs, each of which produces a small but significant reduction in HC and/or NO_x emissions. The California program to retrofit 1966-70 light-duty motor vehicles with a device to control NO_x emissions, which was instituted in 1973, was one such "incremental" control strategy. As a part of a review of the effectiveness of this strategy, the HC-NO_x-O_3 data base, which had been generated in the ARB-supported surrogate chamber program described above, was utilized to

evaluate the changes in ambient ozone levels which might be expected on the basis of observed reductions in NO_x and HC emissions achieved with the retrofit devices. To carry out such an evaluation, it was necessary to have, in addition to the HC-NO_x-O_3 data base, (a) data concerning initial (i.e., precontrol strategy) ambient levels of HC and NO_x present in the early morning hours, (b) an estimate of the emissions reductions to be achieved by the NO_x retrofit control program, and (c) a method for predicting the ambient HC and NO_x levels resulting from such emission reductions.

Briefly, the initial HC and NO_x levels were based on ambient air monitoring data from the Los Angeles Air Pollution Control District at the downtown Los Angeles (001) and Pasadena (083) stations. Average 6-9 am average NMHC and NO_x levels in Los Angeles for the 10 worst oxidant days in Pasadena in 1973 were calculated to be 2.35 ppmC of NMHC and 0.336 ppm of NO_x (NMHC/NO_x = 7). Data concerning the effectiveness of the retrofit devices in reducing NO_x and HC's were obtained by the ARB in a number of certification tests and surveillance programs which tested emissions from cars under both laboratory and field conditions. The ARB also provided projections of the changes in total emissions (i.e., from all sources) to be expected based on the surveillance data for reductions in exhaust emissions. It was then assumed that the percent change in total emissions resulting from installation of NO_x retrofit devices would give a corresponding change in the ambient nonmethane hydrocarbon (NMHC) and NO_x levels.

The chamber data for ozone levels (after six hours of irradiation) as a function of initial NMHC and NO_x levels as presented in Figure 1 readily gives a qualitative understanding of the changes in ozone levels to be expected for incremental changes in the precursor NO_x and NMHC levels. Starting at the precontrol ambient conditions it can be seen that:

- a decrease in emissions of NO_x which is accompanied simultaneously by an approximately equivalent reduction in NMHC (i.e., constant NMHC/NO_x) should lead to a reduction in ozone levels, whereas a reduction in NO_x emissions (i.e., increase in NMHC/NO_x) alone will tend to increase ozone levels.

The magnitude of these effects, of course, depends upon the specific emission levels involved and does not take into account other possible

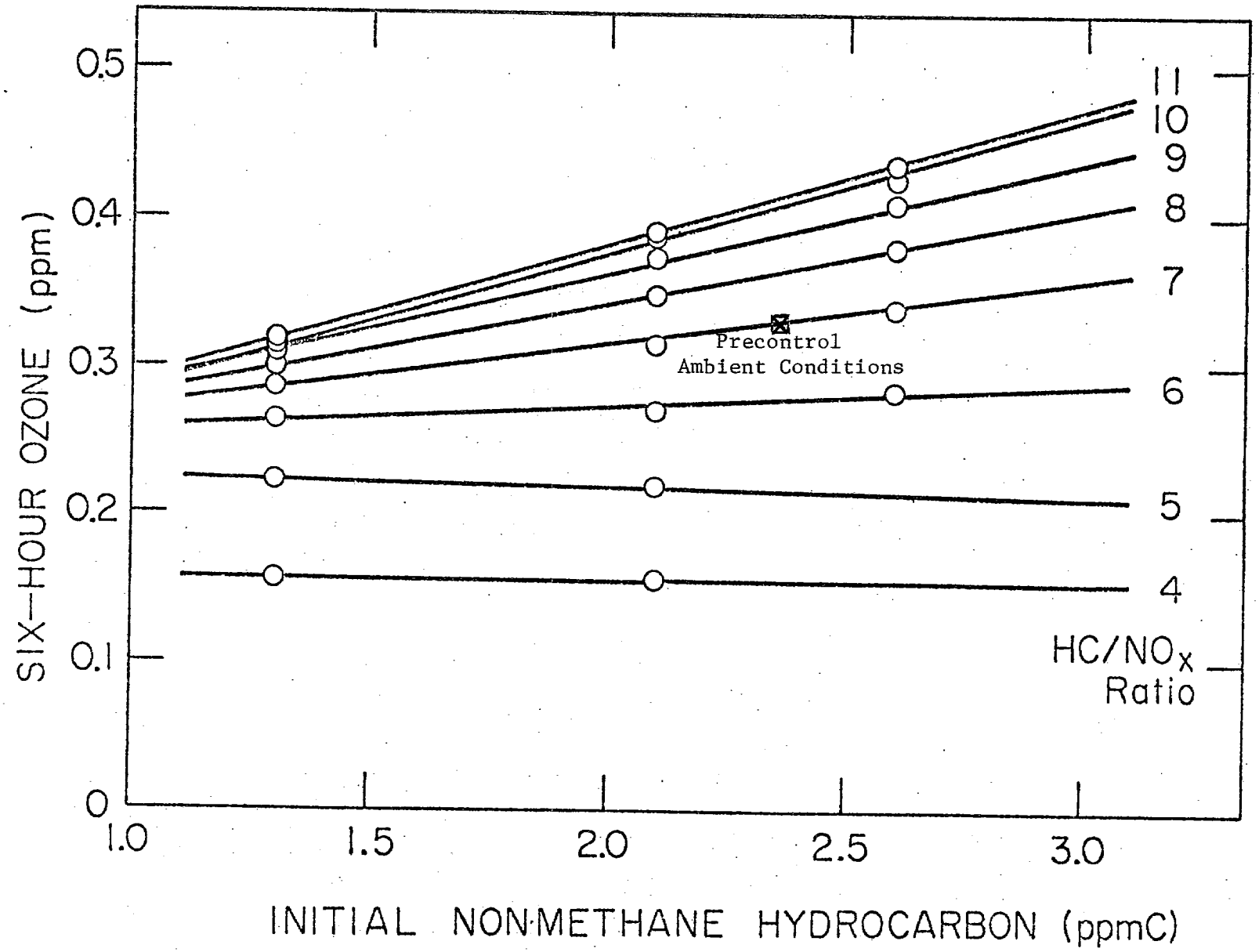

Figure 1. Six-Hour Ozone Concentration as a Function of Initial Nonmethane Hydrocarbon at Various HC/NO_x Ratios Obtained in the SAPRC Surrogate Study.

benefits from reduced NO_x emissions, such as reduced PAN and nitrate aerosol levels.

To provide a more quantitative evaluation of changes in ozone levels expected from various NO_x and/or NMHC concentration changes, equation (1)

$$\Delta O_3(\%) = -1.29(\%\ \text{HC reduction}) + 0.96(\%\ NO_x\ \text{reduction}) \qquad (1)$$

was derived from the data of Figure 1 and is applicable over a region corresponding to as much as a 10% reduction in NO_x and/or NMHC and to locations such as Pasadena (i.e., 4-6 hours downwind from the principal 6-9 AM emission sources). In collaboration with John Holmes and Frank Bonamassa of the ARB, a similar equation was developed for far downwind locations in the South Coast Air Basin (e.g., Upland) by extrapolating our 6-hour chamber data for 10 hours (prior to the validated extrapolation discussed in the following section).

From the quantitative evaluations of the data for changes in emissions provided by the ARB, it was concluded that

- For most of the vehicle emissions data obtained during partial implementation of the NO_x retrofit program, either no change or small increases (1-4%) in ozone would result in the western end of the South Coast Air Basin, while somewhat larger (3-10%) decreases in ozone would occur downwind in eastern portions of the South Coast Air Basin for full implementation of the program.

Development of Air Parcel Transport Simulation Methodology. The goal of this program was to provide a basis for designing chamber experiments which would realistically simulate air parcel transport, in locations such as the California South Coast Air Basin, with respect to both injection of fresh oxidant precursors and dilution and dispersion effects. The first step in this development was an investigation of characteristic air parcel histories in the South Coast Air Basin, with special emphasis on an air parcel which followed a trajectory from southeast Los Angeles to Pasadena between approximately 5 AM and 12 noon on July 25, 1973, the day of highest oxidant observed in 1973 (0.45 ppm oxidant observed in Pasadena).

The trajectory of an air mass was determined by numerical interpolation on the meteorological data recorded at the various air monitoring stations within the South Coast Air Basin. The trajectory program was taken

directly from the DIFKIN model of the General Research Corporation. The wind direction and speed was determined at a given point and used to trace the air parcel trajectory in a forward or backward direction from that point. Having determined the air parcel trajectory, the air quality within that parcel was estimated, using a similar interpolation scheme. In this case, the pollutant concentrations reported at the various air monitoring stations were interpolated by using a similar weighting factor for the three closest stations. The concentrations of the pollutants reported were then estimated at specific times of day along the trajectory.

To determine the dilution and addition rates for a given air parcel, a diffusion model is needed to account for the transport of pollutants in vertical and horizontal directions. For the GRC-DIFKIN model, which was used in this study, the horizontal turbulent diffusion fluxes, both normal to and along the wind trajectory, were assumed negligible, compared to the advection and vertical diffusion. In order to generate a set of diffusion coefficients, which are realistic for the given day being studied, the carbon monoxide air quality data were used as a verification test. The diffusion coefficients were first estimated from the temperature gradient data obtained for the particular day of interest. They were then adjusted to yield calculated (from the diffusion model) ground level carbon monoxide concentrations, which compare well with those estimated from the interpolation on the air quality data. Using these time-dependent diffusion profiles, the concentration of the other primary pollutants, namely NO_x and hydrocarbon, were then determined for the air mass.

The addition rates of fresh pollutants are related to the emissions inventory used for the diffusion model. The dilution rate can also be determined from the results of this model. In general, the accumulation of pollutants within a given air mass is determined by integration of the concentration profile at the beginning and end of the time period under consideration. If the particular air mass of interest is bounded by the ground surface plane, then the incoming mass is determined directly from the source inventory, and the outgoing flux by the difference between the accumulation and the incoming flux. If the lower boundary of the air mass is not the ground plane, then the incoming or outgoing mass flux can be determined by using the Fickian diffusion equation and the turbulent

diffusivities assumed in the diffusion model. The term "dilution" indicates that there would be a net reduction in the concentration of primary pollutants in the air mass. This is often not the case for trajectories which remain over areas of high primary pollutant fluxes. Thus, the dilution and/or buildup of pollutants within the air mass is strongly dependent upon the trajectory and the time of day for a given trajectory. This method for determining the trajectory and air quality for an air mass was applied to a given trajectory for July 25, 1973 and the results are presented in Section III-C.

In summary,

- A methodology has been developed to calculate both pollutant addition and dilution rates required during dynamic smog chamber experiments in order to more accurately simulate full-day irradiation and air parcel transport effects for characteristic air parcel trajectories in an air basin for which ground level meteorological and pollutant concentration data are available.

Long-Term Irradiations and Aged Smog Studies. Achieving reductions in oxidant formation in regions downwind of major emission sources requires data concerning the oxidant-precursor relationships which occur (a) during long-term (i.e., ~6-10 hrs) irradiation and transport periods, and (b) during multiple-day irradiations of polluted air masses. At the time of the present study, few (if any) smog chamber data relevant to this problem were available. Specifically, most, although not all, published data from previous chamber studies are for irradiation periods of 6 hours, or, in many cases, for 2-4 hours. Accordingly, we have attempted to provide data of utility with regard to assessing the dependence of oxidant formation on initial HC and NO_x concentrations for irradiation periods longer than 6 hours.

Two approaches have been taken. First, we have experimentally generated new O_3-NO_x-HC data for 9-hour or longer irradiations for NMHC and NO_x concentrations corresponding to present ambient levels in the South Coast Air Basin. Second, we have developed methodologies for extrapolating the previously obtained 6-hour SAPRC-ARB data base to periods as long as 10 hours. Detailed results from these studies are presented in Section III-D. Using these results we have calculated the 9-hour ozone concentrations for 60 sets of

initial NMHC and NO_x concentrations (corresponding to 60 experimental runs), and the values are shown in Figure 2. Thus,

- The previous 6-hour HC-NO_x-O_3 data base has been extrapolated to 9 hours on the basis of 9-hour HC-NO_x surrogate irradiations conducted during the current program. These data are believed to be applicable to assessments of the effects of control strategies on oxidant concentrations in the downwind portions of the South Coast Air Basin.

Having obtained 9-hour ozone concentrations it was possible to examine the dependence on irradiation period of the maximum in the ozone vs initial NO_x function (for a given initial NMHC concentration). An example of this dependence is shown in Figure 3 from which we conclude that:

- At intermediate NO_x and NMHC levels (i.e., NMHC/NO_x ratios of ~5 to ~15), the maximum ozone levels occur at NMHC/NO_x ratios which are determined largely by the irradiation period.

Aldehydes occur in the atmosphere both as primary emissions and as the result of atmospheric photochemistry and are important photoinitiators. In an "aged smog" study, irradiations of the standard surrogate mixture (2450 ppbC nonmethane HC, 0.33 ppm NO_x, 7.0 ppm CO, and 2.8 ppm CH_4) were carried out for several different initial formaldehyde concentrations. The quantitative effects of increasing HCHO on both initial rates of reaction and on 6-hour ozone levels are summarized in Section III-D. The 6-hour ozone concentration as a function of HCHO is shown graphically in Figure 4. An experiment carried out with acetaldehyde (CH_3CHO) instead of HCHO gave comparable results. The effect of added HCHO on ozone levels throughout a series of 9-hour irradiations of the HC-NO_x surrogate mixture is shown in Figure 5. The enhancement in ozone production was striking. Thus,

- Ozone production was experimentally observed to be catalyzed by the addition of formaldehyde and acetaldehyde to the HC-NO_x surrogate mixture and to exert effects throughout a 9-hour irradiation period.

Investigation of the 2% Neutral Buffered Potassium Iodide Method for Ozone. The accurate measurement of ozone concentrations is critical to the development of any new major HC-NO_x-O_3 data base, such as the one being generated in this research program. In June 1974, at a time when a major

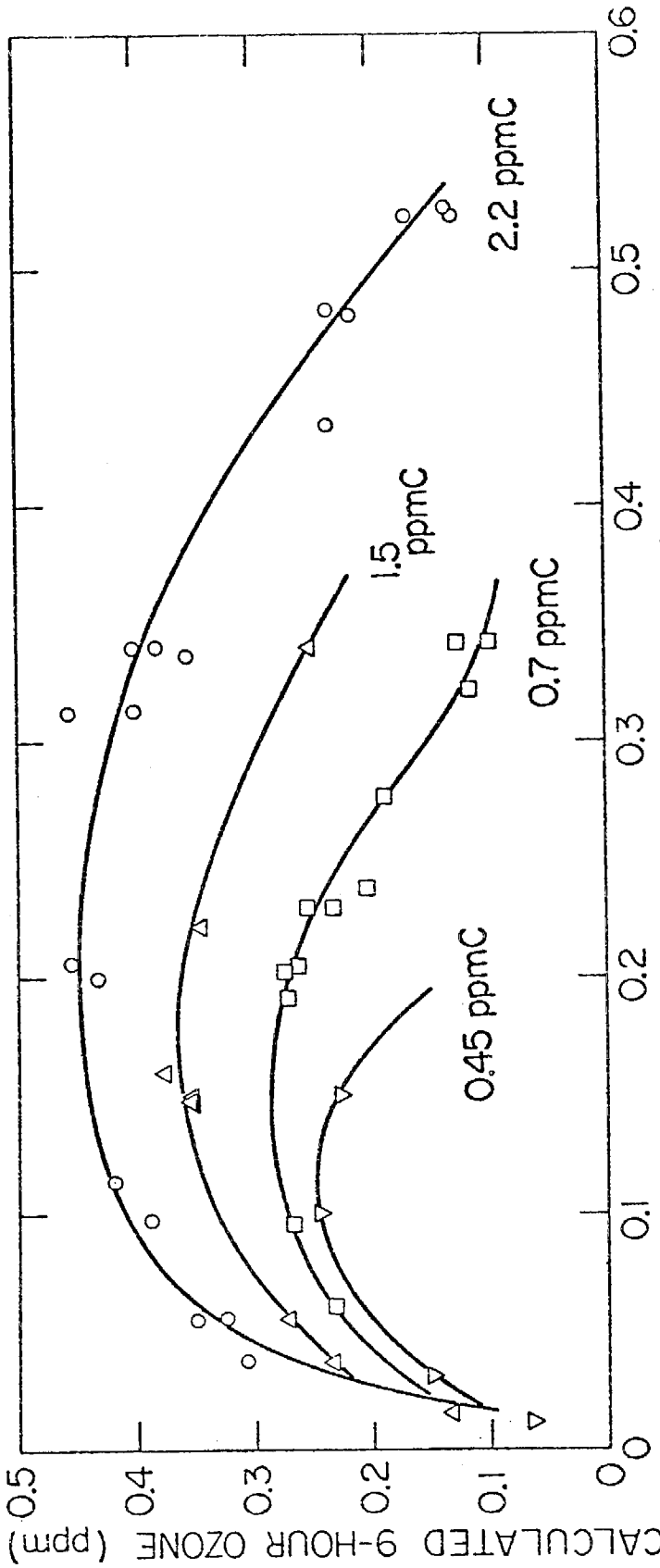

Figure 2. Nine-Hour Ozone Concentrations Calculated Using Regression Functions vs. Initial NO_x at Various Nonmethane Hydrocarbon Concentrations.

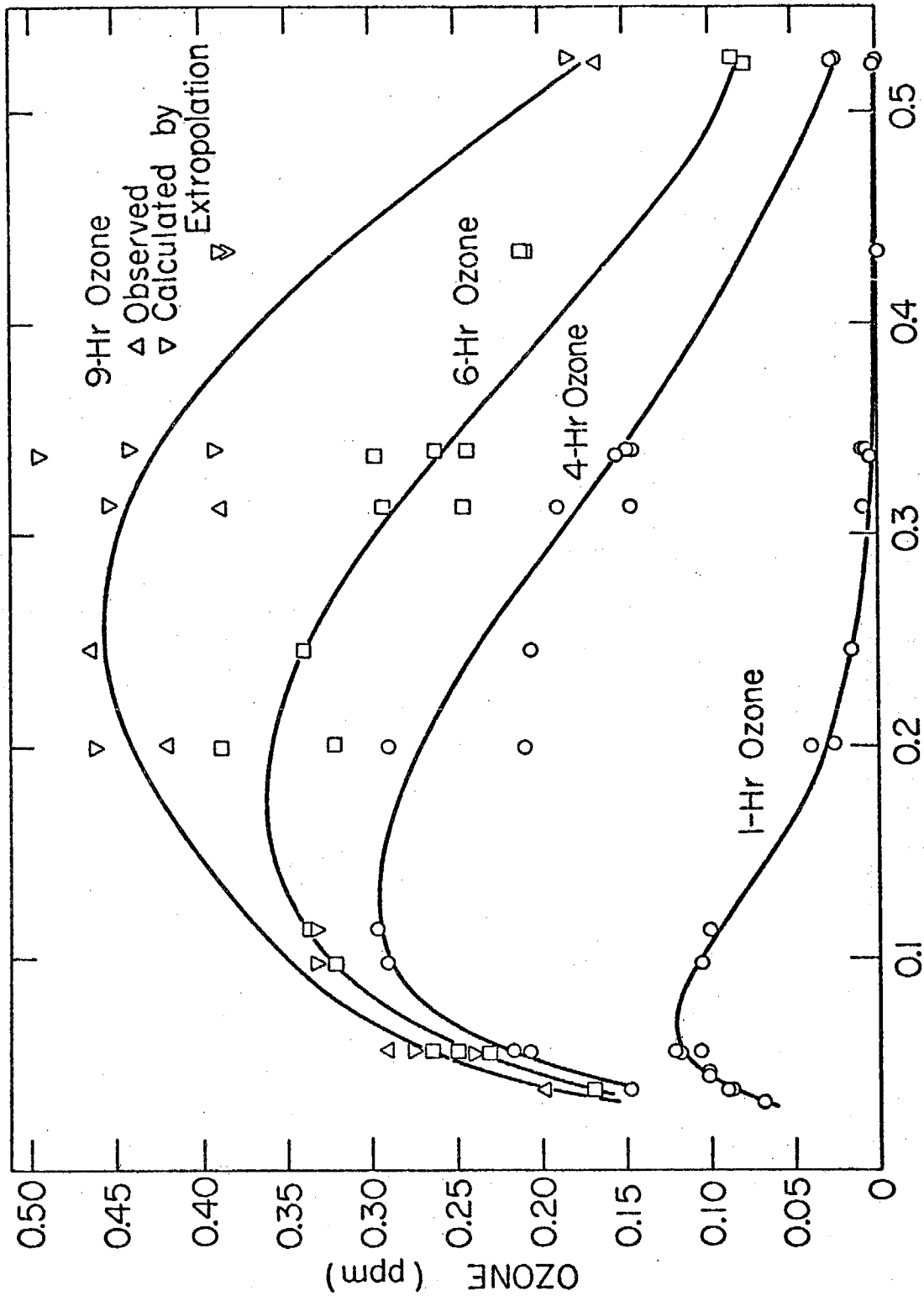

Figure 3. Maximum Ozone Observed During 1-, 4-, 6-, and 9-Hour Chamber Irradiations as a Function of Initial NO_x for Initial NMHC of 2.2 ppm.

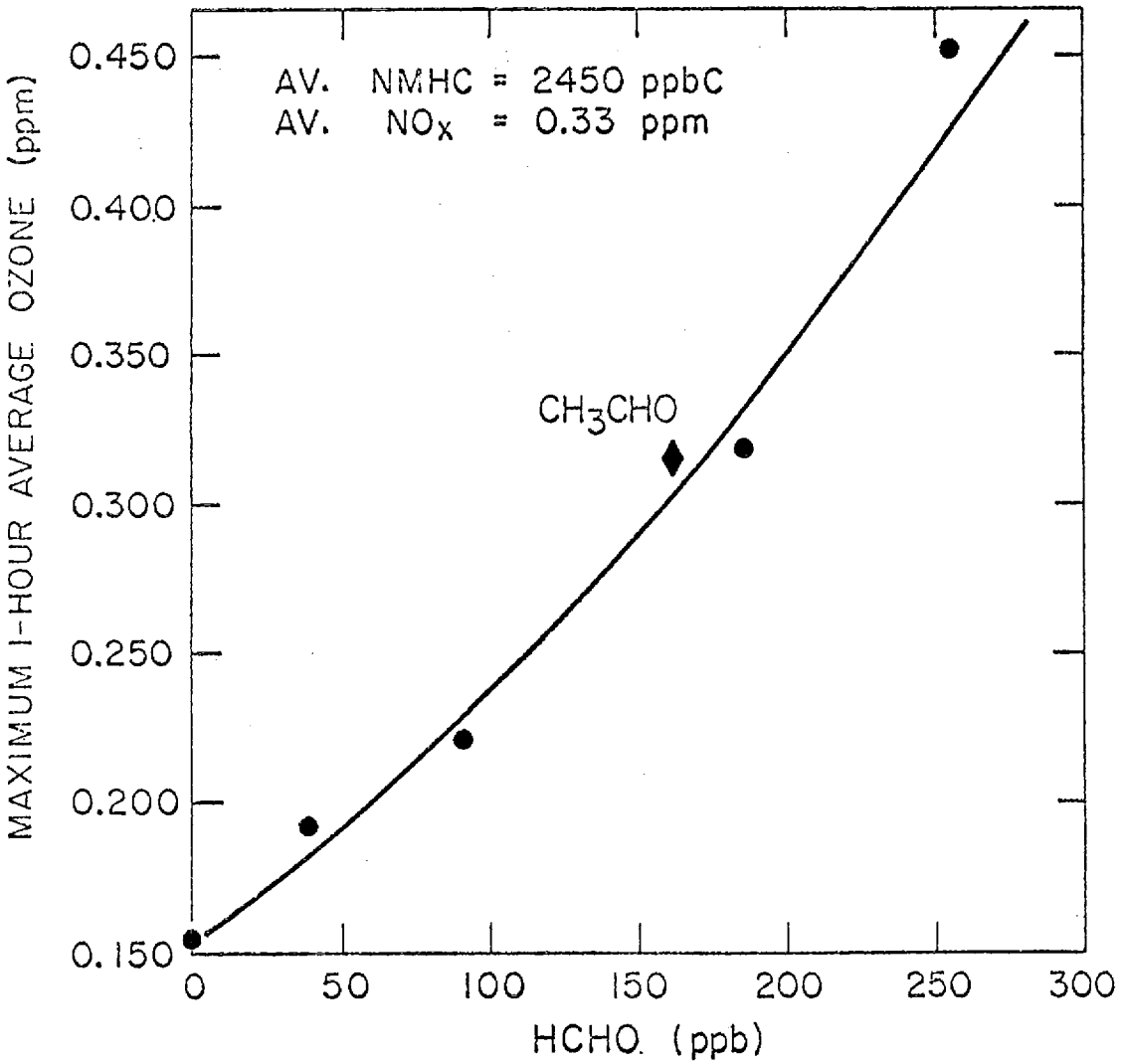

Figure 4. Effect of Added HCHO on Six-Hour Ozone Concentration During Irradiation of Surrogate Mixture.

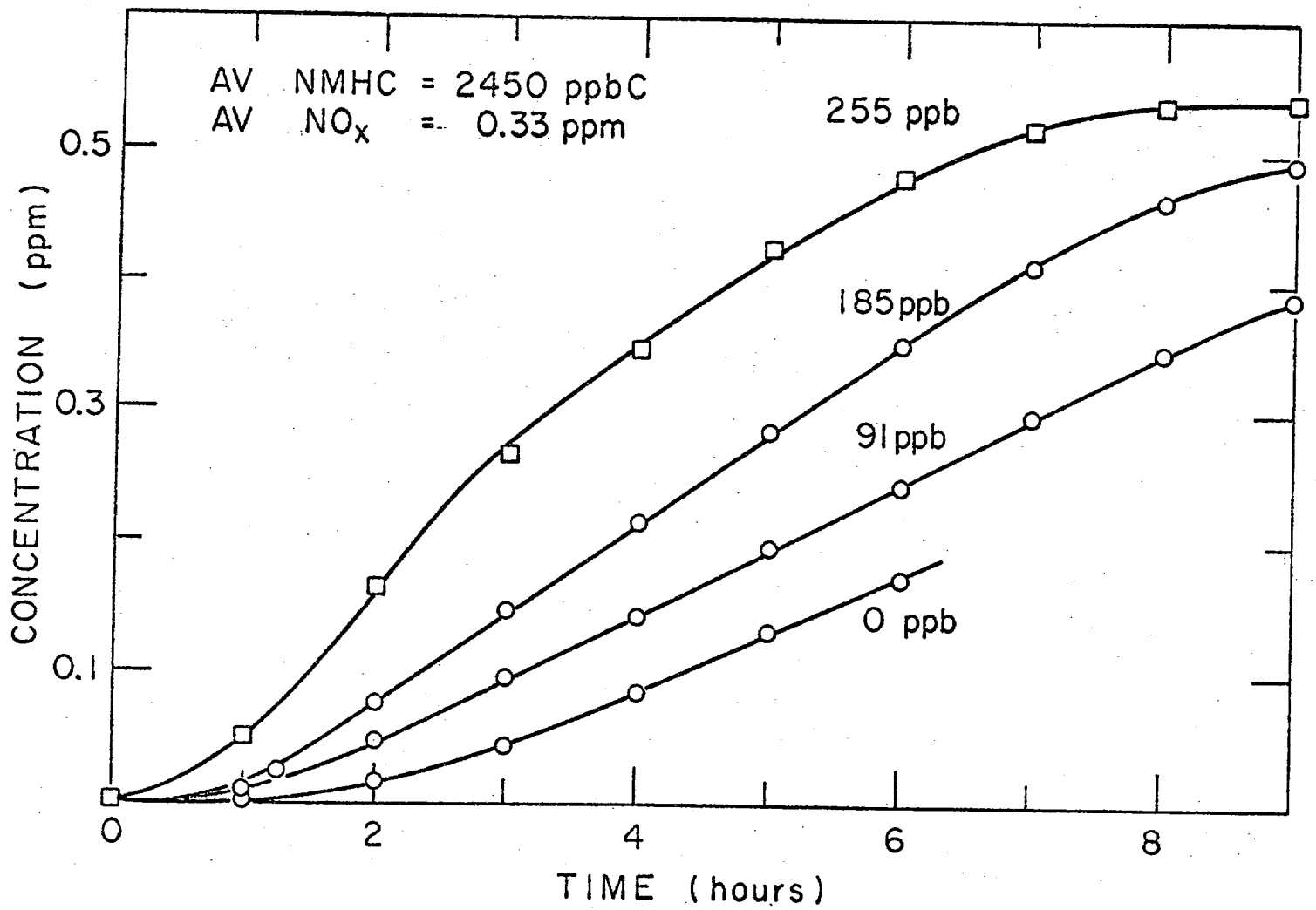

Figure 5. Effect of Added HCHO on Ozone Formation in Long-Term Irradiations of Surrogate Mixture.

body of data relating ozone production to initial HC and NO_x levels had already been generated in this chamber program, it was disclosed by the California Air Resources Board (ARB) and the Los Angeles Air Pollution Control District (LAAPCD) that a significant discrepancy (approximately 30%) existed between ozone concentrations measured by their respective calibration procedures. Inasmuch as the 2% neutral buffered potassium iodide (NBKI) method for determination of ozone (i.e., the ARB method) had been employed in our laboratories in the calibration of ozone monitors used in our HC-NO_x-O_3 research program, we felt that it was critical to understand the implications of this discrepancy for our data. Thus, we undertook an investigation of the stoichiometry of the 2% NBKI method at ambient concentrations of ozone using long-path infrared (LPIR) spectroscopy.

In the first phase of this investigation the absolute absorptivity of the 9.6-micron band of ozone was determined as a function of both spectral resolution and abundance, since such data have not been previously reported. The results from this study are summarized in Figure 6.

- At a spectral resolution of approximately 1 cm^{-1} the absorptivity was determined by two independent methods to be 4.23×10^{-4} ppm^{-1} m^{-1}.

In the second phase of this investigation, the correlation between the 2% NBKI method and the infrared absorption of ozone was investigated over an ozone concentration range from 0.1 to 1.2 ppm and as a function of relative humidity using an LPIR spectrophotometer interfaced to the SAPRC 5800-ℓ evacuable environmental chamber. Data obtained for relative humidities of approximately 18 and 50% are shown in Figures 7 and 8, respectively. Our principal findings were that:

- The stoichiometry of the 2% NBKI ozone analyzer calibration procedure, employed by the California Air Resources Board from 1960 until June 1, 1974, ranged from ~1.12 to ~1.25, depending upon whether the relative humidity of the sample stream was high or low, respectively.

- The infrared method employed in this investigation is consistent with the UV absorption method as shown in a collaborative study with W. B. DeMore in which the linear regression equation between LPIR and UV measurements of ozone samples in dry matrix air (RH ~3%) was $[O_3]^{UV} = (0.99 \pm 0.02)$ $[O_3]^{IR} + (0.016 \pm 0.011)$.

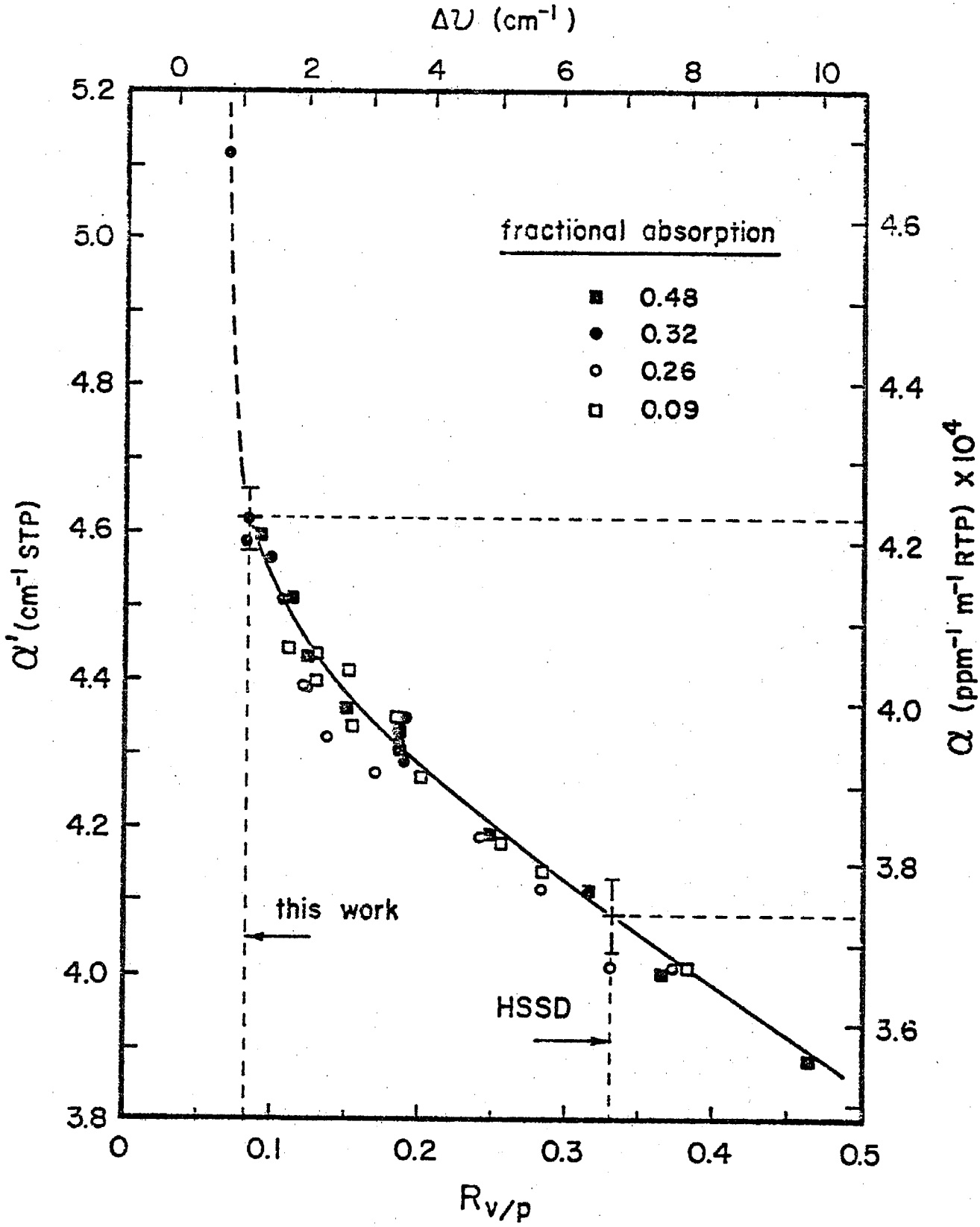

Figure 6. $R_{v/p}$ vs. Absorptivity (α) for the 9.48-Micron Ozone Absorption.

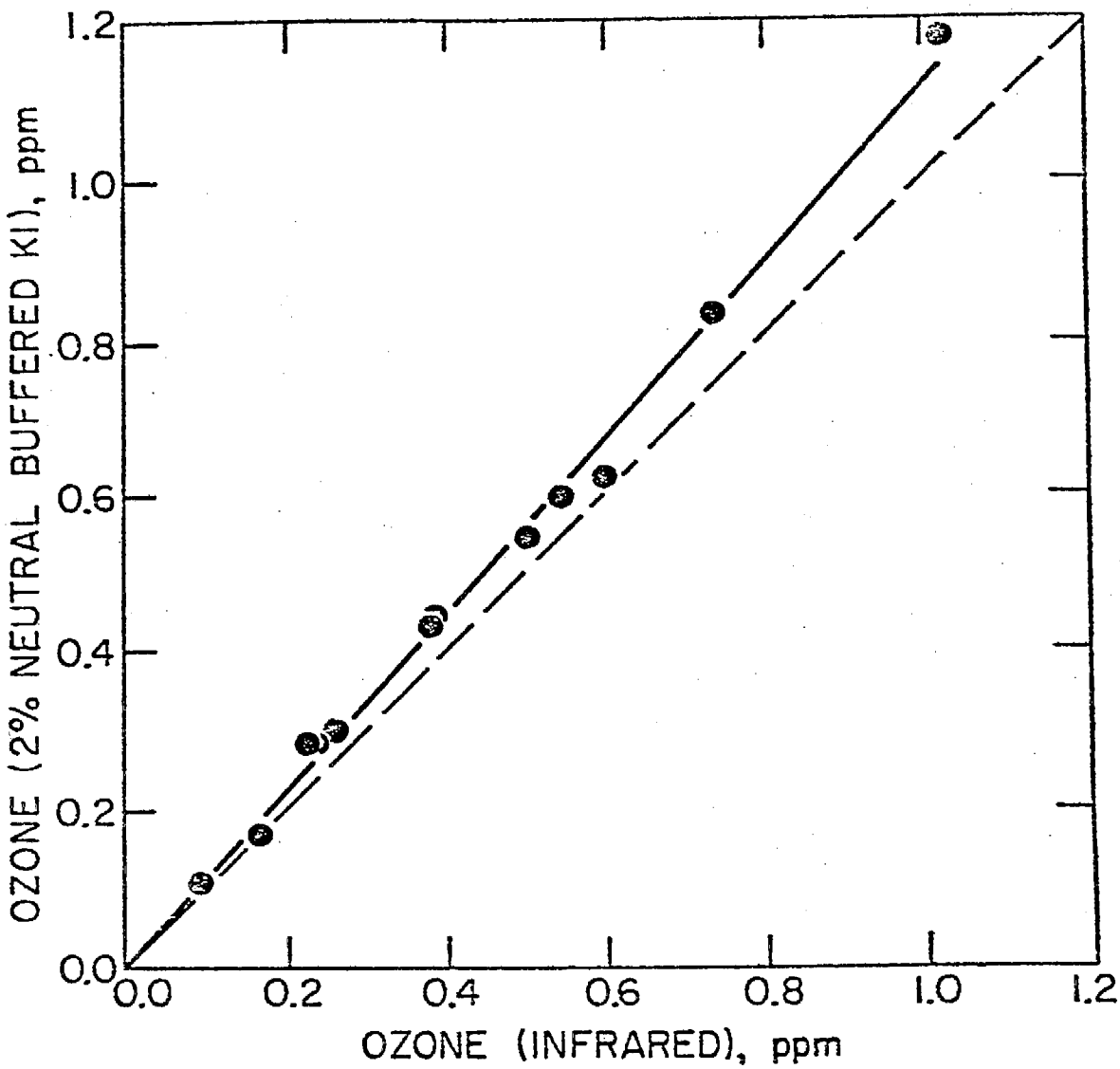

Figure 7. Linear Regression Fit of Ozone Concentrations Measured by LPIR and 2% NBKI Methods at an Average Relative Humidity of 18%; Slope = 1.12 ± 0.03, Intercept = 0.001 ± 0.014.

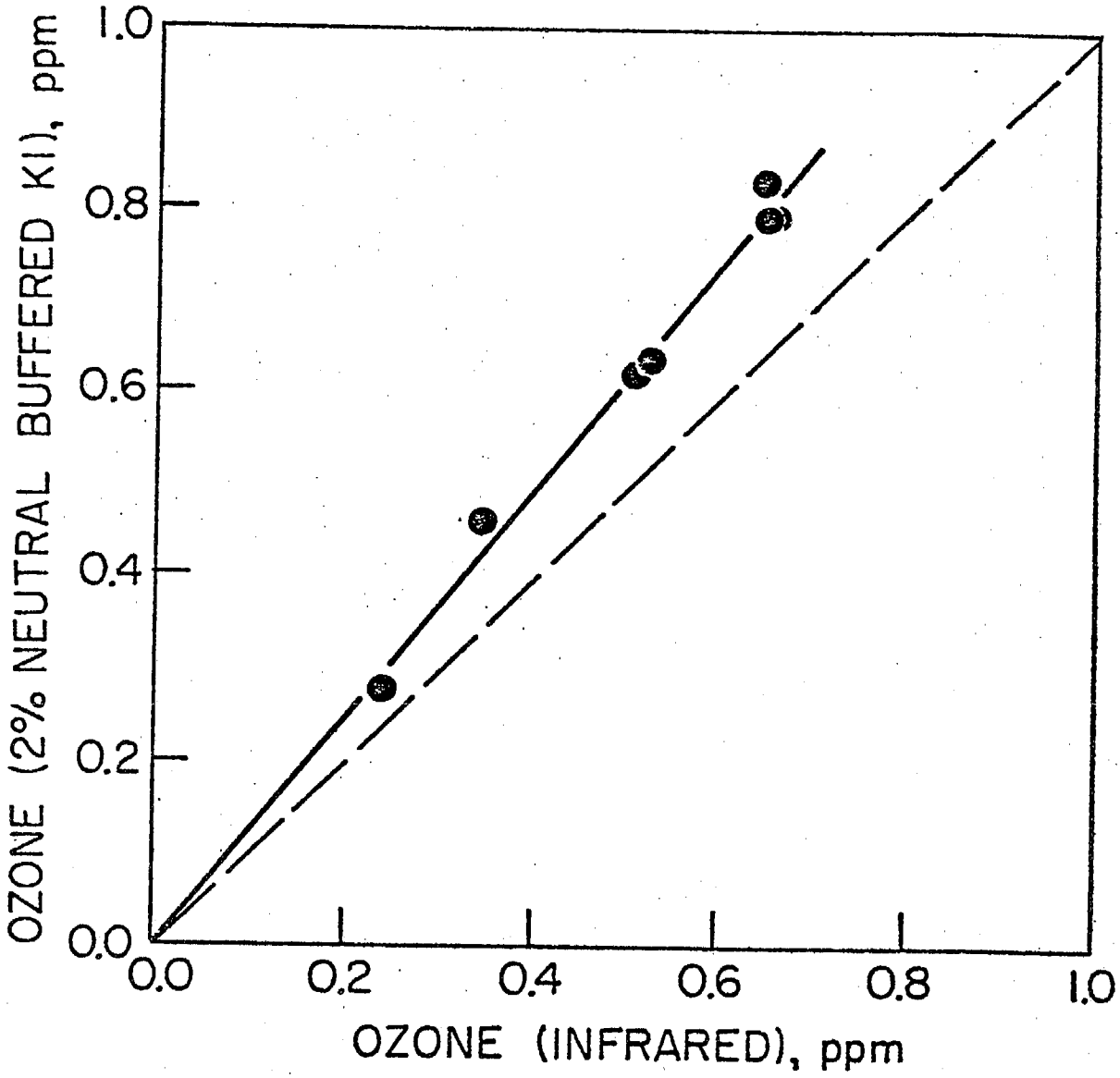

Figure 8. Linear Regression Fit of Ozone Concentrations Measured by LPIR and 2% NBKI Methods at a Relative Humidity of ~50%; Slope = 1.23 ± 0.06, Intercept = 0.001 ± 0.034.

In the final phase of this investigation, SAPRC staff members analyzed the implications for the historical oxidant data base in the South Coast Air Basin of placing the data obtained by both the LAAPCD and the ARB on a common calibration basis. Thus,

- An internally consistent set of oxidant air quality data for the California South Coast Air Basin was generated by scaling existing data for Los Angeles County air monitoring stations by a factor of 1.1 and existing air quality data for non-LAAPCD stations by a factor of 0.8.

- The scaled oxidant data show that, contrary to the indications of the original data, the cities of Azusa and Pasadena (in Los Angeles County) have higher yearly total oxidant levels than the cities of Riverside and San Bernardino in the eastern portion of the South Coast Air Basin.

RECOMMENDATIONS

- Very recent disagreements in the literature concerning the precise rates of dilution and fresh pollutant addition which should be employed in air parcel transport simulation studies in environmental chambers indicate that additional investigation and better methodologies are required in this research area.

- Additional data from long-term irradiation (> 9 hour) experiments are required to more fully elucidate oxidant-precursor relationships which are applicable to regions considerably downwind from major urban sources.

- There continues to be a need for consistent and experimentally valid hydrocarbon reactivity assessments and recent SAPRC environmental chamber studies appear promising in this regard. These studies should be continued on a formal basis.

- The HC-NO_x-oxidant data base which has been generated in this program should now be extended by the inclusion of SO_2 and by investigation of SO_2 to sulfate aerosol conversion rates under simulated atmospheric conditions.

- In the course of the added aldehyde experiments and HC-NO_x-ozone studies reported here and in our previous report (Final Report - Contract No. 3-017), it has been established that the initial formaldehyde concentration is a critical parameter in the rate of formation of ozone. However, the uncertainties associated with the chromotropic acid method for formaldehyde, particularly at the low (< 100 ppb) concentrations present in this study, have complicated quantitative interpretation of our results. It, therefore is important that a systematic study of the applicability and reliability of the chromotropic acid method be carried out.

ACKNOWLEDGMENTS

Stimulating discussions and valuable exchanges of technical information, for which we express our appreciation, took place at various times during this program with the following members of the California Air Resources Board staff:

Mr. Frank Bonamassa
Dr. Robert C. Grant
Dr. John R. Holmes
Mr. Tom Quinn
Dr. Jack K. Suder

We wish to specifically acknowledge the collaboration of John Holmes and Frank Bonamassa during our study of the NO_x retrofit program, and the work of William C. Kuby in developing the methodology for designing air parcel transport simulation experiments. In addition, we thank our colleagues Jeremy L. Sprung, Marian C. Carpelan, Minn P. Poe, and Alan C. Lloyd for preparing Section III-G of this report.

Contributions from the Various Donors Fund of the Statewide Air Pollution Research Center, the U. S. Environmental Protection Agency (Grant No. R-800649), and the National Science Foundation--Research Applied to National Needs (Grant Nos. GI-41051 and AEN73-02904-A02), which supported in part the purchase of a computer data acquisition system employed in the ARB program, are gratefully acknowledged.

Finally, we thank the California Air Resources Board for their financial support of the work performed under this contract.

ALL OZONE AND OXIDANT DATA REPORTED IN THIS STUDY HAVE BEEN CORRECTED BY A FACTOR OF 0.8 SINCE THE 2% NEUTRAL BUFFERED POTASSIUM IODINE CALIBRATION PROCEDURE WAS EMPLOYED IN THESE EXPERIMENTS.

I. INTRODUCTION

A. Scope and Purpose

Despite two decades of intensive research concerning the photochemistry of polluted atmospheres, and the concerted attention during the past ten years of local, state, and federal air pollution control agencies to the problem of reducing photochemical oxidant in urban areas, substantial uncertainty still remains as to the most cost-effective and societally acceptable means of solving this major environmental problem. Three critical issues which still have not been adequately resolved are (a) the degree to which oxides of nitrogen (NO_x), as well as nonmethane hydrocarbons (NMHC), must be controlled to achieve optimal reduction in oxidant formation;[1] (b) whether ambient air monitoring data, smog chamber data, or both, should provide the basis for developing oxidant control strategies;[2] and (c) whether different strategies must be pursued to control oxidant in downwind regions, as opposed to those strategies which apply to urban centers, and, if so, whether the differing approaches to levels and kinds of source control can be reconciled.[3]

A major goal of this continuing research program is to provide an experimental data base with which further resolution of such issues can be achieved. Toward this end, the SAPRC environmental chamber facility, which was designed and constructed with support from the California Air Resources Board,[4,5] has been utilized[6] for the past two years in a study of hydrocarbon-oxides of nitrogen (HC-NO_x) mixtures irradiated under conditions simulating those found in the California South Coast Air Basin. The systems studied included HC and NO_x concentrations ranging from those found in present day polluted atmospheres down to those to be expected from the implementation of emission control strategies aimed at meeting the State and Federal ambient air quality standards.

Emphasis during the current period has been on extension, refinement, and application of the oxidant-precursor data base generated in this program and some 80 additional chamber experiments have been conducted. Specific applications carried out during the current contract period include (1) the utilization of the SAPRC chamber data to an assessment of the impact of the NO_x retrofit program for 1966-70 light duty vehicles in the South

Coast Air Basin with respect to reduction (or increases) in ozone levels; (2) the extension of our program to longer irradiation times, with a view toward evaluating oxidant-precursor relationships during the critical later stages of a long irradiation day; and (3) an investigation of the effects of added aldehydes on oxidant-precursor relationships as part of our continuing study of aged smog effects.

Preliminary work has also been carried out concerning the design of the dynamic chamber experiments which would attempt to more realistically simulate air parcel transport in a location such as the South Coast Air Basin. Thus, a diffusion model has been employed to investigate the rates of dilution and fresh pollutant addition occurring during characteristic air parcel histories. Finally, as a result of the disclosure, in June 1974, of differences in ozone concentrations measured by different potassium iodide calibration procedures, and because accurate ozone measurements are critical to the acquisition and interpretation of the data being generated in this research program, we undertook an investigation of the stoichiometry of the 2% neutral buffered potassium iodide method for ozone at ambient concentrations using long-path infrared spectroscopy. As an adjunct to this experimental program, SAPRC workers also analyzed the implications for the historical oxidant data base for the South Coast Air Basin of placing the data obtained by both the Los Angeles Air Pollution Control District and the Air Resources Board on a common calibration basis.

The specific results obtained with respect to each of the subprograms outlined above, as well as analysis and discussions of these results, are given in Section III. In the section which follows immediately, a brief background to this SAPRC-ARB program is provided.

B. Background

Previous Smog Chamber Studies. For more than 20 years, a great variety of smog chamber data have been generated concerning many facets of the mechanism of photochemical air pollution, and considerable insights into the kinetics, mechanisms, and products of this phenomenon have been gained. Unfortunately, with respect to the formulation of quantitative control strategies, most, if not all, early chamber data suffer one or more serious limitations, which can considerably limit their applicability to

the real atmosphere. Such limitations include the use of pollutant concentrations significantly higher than those encountered in the atmosphere, use of hydrocarbon compositions bearing little resemblance to current hydrocarbon mixes in urban atmospheres, substantial deviation in irradiation intensity and spectral distribution from that occurring in the troposphere, and limitations in analytical methods imposed by the state-of-the-art at the time the studies were conducted.

Previous chamber studies dealing with the interrelations of HC, NO_x and photochemical smog manifestations have generally utilized either auto exhaust or pure organic compounds (e.g. propene or butane) as the hydrocarbon component. Studies using pure hydrocarbons, either singly or in simple mixtures have provided valuable information on the mechanisms of reaction and on the relative reactivity of these compounds,[7-12] but they are not directly applicable to predicting the production of oxidants under ambient conditions which involve complex multi-component mixtures of hydrocarbons. Chamber studies utilizing auto exhaust[12-17] have more closely approximated the pollutant composition found in ambient air and have provided the basis for the view that both NMHC and NO_x must be controlled in order to reduce photochemical oxidant. The relatively recent work of Dimitriades[16,17] is the most important example of such a study.

In his investigations, Dimitriades attempted, with considerable success, to deal with many of the problems encountered in previous smog chamber studies and consequently generated a useful body of data with respect to control strategy formulations. Recently these data have been employed[18,19] by air pollution scientists and control officials in their attempts to assess the relative reductions in ambient oxides of nitrogen and hydrocarbons required to effect various reductions in photochemical oxidant. This renewed attention to smog chamber data has resulted from the realization that ambient air monitoring data, which to date have formed the sole basis for the Federal approach to controlling photochemical oxidant, suffer serious limitations, not only in accuracy and detail, but also with respect to their applicability to oxidant problems in areas other than urban centers, a problem which has become of increasing concern in recent years.[20]

The Present Study. For the SAPRC-ARB study of precursor-oxidant relationships, a mixture of hydrocarbons, carbon monoxide and oxides of nitrogen (a primary pollutant "surrogate"--see Table 2) was chosen to represent the ambient air pollutant burden from all sources in the South Coast Air Basin of California.[21] This choice was made, in part, to avoid four serious difficulties associated with the use of auto exhaust: (1) non-reproducible starting composition, (2) particulate contamination of the chamber, (3) inability to achieve very low NO_x concentrations, and (4) the absence in auto exhaust alone of other hydrocarbons which are found in abundance in the Los Angeles atmosphere from natural gas and evaporative and geogenic sources.

Based on direct comparisons with observed ambient air monitoring data and chamber irradiations of ambient air,[21] the following criteria were selected for determining the acceptability of the surrogate mixture:

(1) oxidant concentration (2% neutral buffered KI method) $\simeq$ 0.45 ppm (uncorrected) after 3-4 hours of irradiation;

(2) nitrogen dioxide peak concentrations $\lesssim$ 0.25 ppm;

(3) aldehyde concentrations after 3-4 hours of irradiation should be 100-200 ppb each of formaldehyde, and total aldehydes except formaldehyde;

(4) comparable rates of hydrocarbon disappearance for the surrogate mixtures and an ambient sample irradiated in the chamber under comparable conditions.

Using these direct comparisons, as well as several indirect criteria, it was found that the standard surrogate mixture with the nominal concentrations given in Table 2 gave satisfactory results when irradiated in the glass chamber at a light intensity 70% of the maximum possible.[21] In the first year (1973-74) following this validation of the "surrogate", more than 60 irradiation experiments were conducted in a systematic study of the effect on production of ozone and oxidants of across-the-board reductions in hydrocarbon and carbon monoxide levels at nitrogen oxides concentrations varying from very low levels to levels approaching worst day ambient concentrations in Los Angeles (~0.4 ppm). Table 3 summarizes the average observed initial methane (CH_4), carbon monoxide (CO) and nonmethane hydrocarbon (NMHC) concentrations employed for irradiations at each of the five sets of concentrations studied.[6] Most of the irradiations were carried out for 6 hours with a few of ~2 hour duration.

Table 2. Prototype Surrogate Composition and Typical Central SCAB Concentrations of Components[21]

	Variable	Component	Carbon-Weighted Mole (percent)	Typical Concentration (ppb or ppbC)
1.	Nitrogen oxides		100.0[a]	Total 300 ppb
		Nitric oxide	90.0[a]	270 ppb
		Nitrogen dioxide	10.0[a]	30 ppb
	"Automotive hydrocarbons"	--	100.0	Total 2201 ppbC
	2. Aromatic	Toluene	5.22	115 ppbC
		m-Xylene	14.77	325 ppbC
	3. Saturates	n-Butane	35.66	785 ppbC
		2,3-Dimethylbutane	27.94	615 ppbC
	4. Olefins	cis-2-Butene	2.73	60 ppbC
		2-Methyl-2-butene	3.18	70 ppbC
	5. Cracking products	Ethylene	3.82	84 ppbC
		Propene	1.59	35 ppbC
		Acetylene	4.59	101 ppbC
	6. FID oxygenates	Acetaldehyde	0.23	5 ppbC
		Acetone	0.27	6 ppbC
7.	Formaldehyde[b]	Formaldehyde	--	Total 54 ppbC
8.	Natural gas[c]	--	100.0	Total 3000 ppbC
		Methane	93.34	2800 ppbC
		Ethane	5.33	160 ppbC
		Propane	1.33	40 ppbC
9.	Carbon monoxide	Carbon monoxide	100.0[a]	Total 7000 ppb

a. Mole percent only.
b. Treated as a separate variable for analytical reasons; determined by separate wet chemical method, as it gives little FID response and cannot be analyzed by GLC methods at these concentrations.
c. Includes background methane (∿1400 ppb) in its definition.

Table 3. Average Initial Concentrations in Surrogate Experiments (1973-74)

NMHC (ppbC)	CH_4 (ppm)	CO (ppm)
2610	2.8	8.3
2110	2.5	6.0
1310	2.1	3.7
690	1.8	1.9
460	1.6	1.4

The extension of this work during the current year, as outlined in Section A above, is discussed in detail in the following sections. The results of last year's experiments have been combined with those of the current year and the composite data set has provided the basis for application to evaluation of emission control strategies.

II. FACILITIES AND METHODS

A. Chamber Facility and Analytical Methods

Most of the experiments in this study were carried out in a 6400-liter (226-ft^3), all-glass (Pyrex) chamber[22,23] which has a surface-to-volume ratio of 3.4 m^{-1} (1.04^{-1}). The dimensions of the glass chamber are 8' x 8' x 4' (i.e., a flat box). Photolyzing radiation is provided by two externally mounted, diametrically opposed banks of forty Sylvania 40-W BL (black light) lamps, which are backed by arrays of Alzak-coated reflectors. Half-lives for ozone decay, measured at various times in this program under standard conditions of temperature, relative humidity, and light intensity, were $\geq$ 25 hours in the dark and 12 to 15 hours with irradiation. These half-lives are significantly longer than those reported for other chambers with comparable dimensions, surface-to-volume ratios, and light intensities and result in correspondingly smaller perturbations on ozone rates of formation and maximum ozone concentrations in the glass chamber experiments.

The supporting analytical facilities employed in the glass chamber studies are shown schematically in Figure 9 and are described in detail below. The on-line computer data acquisition system was installed in November 1974, and became fully operational near the end of this program. Use of the computer system is greatly facilitating data handling for measurements of physical parameters and concentrations obtained from continuous analyzers.

The SAPRC evacuable chamber[22,24] was employed in the investigations of the stoichiometry of the 2% neutral buffered potassium iodide method for ozone and the analytical methods used in this study are described in Section III-E.

The current physical and chemical measurement methods and the range, precision, and accuracy of measurement of each of these parameters are given in Table 4. The details of the analytical and data processing procedures are described below for each species or variable monitored. The data obtained (except for hydrocarbons) are tabulated for each run on an inorganic data sheet (Appendix A) and have not been corrected for losses due to sampling from the chamber.

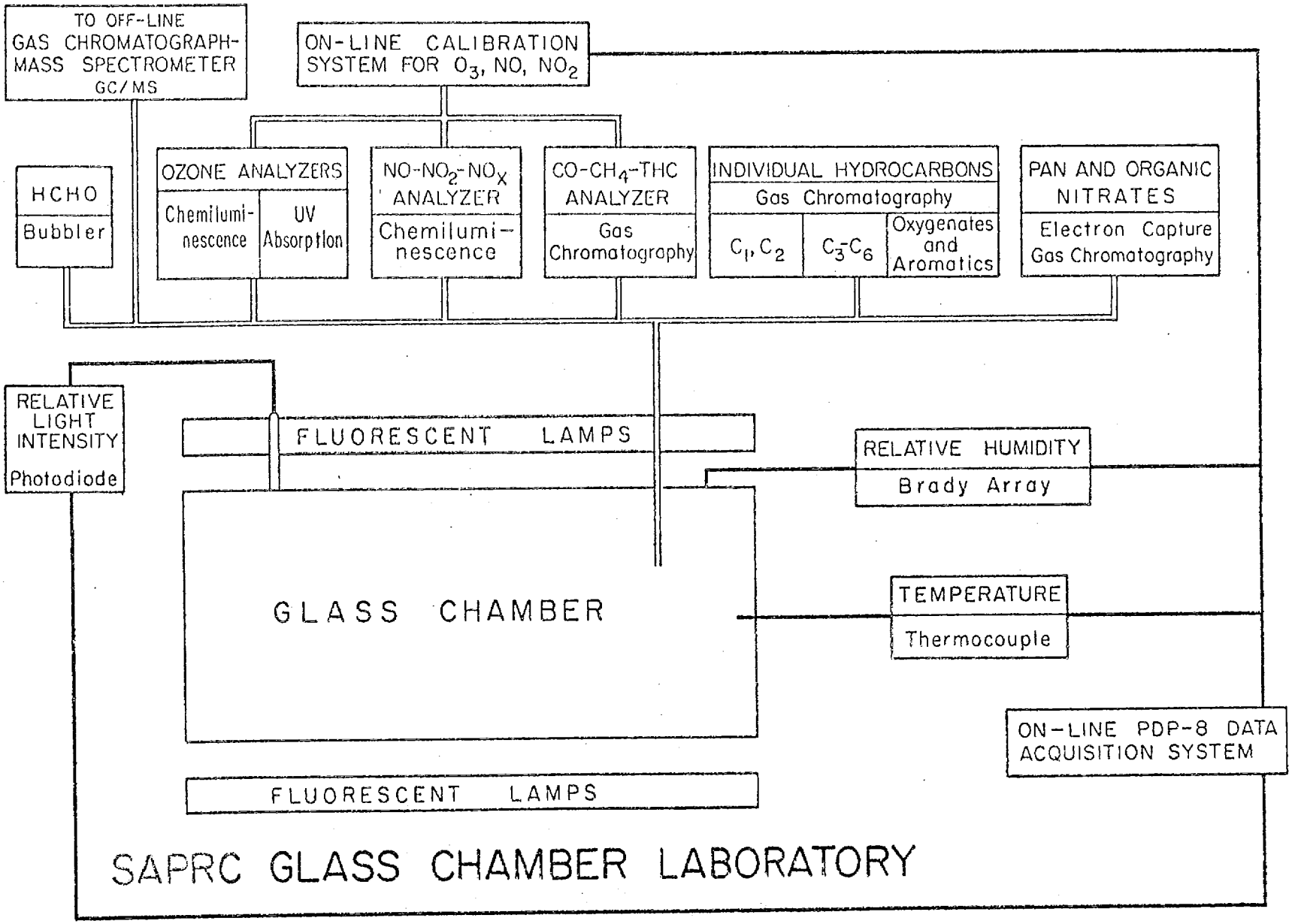

Figure 9. Schematic Drawing of Glass Chamber Facility.

Table 4. Chemical and Physical Parameters Measured in Glass Chamber Studies

Parameter	Range	Method	Sampling Rate	Precision	Accuracy
Ozone	0-20 ppm	UV Absorption Analyzer	570 ml/min	± 0.005 ppm	± 5%
Total Oxidant	0-1 ppm	Mast Analyzer	134 ml/min	± .05 ppm	
NO	0-10 ppm	Chemiluminescent Analyzer	895 ml/min	± 2% F.S.	± 5%
NO_2	0-10 ppm			By difference	By difference
NO_x	0-10 ppm			± 2% F.S.	± 5%
PAN	>1 ppb	GC		± 0.5 ppb	± 10%
Formaldehyde	>10 ppb[a]	Chromotropic Acid	1 ℓ/min (30 min samples)	± 7 ppb	± 10%
Individual HCs	0.5-1 ppb	GC		± 15%	Limited by calibration standard (typically ± 5%) and/or by sampling techniques
	1-2 ppb	GC		± 10%	
	>2 ppb	GC		± 2%	
CO	0-10 ppm	GC	100 ml/min	± 2% F.S.	± 10%
Temperature	15° to 40°C	Thermometer Thermocouple		± 0.02°C ± 0.1°F	± 0.5°C ± 2°F
Light Intensity	0-1 Solar Constant	NO_2 Actinometry		± 5%	b
	Relative	Photodiode			
Relative Humidity	0-100%	Brady Array		± 1% RH	± 5%

[a]Determined by practical values of sampling time and flow rate

[b]See discussion on page 14.

OZONE (O_3) was monitored by ultraviolet absorption analyzers (Dasibi-1003 or AH-1003) calibrated against 2% neutral buffered potassium iodide.[25] Since it has subsequently been demonstrated[26,27] that at ~50% RH this calibration procedure yields ozone values which are too high by a factor of ~1.25, all ozone data reported have been corrected by a factor of 0.8.

TOTAL OXIDANT was monitored (in Runs 74-102) using a Mast analyzer which was calibrated in tandem with the Dasibi ozone monitor using 2% neutral buffered potassium iodide. The original calibration factor is given on each data sheet. The oxidant data have been corrected by a factor of 0.8 as discussed above. Data points were read from the strip chart.

NITROGEN OXIDES (NO, NO_2, and NO_x) were monitored by chemiluminescent detection (TECO 14B). The NO_2 and NO_x modes of this and similar chemiluminescent NO-NO_x analyzers have been shown to respond quantitatively to other nitrogen-containing compounds, such as peroxyacetyl nitrate (PAN) and organic nitrates and nitrites.[28,29] All NO_2 and NO_x data reported here have been corrected by subtraction of measured or interpolated PAN concentrations.

CARBON MONOXIDE (CO) was monitored by gas chromatography (Beckman-6800). The instrument was calibrated daily with a standard gas sample.

PEROXYACETYL NITRATE (PAN) was monitored by gas chromatography with electron capture detection (GC-ECD).[30,31] Samples were taken in a 100-ml precision bore syringe and transferred to the GC sampling system as quickly as possible. Peak heights were read from the strip chart and converted to concentration units using a calibration function which was determined periodically. PAN data are given on both the inorganic and hydrocarbon data sheets.

FORMALDEHYDE (HCHO) was monitored using the chromotropic acid method.[32] Air from the chamber was drawn through a bubbler at the rate of 1 ℓ min^{-1} and the total volume per sample was determined using a timer-controlled shutoff system. Generally, a 30-min. sample was taken. The concentration was recorded at the midpoint of this time interval, except for the initial value, which was taken in the 30 minutes prior to lights on, and the final sample, which was taken in the 30 minutes prior to lights off. Absorbances were read on a Bausch and Lomb Spectronic 20, and calculations of

the HCHO concentration from the absorbance and volume of air sampled (HCHO vol) were made from the following equation:

$$\text{HCHO (ppm)} = \frac{\text{HCHO}(\mu g) \times 2.037}{\text{HCHO(vol)}}$$

where HCHO (μg) is taken from the least squares fit of the experimentally determined calibration function of HCHO (μg) vs. absorbance. HCHO data are given on both the inorganic and hydrocarbon data sheets.

RELATIVE LIGHT INTENSITY (PD #2) was monitored using a photodiode (CL 905 HL) equipped with a 338 nm interference filter and a 1.5-V, 30-KΩ bridge. The absolute magnitude of the voltage as read with a digital voltmeter is reported. With this device, increasingly negative values correspond to increasing light intensity. The response function for the device has not been determined quantitatively and the data are employed only for relative information concerning the trend in the intensity of a given set of lamps over their useful life. The photodiode was positioned on one side of the chamber facing the bank of lamps on the opposite side.

Late in this program, an EG & G Inc. absolute radiometer was installed on the end of the chamber to provide an estimate of the magnitude of the variation of light intensity during the run. Values of the photon flux in $\mu W\ cm^{-2}$ near the beginning and end of each run are noted in the comments on the data sheets and typically differed by less than 3%.

The SAMPLE TEMPERATURE was read from either a Doric Thermocouple indicator (°F), using a thermocouple suspended in the chamber (TS2), or from a 19-35°C (0.01 degree/division) thermometer hung free inside the chamber close to the end window, but not in the direct light path (TS1).

RELATIVE HUMIDITY (RH) was measured using a Brady array (Thunder Scientific). The response in volts (V) was converted to percent RH, using the calibration function supplied by the manufacturer. The Brady array was sent to the manufacturer for recalibration midway through this program. Humidity data are unavailable for runs conducted during this period.

HYDROCARBONS (HC) were monitored by gas chromatography with flame ionization detection (GC-FID), using the columns and methods developed by Stephens and Burleson.[33,34] Methane and C_2 HC's were analyzed using a

5' Poropak N Column, C_3-C_6 HC's using a 36' 2,4-dimethylsulfolane column, and aromatics and oxygenates using a special three-part column. Oxygenates were also monitored using a 10' Carbowax 600 column. Each GC was calibrated frequently using specially prepared samples.[33] Peak heights were read from the strip charts in ppb using calibrated transparent overlay charts. Computer processing of the data includes calculation of the concentration in ppbC for each data point. These data are given for each run on the hydrocarbon data sheets (Appendix C). Further information to facilitate use of the organic data is given at the beginning of Appendix C.

B. General Experimental Procedures

Following each experiment in this program, the glass chamber was flushed with dry air provided by an air purification system[35] (see Figure 10) for about 2 hours at a flow of ~12 cfm. The chamber was then flushed with humidified pure air for about one hour just prior to the start of a run to achieve the desired initial RH of ~50%. The temperature of the chamber prior to turning on the lamps was adjusted to the operating temperature anticipated during the irradiation by means of infrared lamps. During all flushing procedures, the two sonic pumps were in operation to provide maximum release of materials from the chamber walls.

The matrix air used during the flushing procedure and for the final fill for the experiment generally contained less than a total of 60 ppbC of all hydrocarbons except methane, which was typically at a concentration between 550-850 ppb.[35] After completion of filling, analysis of the matrix air prior to injections showed somewhat higher hydrocarbon values due to off-gassing from the chamber walls, but generally these values were less than 200 ppbC nonmethane hydrocarbon.

Following flushing, starting materials were injected by using 100-ml precision bore syringes, and rapid mixing was obtained by brief (~5 minutes) use of the sonic pumps. The surrogate hydrocarbons were injected as samples from previously prepared mixtures. The liquid hydrocarbons were contained in a nitrogen-filled 20-ℓ Pyrex bottle, and the gaseous hydrocarbons were contained in an LPO bottle pressurized with nitrogen.

During the run, the sample temperature was controlled at 32 ± 2°C by means of a variable air flow past the chamber walls.

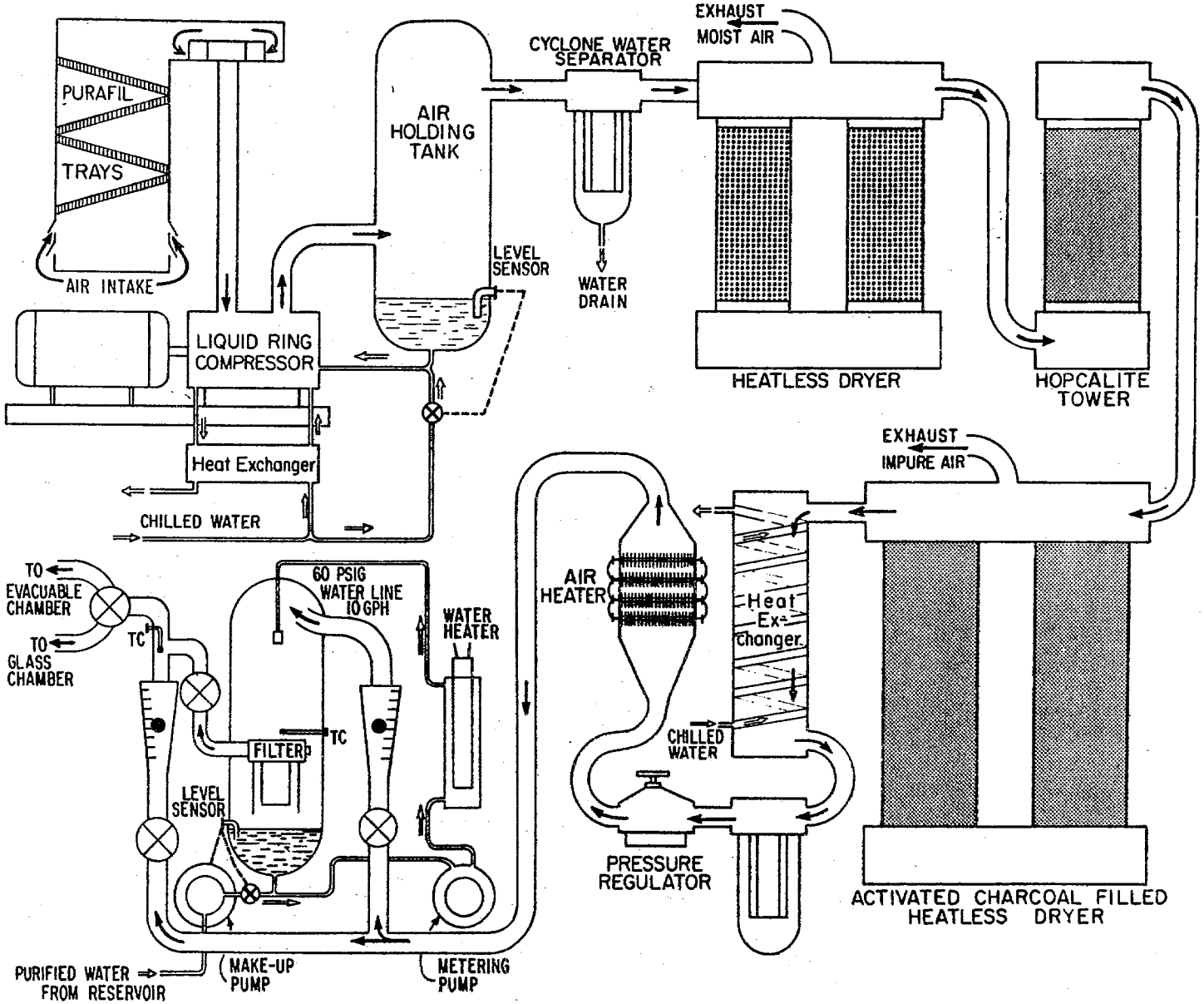

Figure 10. Air Purification System (from Reference 35).

Light intensity (k_1) was periodically determined, using the method of Holmes et al.,[36] which employs the initial rate of NO_2 photolysis in N_2 as a measure of absolute photon flux in the glass chamber in the actinic region (300-450 nm). However, some O_2 (of order tens of ppm or higher) will be present in the chamber which cannot be evacuated, but instead must be flushed repeatedly with N_2. Oxygen present in concentrations greater than approximately 10 ppm will lead to somewhat low values for k_1 as they were calcululated in this study relative to the true k_1 which would be observed for the complete absence of O_2.[36] Based on the purity of the nitrogen used (with respect to oxygen content) and a calculated efficiency for repetitive flushing of the chamber, it is estimated that the observed k_1 could be as much as 25% low with respect to the true k_1.

In September 1974, it was found that the k_1 for the original set of lamps (Sylvania) had dropped to ~0.20 min^{-1}. These lamps were replaced with a new set of presumably comparable General Electric (G.E.) lamps which were found to be actually less effective than even the old Sylvania lamps (in the actinic region corresponding to NO_2 photolysis). Relative light intensities were measured with a photodiode equipped with a 338-nm interference filter and a 1.5-V, 3 KΩ bridge as discussed above. Standard propene-NO_x experiments were also used to confirm the unsuitability of the G.E. lamps. Results of these experiments are summarized in Table 5. Replacement of the G.E. lamps with new lamps manufactured by Sylvania provided a substantial improvement in light intensity. After 100 hours' "burn in" time, there appeared to be good reproducibility for surrogate runs carried out at both high (.34 ppm) and low (.06 ppm) NO_x levels. After ~150 hours of use (February 13, 1975), a k_1 of 0.32 min^{-1} was observed for the new set of lamps. On March 21, 1975 after 17 additional runs had been conducted, a k_1 value of 0.25 min^{-1} was measured.

Table 5. Sylvania and G.E. 40-BL Lamp Comparisons Under Normal Operating Conditions of the Glass Chamber

Lamps	Light Intensity at 338 nm[a] (volts)	dNO_2/dt[b] (ppb/min)
Used Sylvania	-0.0556	3.0
New G.E.	+0.015	2.4
New Sylvania	-0.226	3.8

[a]Negative values correspond to higher light intensities.

[b]Standard propene-NO_x experiment; rate for period 0.25 to 1 hour.

III. RESULTS AND DISCUSSION

A. Extension of the HC-NO_x-O_3 Data Base

We have previously reported[1] results from more than 60 surrogate mixture irradiations representing a systematic study of the effect on production of ozone and other oxidants of across-the-board reductions in hydrocarbon and carbon monoxide levels at nitrogen oxide concentrations ranging from very low levels (~0.01 ppm) to levels approaching worst-day ambient concentrations in Los Angeles (~0.4 ppm). In the present program, a total of 80 chamber runs were conducted, including chamber characterization experiments (i.e., determinations of k_1, ozone decay rates, standard propene runs, etc.), as well as irradiations of HC-NO_x surrogate mixtures.

We are reporting detailed data resulting from a total of 64 surrogate runs. These runs were designated to (a) provide data for 6-hour irradiations, which would supplement those obtained in the previous year's program,[1] (b) establish a data base for long-term irradiations (i.e., 9 hours or longer), and (c) determine the effects of added aldehydes and aged smog on ozone production.

Data sheets listing O_3, NO, NO_2, NO_x, CO, PAN, HCHO, RH, and temperature values for each run are given in Appendix A. Concentration-time plots showing O_3, NO, NO_2, and PAN are given in Appendix B. Individual hydrocarbon analyses are given in Appendix C. A summary of the initial reactant concentrations, values for the maximum ozone and PAN levels observed, and the maximum 1-hour average ozone levels are given in Table 6 for 6-hour irradiations and in Table 7 for the long-term irradiations (including three runs from last year's program) and added aldehyde experiments. These results are discussed in detail in the following sections.

Table 6. Initial Reactant Concentrations and Values of Reactivity Parameters for Six-Hour Surrogate Irradiations

Surrogate Run No.	Initial Concentrations				Ozone		6-Hour PAN (ppm)
	NMHC (ppbC)	NO_x (ppm)	NO_2/NO_x	HCHO (ppb)	6-Hour (ppm)	Maximum 1-Hour Average During 6-Hour (ppm)	
74-G	2685	.600	.100	102	.079	.064	
75-G	1998	.526	.103	46	.087	.071	.002
76-G	2718	.534	.101	31	.102	.083	.003
77-G	2202	.348	.166	20	.322	.283	.008
78-G	2118	.090	.256	31	.372	.367	.011
79-G	1341	.380	.100	16	.069	.057	.002
80-G	2756	.430	.198	0	.186	.162	.006
81-G	2467	.190	.153	0	.378	.366	-
83-G	2735	.433	.111	67	.222	.196	.010
84-G	2836	.530	.094	35	.107	.090	.005
85-G	2250	.433	.268	99	.234	.205	.011
86-G	2270	.349	.100	104	.234	.204	.012
101-G	2373	.337	.107	65	.159	.135	.014
102-G	2312	.358	.123	28	.139	.117	.011
107-G	2339	.330	.139	73	.214	.188	.017
118-J[a]	2603	.313	.118	110	.293	.265	.028
119-J	2534	.340	.121	38	.244	.218	.018
124-J	1591	.100	.180	39	.287	.272	.031
125-J	1619	.150	.107	34	.238	.217	.018
D-130-J[b]	2416	.340	.124	-	.206	.185	.017
D-137-J[b]	2330	.526	-	2	.045	.038	-
138-J	2331	.523	.096	60	.031	.025	.002
D-139-J[b]	2296	.511	.121	8	.062	.050	.004
153-J	2395	.481	.121	-	.068	.057	.004
154-J	2548	.483	.166	140	.078	.068	.003
157-J	2309	.198	.131	40	.309	.282	.015

[a]New lamps installed prior to 111-G. Runs 111 through 116 were used to bring the lamps to a reasonably stable intensity.

[b]Following ozone conditioning of the chamber.

Table 7. Initial Reactant Concentrations and Values of Reactivity Parameters for Long-Term (≥ 9 Hours) Surrogate Irradiations and Added Aldehyde Experiments

Surr. Run No.	Irradiation Time (hrs)	Initial Concentrations				Ozone			Maximum 1-Hr Average Ozone During		PAN	
		NMHC (ppbC)	NO_x (ppm)	NO_2/NO_x	HCHO (ppb)	6-hr (ppm)	9-hr (ppm)	Final (ppm)	6-hr (ppm)	9-hr (ppm)	6-hr (ppm)	9-hr (ppm)
117-G	12.75	1975	.298	.107	4	.209	.346	.470	.186	.322	.025	----
121-J	9.0	2427	.056	.214	-	.264	.290	----	.257	.286	.025	.025
122-J	9.0	1639	.098	.122	94	.297	.337	----	.283	.334	.029	.023
132-J	10.25	1529	.161	.112	-	.284	.368	.380	.261	.358	.014	----
133-J	9.0	1581	.097	.134	5	.298	.326	----	.288	.323	.014	.012
134-J	9.0	2490	.038	.211	31	.170	.198	----	.164	.194	.008	.008
135-J	9.0	1477	.037	.189	27	.188	.218	----	.181	.214	.008	.008
136-J	9.0	2412	.271	.111	15	.255	.394	----	.229	.374	.015	.024
141-J	6.0	2374	.333	.117	0 CH_3CHO	.176	----	----	.155	----	----	----
142-J	9.5	2796	.332	.104	162	.351	.541	.558	.317	.514	.037	.048
144-J	6.25	2329	.337	.122	38	.218	----	----	.192	----	.011	----
145-J	9.0	2570	.337	.116	185	.351	.496	----	.319	.480	.020	.028
148-J	9.0	2460	.321	.112	255	.480	.539	----	.452	.537	.027	----
149-J	11.25	2275	.313	.125	91	.246	.389	.463	.222	.368	.012	.019
150-J	9.25	2448	.523	.139	134	.078	.166	.172	.064	.149	.004	----
151-J	10.25	2483	.245	.102	111	.340	.463	.477	.310	.448	.019	.025
156-J	9.0	2226	.206	.155	10	.321	.419	----	.298	.408	.017	.021
158-J	9.0	3116	.430	.107	107	.174	.295	----	.153	.274	.009	.014
48-E	10.0	350	.077	.026	0	.146	.214	.228	.128	.206	.004	.005
55-G	9.0	1357	.016	.312	56	.096	.136	----	.088	.130	.003	----
62-G	9.0	746	.096	.260	69	.238	.281	----	.224	.274	.008	.008

B. Application of SAPRC-ARB Chamber Data to NO_x Retrofit Program for 1966-70 Light-Duty Motor Vehicles in the SCAB[37]

An important goal of this SAPRC-ARB investigation has been to define ranges of initial ambient NO_x and nonmethane hydrocarbon (NMHC) concentrations for which the Federal ambient air quality standard for oxidant would be met. However, it now appears that interim improvements in air quality, as well as the ultimate achievement of air quality satisfying the oxidant standard, will come about largely through a series of control programs--each of which produces only relatively small, discrete reductions in HC and/or NO_x emissions. Such a control program was instituted in 1973 in the California South Coast Air Basin, in which 1966-70 light-duty motor vehicles were to be retrofitted with a device to control NO_x emissions.[38] In early 1974, after only partial implementation of this program, it appeared that repeal of the program by legislative action might occur. This led to a request from the ARB chairman that we apply the data obtained in our ARB-sponsored HC-NO_x surrogate irradiation program to a quantitative evaluation of the effect on maximum ambient ozone levels, in both Los Angeles and downwind regions of the South Coast Air Basin, of the fully implemented NO_x retrofit program.

The resulting development of a method to provide an evaluation of incremental reductions in ambient HC and/or NO_x levels has been described in a previous report.[1] The following four elements are necessary to carry out such an evaluation: (a) a valid data base relating precursor levels to production of ozone, (b) data concerning initial (i.e., precontrol strategy) ambient levels of HC and NO_x present in the early morning hours, (c) an estimate of the emissions reductions to be achieved by the control program under consideration, and (d) a method for predicting the ambient HC and NO_x levels resulting from such emission reductions. Each of these elements, and the assumptions involved in their use, will be discussed below in relation to their specific application to evaluation of the NO_x retrofit program.

HC-NO_x-Ozone Data Base. The data base relating ozone formation to initial NMHC and NO_x levels, which was largely developed in the previous year,[1] has been supplemented and extended as described in the preceding section (see Table 6). From these combined sets of data, we have taken the ozone concentration after 6 hours of irradiation (the maximum

observed during that period), as a function of initial NMHC and NO_x concentrations (Figure 11), as the basis for developing the following assessments of effects on ozone maxima resulting from incremental reductions in precursor levels. We have assumed that the chamber irradiation results provide a reliable indication of the results to be expected for similar conditions in the atmosphere in the South Coast Air Basin. Some evidence for the validity of this assumption will be discussed below.

Initial Ambient Concentrations of the NMHC and NO_x Precursors. In order to calculate the magnitude of effects on ambient ozone levels due to a given reduction in ambient NMHC and NO_x levels, it is necessary to establish base conditions, i.e., the levels of NMHC and NO_x present prior to implementation of a control program. We chose to define initial conditions on the basis of air monitoring data from stations 001 and 083 of the Los Angeles Air Pollution Control District which are located in downtown Los Angeles and Pasadena, respectively. Extensive trajectory and air parcel transport studies by a number of groups[39-41] have shown that on days of high oxidant, Pasadena is frequently a receptor at about noon (i.e., approximately 4 hours after the morning traffic peak) for air parcels originating in the Long Beach-Central Los Angeles area in the 6-9 AM period. Since the surrogate mixture was designed to reflect the 6-9 AM ambient NMHC and NO_x levels in Los Angeles, the smog manifestations observed toward the end of a 6-hour irradiation are taken to correspond in this case to ambient photochemical oxidant concentrations observed in the Pasadena area (see discussion and validation of this concept below).

Two sets of initial conditions, utilizing air monitoring data for oxidant (ozone)[42] in Pasadena and NO_x and NMHC in downtown Los Angeles (Station 001), have been selected. The first case is based on the highest oxidant (0.45 ppm hourly average) observed in Pasadena in 1973. This occurred on July 25, for which date the hourly average NMHC and NO_x concentrations at 8 AM (PST) at Station 001 were 3.0 ppmC and 0.3 ppm, respectively. These precursor concentrations yielded the highest hourly average NMHC/NO_x ratio observed at Station 001 during the 6-9 AM period for the 12 days of highest oxidant observed in Pasadena during 1973.[43] The second case is derived from data for July 3 and 24, August 18, and October 4, 1973--four days of high

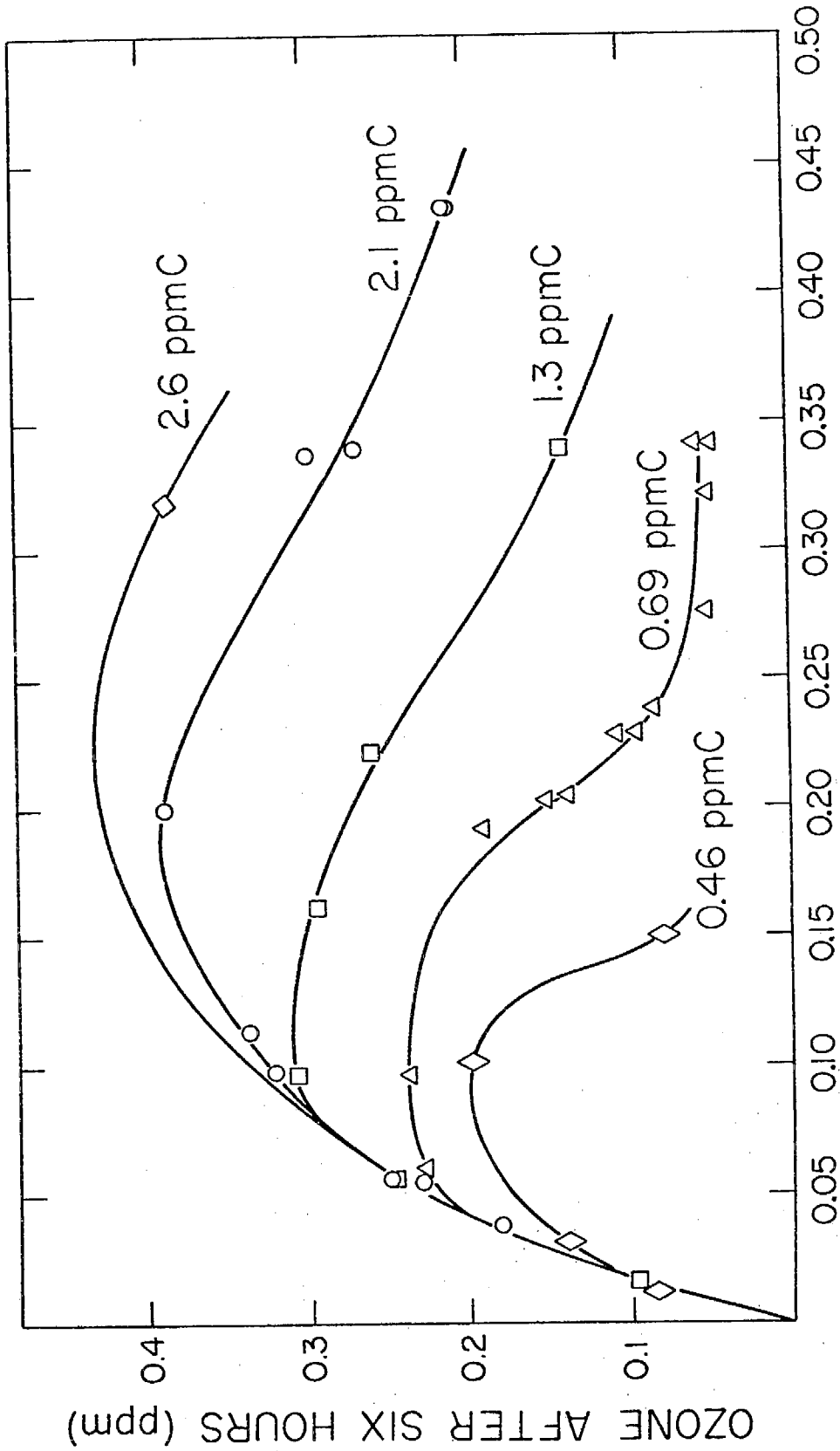

Figure 11. Six-Hour Ozone Concentrations as a Function of Initial NO_x at Various Nonmethane Hydrocarbon Levels.

oxidant in Pasadena for which (with the exception of July 25) the highest 6-9 AM NMHC was observed at Station 001 in 1973.[43] For these four days, 6-9 AM average NMHC was 2.35 ppmC, and a more typical NMHC/NO_x ratio of about 7 (average of 6-9 AM average values) was observed.

Reductions in Emissions and Ambient NMHC and NO_x Levels. The data on reduced emissions from vehicles retrofitted with NO_x devices were obtained by the ARB by measuring the emissions from a large number of vehicles both with and without the device. A number of surveillance programs were conducted, and, from the observed changes in emissions resulting from installation of the NO_x retrofit devices, the ARB provided projections of the resulting change in total emissions (from all sources) of NMHC and NO_x. The assumption that the percent reduction in emissions would give a corresponding percent reduction in ambient NMHC and NO_x levels was made in these calculations.

Application of Chamber Data to the NO_x Retrofit Program. Three different initial estimates of the emissions reductions effected by the retrofit devices and the resulting impact on NO_x and HC emissions in 1975 for the South Coast Air Basin were (a) a 7% reduction in NO_x emissions from all sources with no change in HC emissions, (b) in addition to a 7% NO_x reduction, a 3% decrease in overall HC emissions based on an approximate 21% reduction in HC exhaust emissions which was observed as a side benefit from the retrofit devices in some early surveillance tests, and (c) a 3.3% decrease in NO_x emissions and a 3.7% decrease in HC emissions.[44,45]

Initially, we calculated the effects of various small reductions in NO_x and/or NMHC on ozone formation by linear interpolation on the SAPRC chamber data as presented in Figure 12.[1] Evaluation of the impact of the three emissions reduction scenarios cited above, using an initial NMHC/NO_x ratio of 10 and of 7 (as discussed previously), is given in Tables 8 and 9, respectively. It can be seen that slightly more pessimistic results are obtained for an initial NMHC/NO_x ratio of 7. This result can be predicted qualitatively from Figure 11 as well, where it can be seen that, for the two highest HC levels, the greatest ozone levels are produced at HC/NO_x ratios of about 10. Thus a change in NO_x in either direction will tend to lead to a reduction in ozone. However, at an HC/NO_x ratio of 7, a decrease in NO_x only will lead to an increase in ozone.

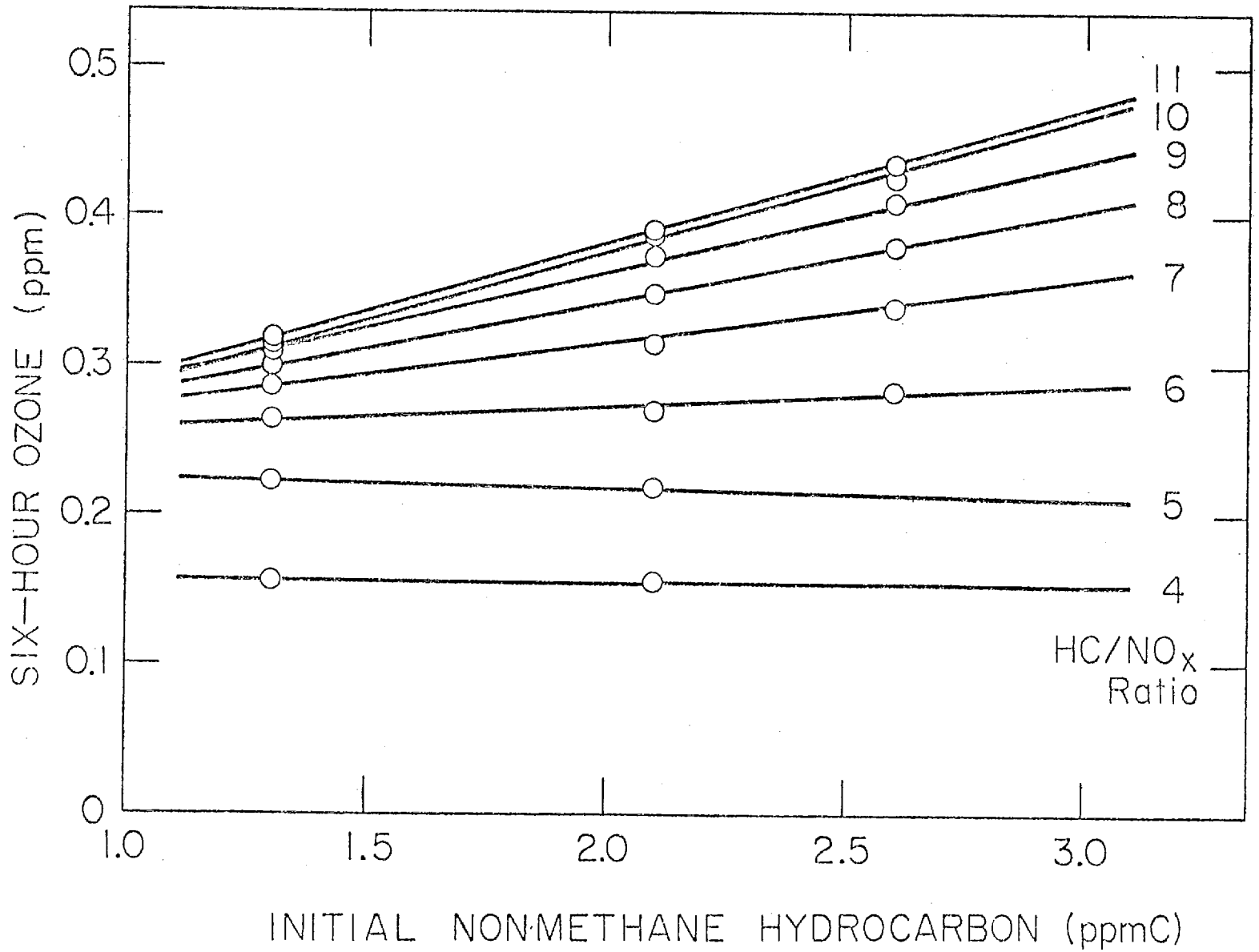

Figure 12. Six-Hour Ozone Concentration as a Function of Initial Nonmethane Hydrocarbon at Various HC/NO_x Ratios.

Table 8. Effects on Ozone Maximum from Early Estimates of Emission Reductions Due to NO_x Retrofit Program for $HC/NO_x = 10$

Case	% Reduction in SCAB Emissions HC	% Reduction in SCAB Emissions NO_x	Concentrations NMHC[#] (ppmC)	Concentrations NO_x (ppm)	Ratio $NMHC/NO_x$	Max Ozone (ppm)	% Change
	0	0	3.00*	0.300*	10.0	.46	-
(a)	0	7	3.00	0.279	10.8	.47	+2
(b)	3	7	2.91	0.279	10.4	.46	0
(c)	3.7	3.3	2.89	0.290	10.0	.45	-2

[#] $NMHC = THC - CH_4$

* LAAPCD Station 001, 8 AM (PST) hourly average, July 25, 1973

Table 9. Effects on Ozone Maximum from Early Estimates of Emission Reductions Due to NO_x Retrofit Program for $HC/NO_x = 7$

Case	% Reduction in SCAB Emissions HC	% Reduction in SCAB Emissions NO_x	Concentrations NMHC[#] (ppmC)	Concentrations NO_x (ppm)	Ratio $NMHC/NO_x$	Max Ozone (ppm)	% Change
	0	0	2.35*	.336*	7.0	.33	-
(a)	0	7	2.35	.312	7.5	.341	+3
(b)	3	7	2.28	.312	7.3	.34	+3
(c)	3.7	3.3	2.22	.325	6.8	.33	0

[#] $NMHC = (THC - 1.35)/1.55$

* LAAPCD Station 001, average of 6-9 AM (PST) averages for July 3 and 24, August 18, and October 4, 1973.

It is of interest to compare the ozone levels predicted from the chamber data with those actually observed on the days used to establish initial conditions. On July 25, 1973, the maximum ozone in Pasadena was 0.48 ppm (instantaneous, uncorrected) at ~12 noon (PST), approximately 4 hours after the air mass passed the Los Angeles area (see Figure 14 in Section III-C) containing 3.0 ppmC NMHC and 0.300 ppm NO_x. For these same conditions in a 6-hour chamber irradiation, an instantaneous maximum ozone value of 0.46 ppm is predicted (Table 8), in very good agreement with the observed maximum ambient ozone level. In view of the fact that the initial NO/NO_2 ratio was 9 in the chamber experiments, but 0.4 (hourly average) for July 25 at 8 AM (PST), and that it would take 1-1.5 hours for the chamber system to reach $NO/NO_2 = 0.4$, the use of these 6-hour chamber experiments to predict ozone levels for areas 4-5 hours downwind of major source areas appears to be validated by our results. Similarly, for the other 4 days in 1973 which were used to establish initial conditions of 2.35 ppmC NMHC and 0.336 ppm NO_x (6-9 AM PST averages), ozone maxima (instantaneous) in Pasadena were 0.44, 0.41, 0.32, and 0.36 ppm. Based on the average initial conditions for these days, the chamber data predict an average ozone maximum of 0.33 ppm. The agreement between experimental (i.e., chamber) and observed (i.e., ambient) absolute values of maximum ozone is such that the previously stated assumption concerning the application of the chamber data to atmospheric conditions seems justified.

Calculations with Additional Surveillance Data--Development of a Generalized Approach. A significant body of additional surveillance data for light-duty motor vehicles operated by the general public and equipped with NO_x retrofit devices were obtained[46] at the time that Governor Brown was facing the decision of whether or not to sign the State Senate bill (SB-41) which would repeal the mandatory NO_x retrofit program for the South Coast Air Basin. Because several data sets were being developed and frequent updating was provided, a more rapid means of calculating the specific effects of various small reductions in NO_x and NMHC emissions was sought. A plot of the percent change in ozone as a function of the percent reduction in NO_x and NMHC (for a range of reductions up to ~10%) was developed and is presented graphically in Figure 13. These data can also be represented by the following equation:

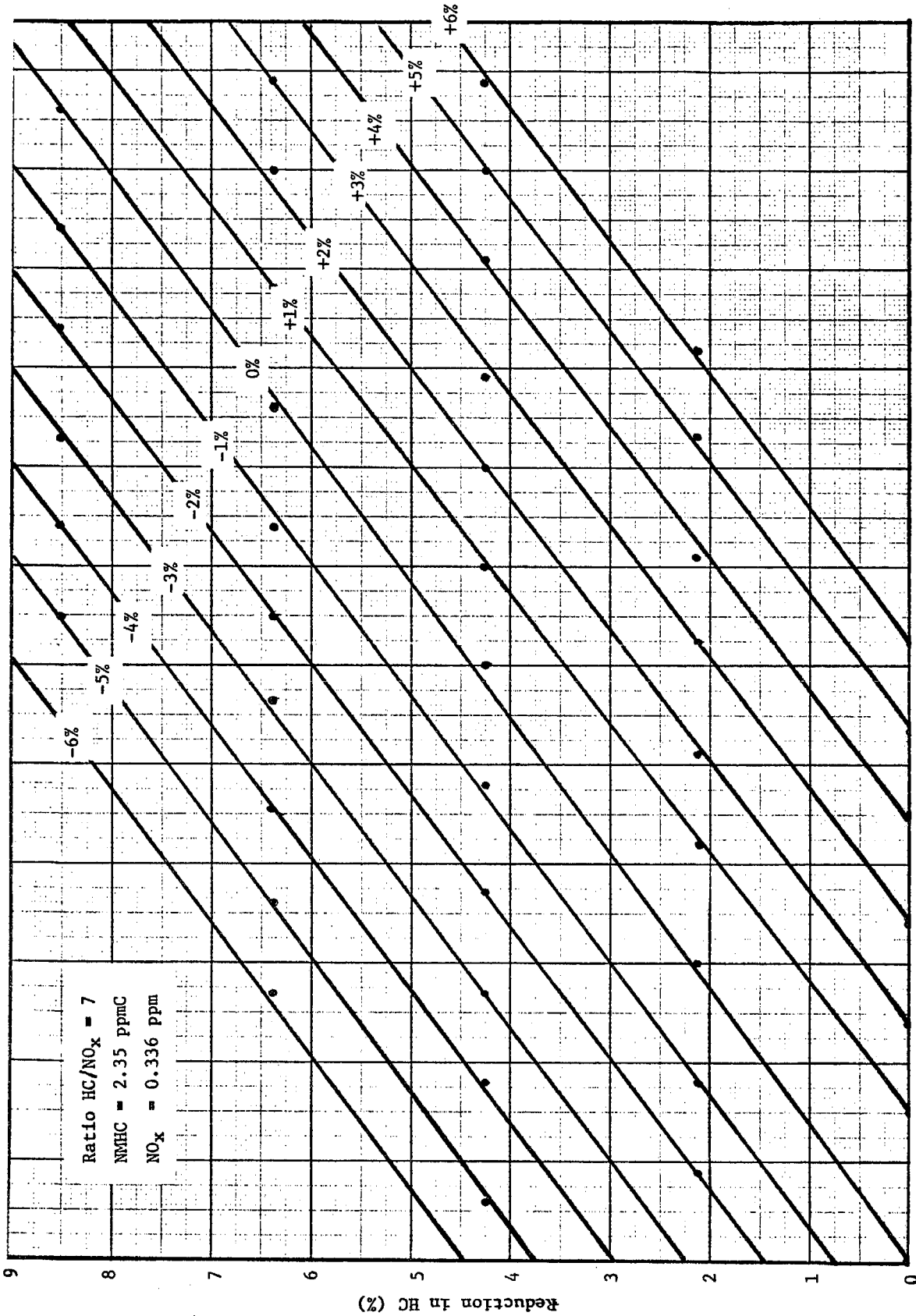

Figure 13. Calculated Change in Maximum Ozone as a Function of Percent Reduction in Initial Nonmethane Hydrocarbon and NO_x.

$$\Delta O_3(\%) = -1.29(\%\ \text{HC reduction}) + 0.96(\%\ NO_x\ \text{reduction})$$

which is taken to apply to locations such as Pasadena (i.e., 4-6 hours downwind from the principal 6-9 AM emission sources).

In collaboration with John Holmes and Frank Bonamassa[47] of the ARB, similar equations were developed for a number of other conditions, specifically for (a) far downwind locations in the South Coast Air Basin (e.g., Upland) by extrapolating our 6-hour chamber data to 10 hours, (b) incorporation of a reactivity "credit" to allow for the fact that exhaust hydrocarbons are generally of high reactivity, and (c) incorporation of a diurnal "credit." The latter corrects the overall emissions reductions estimates (which are based on 24-hour averages of the emission inventory) to account for the fact that 6-9 AM emissions contribute in a disproportionately large way to the formation of ozone downwind later in the day.

The overall equation for far downwind locations in the South Coast Air Basin from extrapolation of the chamber data to 10 hours is:

$$\Delta O_3(\%) = -1.0\ (\%\ \text{HC reduction}) + 0.8\ (\%\ NO_x\ \text{reduction})$$

Ozone changes calculated from this equation were taken to be the smallest reductions in ozone (worst case) to be expected at far downwind locations. Inclusion of the effects of the reactivity and diurnal "credits" noted above led to best-case estimates of the ozone reductions which could be expected for both the 6-hour and 10-hour ozone estimates. The final two columns of Table 10 show the best case and worst case calculated ozone changes for downwind locations corresponding to Pasadena and Upland, respectively, for thirteen different sets of emissions reduction data furnished by the ARB from various NO_x retrofit device test programs.

Conclusions. If only the effect of the NO_x retrofit control strategy is considered and interactions with other concurrent control measures (e.g., new car emission controls, vapor recovery, etc.) are ignored, the major conclusions of this study can be summarized as follows:

(1) In general, a decrease in emissions of nitrogen oxides that is accompanied simultaneously by an approximately equivalent reduction in reactive hydrocarbons should lead to a reduction in ozone levels at all locations in the South Coast Air Basin (SCAB).

Table 10. Oxidant Effects from Retrofit Program for 1966-70 Light Duty Motor Vehicles

CASE (NO. OF CARS)	OUTLIERS	% CHANGE IN RETROFIT VEHICLE EMISSIONS		% CHANGE IN SCAB EMISSIONS		% CHANGE IN OZONE (RANGE)	
						"PASADENA"[a]	"UPLAND"[b]
		HC	NOx	HC	NOx		
1A Original Surveillance (3051)	In	0	-38	0	-4.4	+3.7 to +5.5	-3.5 to -4.6
1B Original Surveillance (2869)	Out	-14	-33	-1.4	-4.0	+1.2 to +2.0	-4.6 to -6.5
2A Accelerated Surveillance (287) (April 15-22)	In	-6	-21	-0.6	-2.5	+1.3 to +1.8	-2.6 to -3.6
2B Accelerated Surveillance (275) (April 15-22)	Out	-20	-20	-2.0	-2.4	-1.8 to -0.3	-3.9 to -5.9
3A Total Surveillance (3338)	In	-1	-36	-0.1	-4.3	+3.4 to +5.2	-3.5 to -4.6
3B Total Surveillance (3144)	Out	-14	-32	-1.4	-3.8	+1.0 to +1.8	-4.4 to -6.3
4 Accreditation Fleet (259)	-	-21	-45	-2.1	-5.4	+1.2 to +2.5	-6.4 to -9.2
5A Proper Installation (178) Accelerated Surveillance	In	-22	-26	-2.2	-3.0	-1.5 to +0.1	-4.7 to -7.0
5B Proper Installation (176) Accelerated Surveillance	Out	-30	-26	-3.0	-3.0	-3.3 to -1.0	-5.5 to -8.3
6A CVS Tests-VSAD (5)	-	-10	-28	-1.0	-3.4	+1.5 to +2.0	-3.7 to -5.2
6B CVS Tests-VSAD (5) with 4° Retard	-	-15	-37	-1.5	-4.4	+1.4 to +2.3	-5.0 to -7.1
6C 7 Mode Tests-VSAD (5)	-	-11	-36	-1.1	-4.3	+2.2 to +2.9	-4.5 to -6.3
6D 7 Mode Tests (5) VSAD with 4° Retard	-	-25	-45	-2.5	-5.4	+0.3 to +2.0	-6.8 to -9.9

[a]Based on 6-hour chamber irradiations. [b]Based on 10-hour chamber irradiations (see text).

(2) A significant reduction in NO_x emissions alone will tend to slightly increase ozone levels in the central and western end of the South Coast Air Basin and tend to decrease ozone levels in the eastern end of the Basin.

The magnitude of these effects will depend on the specific emissions reductions involved, as shown by the data in Table 10.

C. Development of Air Parcel Transport Simulation Experiments Using Trajectory and Diffusion Models

The goal of this subprogram was to provide a basis for designing chamber experiments which would realistically simulate air parcel transport, in locations such as the California South Coast Air Basin, with respect to both injection of fresh oxidant precursors and dilution and dispersion effects. The first step in this development was an investigation of characteristic air parcel histories in the South Coast Air Basin, with special emphasis on an air parcel which followed a trajectory from southeast Los Angeles to Pasadena between approximately 5 A.M. and 12 noon on July 25, 1973, the day of highest oxidant observed in 1973 (0.45 ppm oxidant observed in Pasadena).

In order to carry out this study, three elements are essential; namely, determination of the trajectories, estimation of the air quality within the air mass, and modeling of the diffusion to determine the dilution and fresh pollutant addition rates. Each of these elements is discussed in the following paragraphs. It should be noted here that the basic tool for this investigation was the General Research Corp. (GRC)-DIFKIN computer model,[48] which was altered and expanded as needed to complete the study.

The trajectory of an air mass was determined by numerical interpolation on the meteorological data recorded at the various air monitoring stations within the South Coast Air Basin. The trajectory program was taken directly from the GRC-DIFKIN model. It operates by interpolating on the wind speed and direction reported for the three closest stations to a given point. The weighting of the variables was done either by a $1/r$ or $1/r^2$ weighting factor. In this manner, the wind direction and speed was determined at a given point and used to trace the air parcel trajectory in a forward or backward direction from that point. In this manner, one can determine the trajectory from a given starting point by specifying the meteorological data at the various stations, the geographical location of the starting point, and the time of day. It should be noted that the meteorological data used was obtained essentially at ground level. It is known that transport at higher altitudes occurs at greater speeds than at ground level. This higher altitude transport may be down-mixed with the ground level air masses, thus resulting in higher dilution rates than might be predicted. Accounting for this effect is discussed below.

Having determined the air parcel trajectory, the air quality within that parcel was estimated, using a similar interpolation scheme. In this case, the pollutant concentrations reported at the various air monitoring stations were interpolated by using a similar weighting factor for the three closest stations. The concentration of the various pollutants which are reported was then estimated at specific times of day along the trajectory. In general, this procedure works reasonably well for the following pollutants: carbon monoxide, sulfur dioxide, nitric oxide, nitrogen dioxide, and ozone. It does not work well for nonmethane hydrocarbon (NMHC), since the data for NMHC are reported as total hydrocarbon and methane to the nearest ppm. To obtain NMHC, one must subtract these two large numbers to determine the much smaller nonmethane hydrocarbon concentration. As a result, the accuracy of this determination is generally poor.

To determine the dilution and addition rates for a given air parcel, a diffusion model is needed to account for the transport of pollutants in vertical and horizontal directions. For the GRC-DIFKIN model, which was used in this study, the horizontal turbulent diffusion fluxes, both normal to and along the wind trajectory, are assumed negligible compared to the advection and vertical diffusion. Essentially, the model allows the input of turbulent diffusion coefficients at various altitudes as a function of time of day. In addition, a primary pollutant source inventory, as a function of day and position, is given in the GRC model. This inventory is essentially an extension of the System Applications, Inc. (SAI) inventory[49] for the L.A. Basin in 1968 and yields primary pollutant fluxes on a 2-by-2-mile grid system for oxides of nitrogen, reactive hydrocarbons, and carbon monoxide.

In order to generate a set of diffusion coefficients, which are realistic for the given day being studied, the carbon monoxide air quality estimate was used as a verification test. The diffusion coefficients are first estimated from the temperature gradient data obtained for the particular day of interest. They are then adjusted to yield calculated (from the diffusion model) ground level carbon monoxide concentrations, which compare well with those estimated from the interpolation on the air quality data. Using these time-dependent diffusion profiles, the concentrations of the other primary pollutants, namely NO_x and hydrocarbon, were then determined for the air mass.

The addition rates of fresh pollutants are related to the emissions inventory used for the diffusion model. The dilution rate can also be determined from the results of this model. In general, the accumulation of pollutants within a given air mass is determined by integration of the concentration profile at the beginning and end of the time period under consideration. If the particular air mass of interest is bounded by the ground surface plane, then the incoming mass is determined directly from the source inventory, and the outgoing flux by the difference between the accumulation and the incoming flux. If the lower boundary of the air mass is not the ground plane, then the incoming or outgoing mass flux can be determined by using the Fickian diffusion equation and the turbulent diffusivities assumed in the diffusion model. The term "dilution" indicates that there would be a net reduction in the concentration of primary pollutants in the air mass. This is often not the case for trajectories which remain over areas of high primary pollutant fluxes. Thus, the dilution and/or buildup of pollutants within the air mass is strongly dependent upon the trajectory and the time of day for a given trajectory.

The above analysis for determining the trajectory and air quality for an air mass has been applied to a given trajectory for July 25, 1973. The particular trajectory of interest was started at Pasadena at the time of the peak oxidant level recorded for the day and traced backward to 3:00 PDT for that morning. The actual trajectory is shown in Figure 14, and the ambient air quality profile for NO, NO_2, and oxidant is shown in Figure 15. The hydrocarbon results are also shown in Figure 16, but must be viewed with caution. It is interesting to note that the concentration profiles, as a function of time, are very similar to those produced in a typical smog chamber experiment, and the differences can readily be interpreted in terms of fresh pollutant addition. Note that the NO and hydrocarbons rise in the early morning due to the increased traffic, and, as the sun comes up in the early morning, the NO_2 begins to increase. The traffic falls off at about 9:00-10:00 in the morning, and the NO decreases due to the conversion to NO_2. The NO_2 continues to rise to a peak and then falls off rapidly. During the falloff of NO_2, the ozone rises to its maximum. Unfortunately, for this particular trajectory, the air packet passed over a barrier which was inputted to account for the San Gabriel Mountain range

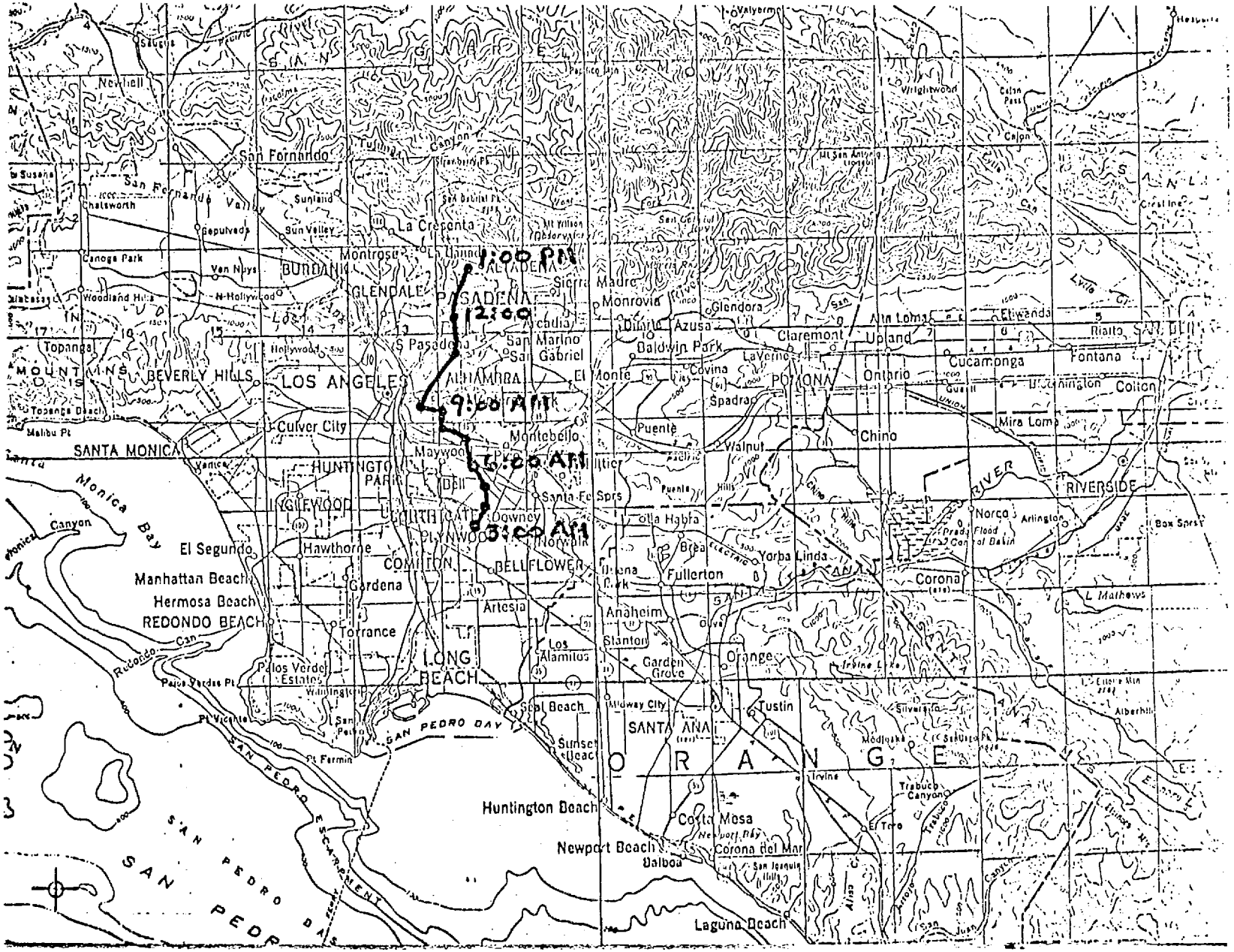

Figure 14. Trajectory Calculated for July 25, 1973, Using Modified GRC-DIFKIN Model.

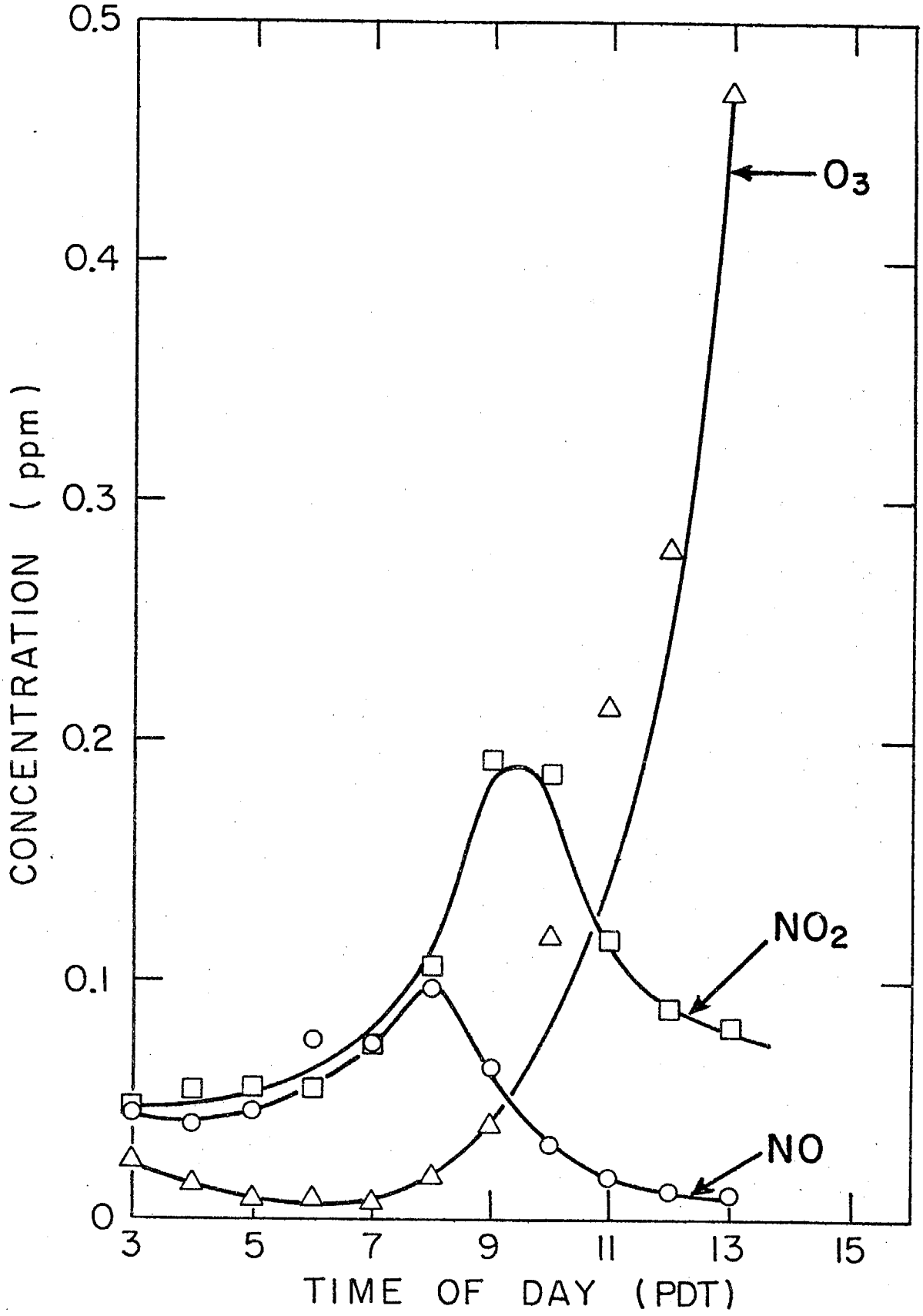

Figure 15. Ambient Air Quality Profiles for NO, NO_2, and Ozone.

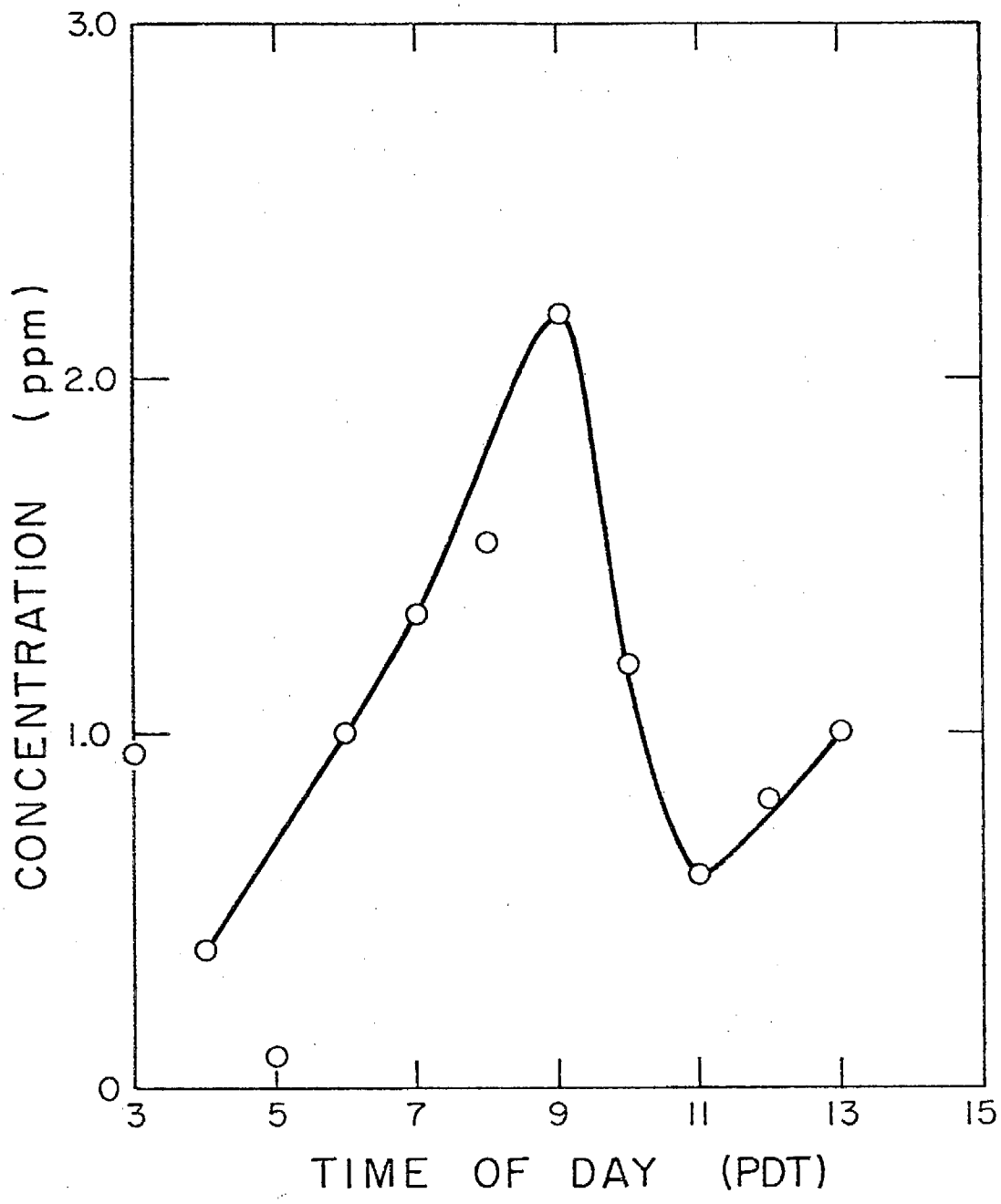

Figure 16. Air Quality Profile for Nonmethane Hydrocarbon.

behind Pasadena just after the peak. Thus, one might assume that the air mass stagnated at that point. Continued analysis is not possible when this occurs.

Figure 17 shows the ground level concentrations of CO as a function of time of day. It is clear that this concentration follows the diurnal variation of traffic, rising to a peak at approximately 9:00 in the morning, falling off just before noontime, and then continuing to rise during the later afternoon. Also shown in Figure 17 is the simulated ground CO concentration predicted by the diffusion model. The earlier falloff of the modeled CO concentration apparently results from the GRC inventory diurnal traffic variation factor being somewhat in error. At the current time, the determination of the dilution rate from the model is not completed so that no further analysis of the CO results can be given. It should be noted that, in other trajectories done to date for which the trajectory could be continued beyond the time of peak ozone, the rapid decline in ozone after the peak is accompanied by a rapid decrease in CO. This might suggest that the decrease in the ozone level beyond the peak is caused by an intrusion of cleaner air via upper altitude transport from the ocean. Further investigation of this point will be made as more trajectories are analyzed.

In the preceding paragraphs, a methodology has been described to analyze the transport of pollutant air masses across an air basin. For a given trajectory, which is determined by interpolation of ground level meteorological data, the ambient air quality is estimated by a similar interpolation procedure using the air quality data. Based on these results, and using the CO concentration history, a diffusion model is generated to allow for the transport of the pollutant in the vertical direction. Using the emissions inventory estimated by GRC and the diffusion model, both dilution and fresh pollutant injection rates can be determined and utilized as a basis for designing realistic chamber experiments simulating full-day irradiation and air parcel transport effects.

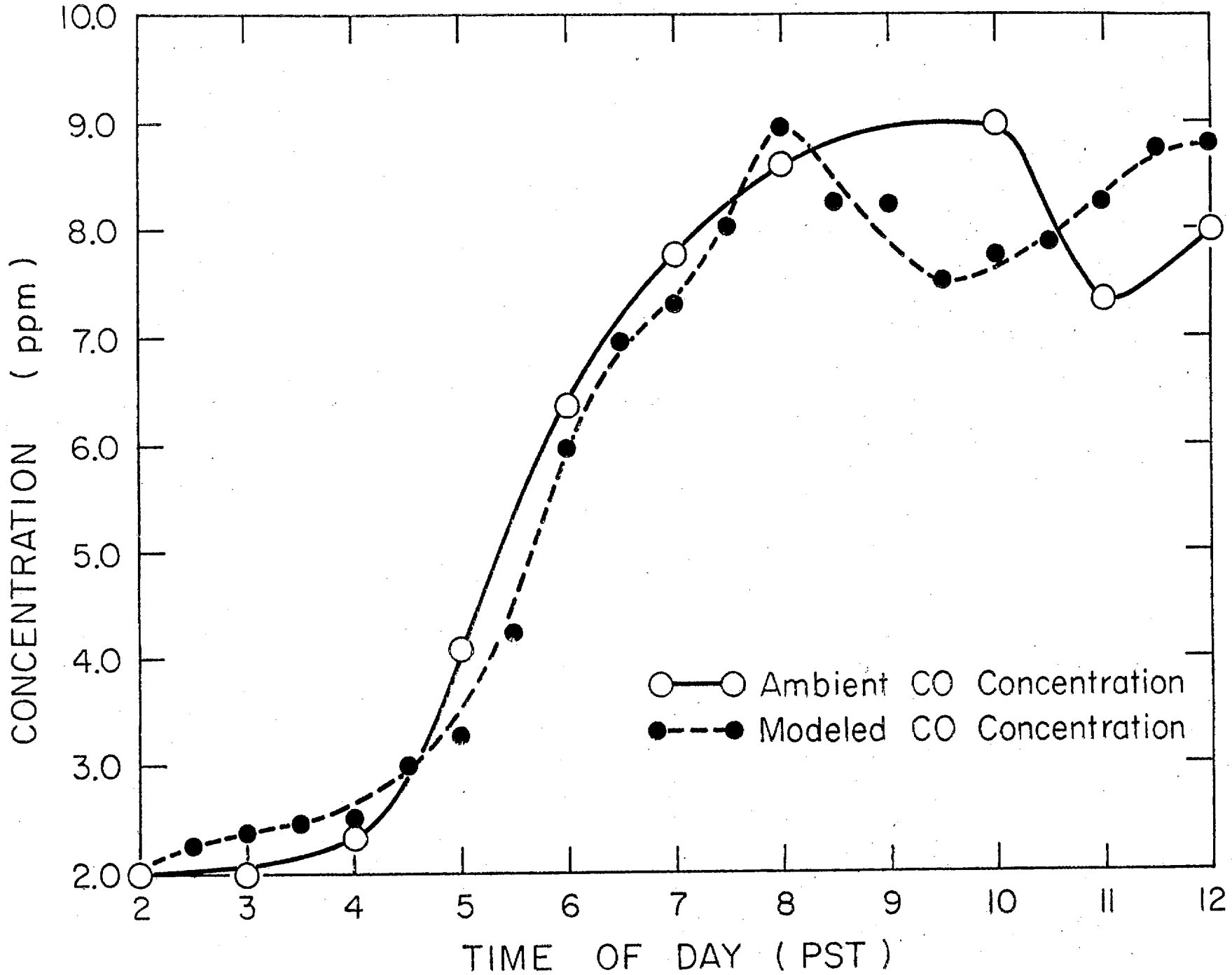

Figure 17. Comparison of Modeled CO Concentrations with the Interpolated Ambient CO Concentration for an Air Parcel Producing High Oxidant in Pasadena on July 25, 1973.

D. Generation and Application of a 9-Hour HC-NO_x-Ozone Data Base and Effects of Aged Smog on the Reduction of Photochemical Oxidants: Added Aldehydes

1. Generation of 9-Hour HC-NO_x-Ozone Data Base

Introduction. Achieving reductions in oxidant formation in regions downwind of major emission sources requires data concerning the oxidant-precursor relationships which occur (a) during long-term (i.e., ~6-10 hrs) irradiation and transport periods, and (b) during multiple-day irradiations of polluted air masses. At the time of the present study, few (if any) smog chamber data relevant to this problem were available. Specifically, most, although not all, published data from previous chamber studies are for irradiation periods of 6 hours, or, in many cases, for 2-4 hours. Accordingly, we have attempted to provide data of utility with regard to assessing the dependence of oxidant formation on initial HC and NO_x concentrations for irradiation periods longer than 6 hours.

Two approaches have been taken. First, we have experimentally generated new O_3-NO_x-HC data for 9-hour or longer irradiations for NMHC and NO_x concentrations corresponding to present ambient levels in the South Coast Air Basin (Section III-A). Second, we have developed methodologies for extrapolating the previously obtained 6-hour SAPRC-ARB data base to periods as long as 10 hours. The purpose of this section is to present the new data and methodologies with a view toward understanding the influences of irradiation period on the interdependencies of absolute NMHC and NO_x concentrations, NMHC/NO_x ratios, and oxidant production. Such an understanding relates directly to a key question posed at the outset of this report--namely, must different views be taken of the problem of controlling oxidant formation in upwind and downwind regions, and, if so, are the different approaches reconcilable?

Extrapolation of the 6-Hour HC-NO_x-Ozone Data Base. Because only a limited number of long-term irradiations have been carried out thus far, we have used the results from these experiments to evaluate methods for extrapolating the data from previous 6-hour runs to longer times. The simplest approach we have taken to estimating 9-hour ozone concentrations was based on a linear extrapolation of the observed 6-hour ozone to 9 hours,

using the observed 5- to 6-hour rate of ozone formation. An estimate of the reliability of this simple extrapolation method may be drawn from data presented in Table 11, which provides a comparison (for those 9-hour, or longer, irradiations conducted to date) of the 9-hour ozone concentration calculated by linear extrapolation (column 5) with that actually observed (column 4). As can be seen from these data, as well as column 6--the ratio of the observed and extrapolated values--for $NO_x \gtrsim 0.3$ ppm, the linear extrapolation works very well (i.e., to within a few percent). For lower NO_x concentrations, the calculated result overestimates the observed 9-hour ozone by amounts varying from 5 to 15%.

A plot of the ratio of the observed to calculated 9-hour ozone concentrations as a function of initial NO_x concentration (Figure 18) suggests that an empirically derived correction factor can be applied to the 9-hour extrapolated ozone values to provide more accurate estimates of the 9-hour ozone levels which would have been achieved in experiments terminated at 6 hours. A limitation of such an approach is that a given (NO_x-dependent) correction factor may not apply at all NMHC concentrations. The majority of the data used in Figure 18 were obtained for initial NMHC concentrations in the range of 1500-2500 ppbC. Although the few points at higher and lower NMHC levels are within the observed scatter, the application of this correction function to the lowest NMHC concentrations investigated during the 6-hour irradiation program should be done with caution.

A second, and considerably more sophisticated approach to extrapolating the 6-hour HC-NO_x-O_3 data base to longer times has recently been developed by G. J. Doyle of our staff. In this approach, the experimental ozone profiles for surrogate runs 10-C to 158-J were fitted to an expansion in orthonormal functions whose coefficients were related to initial NO_x and NMHC concentrations. The resulting regression expressions provide a basis (within specified limitations) for deriving ozone concentrations for any initial NO_x and NMHC concentrations bounded by the experimental data and for extrapolated irradiation times as long as 10 hours. A description of these calculations and the detailed results obtained are presented in Appendix D.

Table 11. Comparison of Experimentally Observed 9-Hour Ozone Values with Those Calculated by Extrapolation of 5- to 6-Hour Values and by Regression.

Surr. Run No.	Initial Concentration NMHC (ppbC)	Initial Concentration NO_x (ppm)	9-Hour O_3 Observed (ppm)	9-Hour O_3 Calculated by Extrap. (ppm)	Obs/Calc (Extrap.)	9-Hour O_3 Calc by Regres. (ppm)	Obs/Calc (Regres)
150-J	2450	.523	.166	.162	1.025	.168	.988
158-J	3120	.430	.295	.297	.993	.338	.873
149-J	2275	.313	.389	.390	.997	.401	.970
117-G	1975	.298	.346	.347	.997	.374	.925
136-J	2410	.271	.394	.411	.959	.434	.908
151-J	2480	.245	.463	.523	.885	-	-
156-J	2230	.206	.419	.462	.907	.454	.923
132-J	1530	.161	.368	.422	.872	.377	.976
122-J	1640	.098	.337	.384	.878	.355	.949
133-J	1580	.097	.326	.355	.918	.352	.926
62-G	746	.096	.281	.325	.865	.269	1.045
48-G	350	.077	.214	.245	.873	.211	1.014
121-J	2430	.056	.290	.306	.948	-	-
134-J	2490	.038	.198	.206	.961	.307	.645
135-J	1480	.037	.218	.230	.948	.234	.932
55-G	1360	.016	.136	.144	.944	.133	1.023

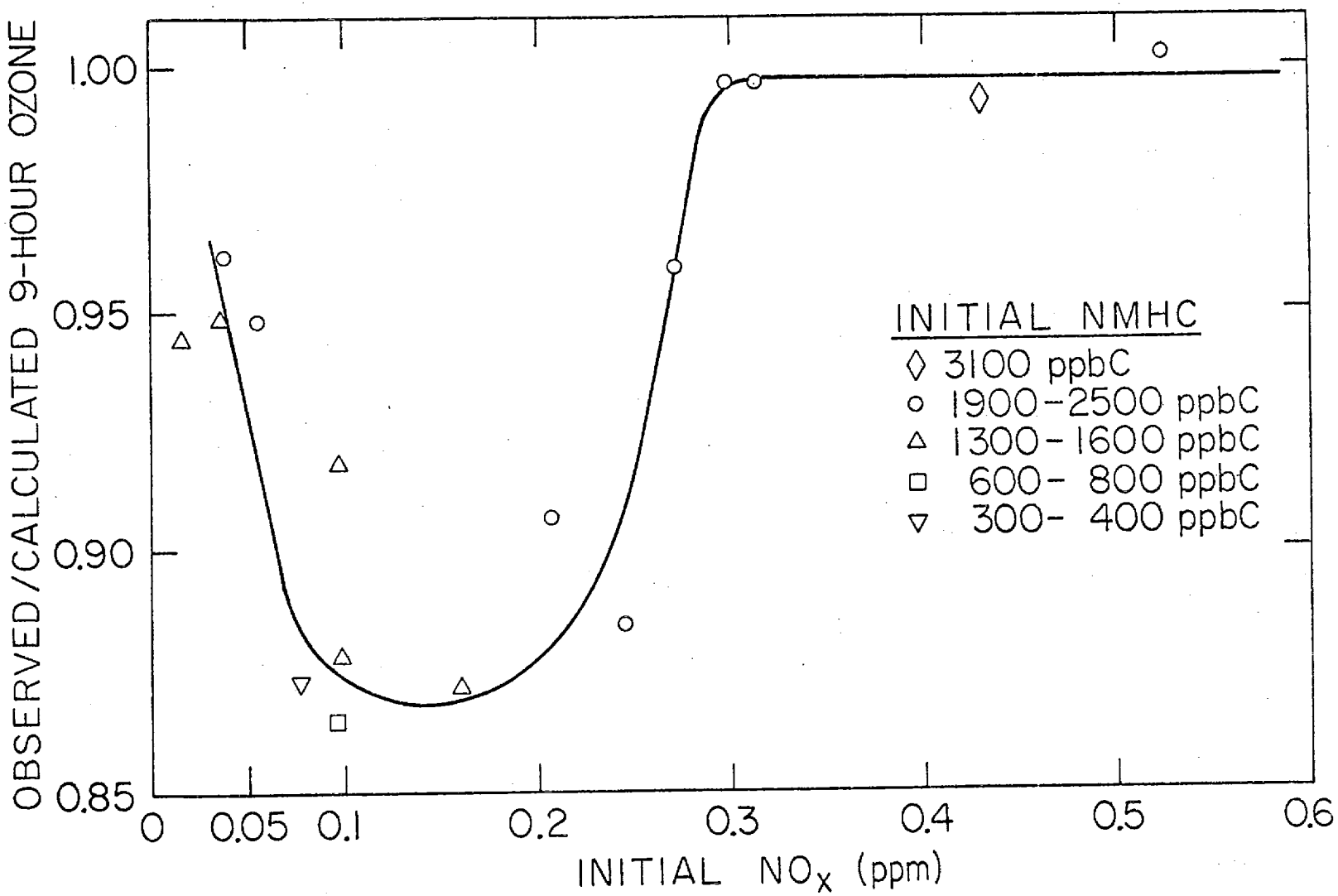

Figure 18. Empirical Correction Function to Be Applied to 9-Hour Ozone Values Calculated by Extrapolation of 5- to 6-Hour Values.

A comparison of the results of the extrapolation to 9 hours, using the regression expressions in Appendix D, to the experimental 9-hour ozone values is shown in columns 4 and 7 of Table 11, and the ratios of calculated and experimental in column 8. With the exception of run 134-J, good agreement was obtained in all cases. Since, however, only a limited number of 9-hour experiments have been performed, and these are limited primarily to the range of initial NMHC concentrations from 1500-2000 ppbC, a further test of the regression analysis method was performed. Specifically, using the initial experimental NO_x and NMHC concentrations from approximately 60 surrogate experiments, the 6-hour ozone concentration was predicted using the regression expressions as discussed. These calculated values are shown as a transparent overlay in Figure 19 and can thus be readily compared to the experimentally observed 6-hour ozone values plotted for the same experiments in Figure 20.

On the basis of the results obtained for the regression expression extrapolation, it appears that this method is of sufficient accuracy and generality that it can be used with some degree of confidence to extrapolate the body of the 6-hour experimental ozone data obtained in this program to time periods between 6 and 10 hours. As a specific case, we have calculated the 9-hour ozone concentrations for some 60 sets of initial NMHC and NO_x concentrations (corresponding to 60 experimental runs), and these values are shown in Figure 21.

Maximum Ozone Levels as a Function of Transport Time. The need for an HC-NO_x-O_3 data base valid for irradiation periods corresponding to air parcel transport to the downwind regions of an air basin has already been demonstrated in Section III-B above, where such data were required for an assessment of the impact of the NO_x retrofit program for 1966-70 light-duty motor vehicles on areas in the eastern portion of the South Coast Air Basin. In this and the following sections, we consider further implications of the effect of irradiation period.

The problem of determining the reductions in NMHC and NO_x levels necessary to achieve maximum reduction in ozone levels is made considerably more complex when one takes into account the irradiation time experienced by the pollutant mass which is to be controlled. This is illustrated in Figure 22, where maximum ozone concentrations after 1, 4, 6, or 9 hours of

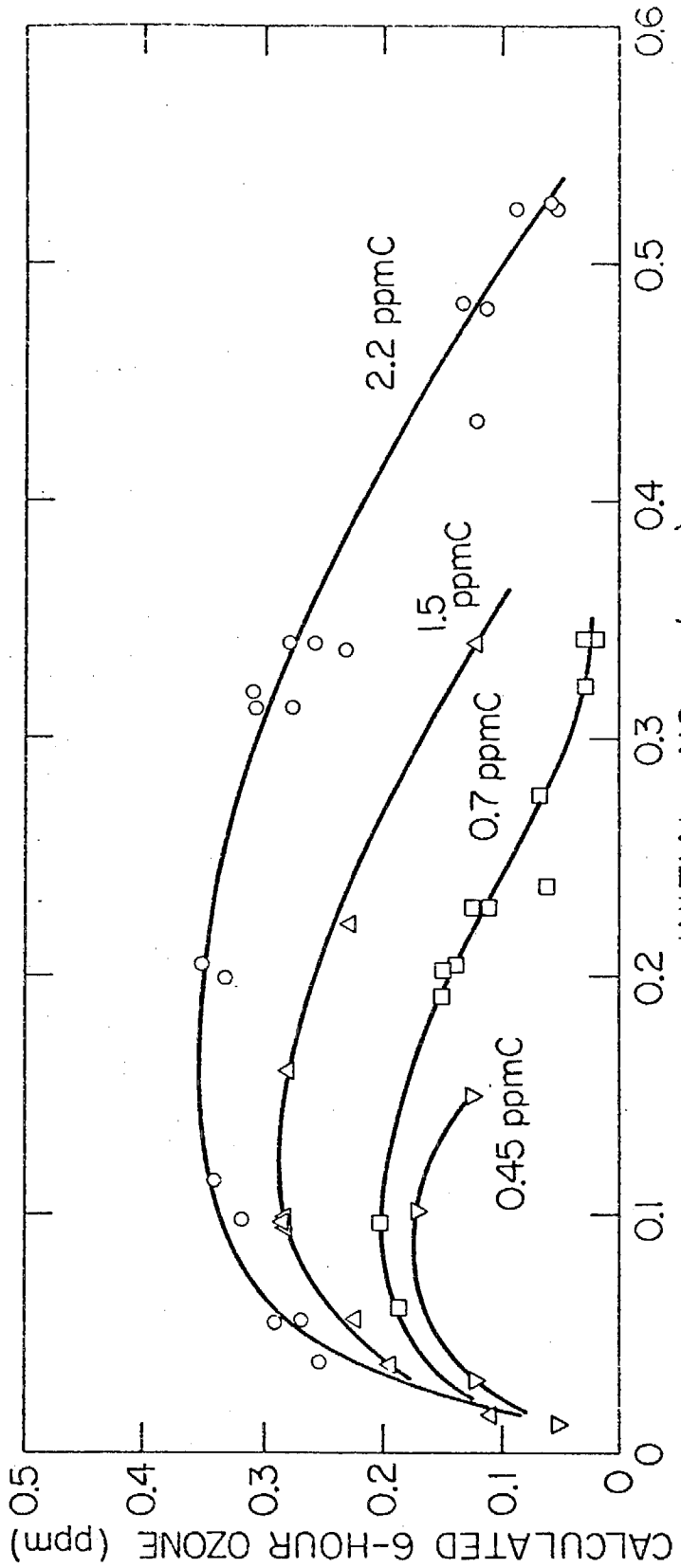

Figure 19. Six-Hour Ozone Concentrations Calculated Using Regression Functions vs. Initial NO_x at Various Nonmethane Hydrocarbon Concentrations (Compare with Figure 20).

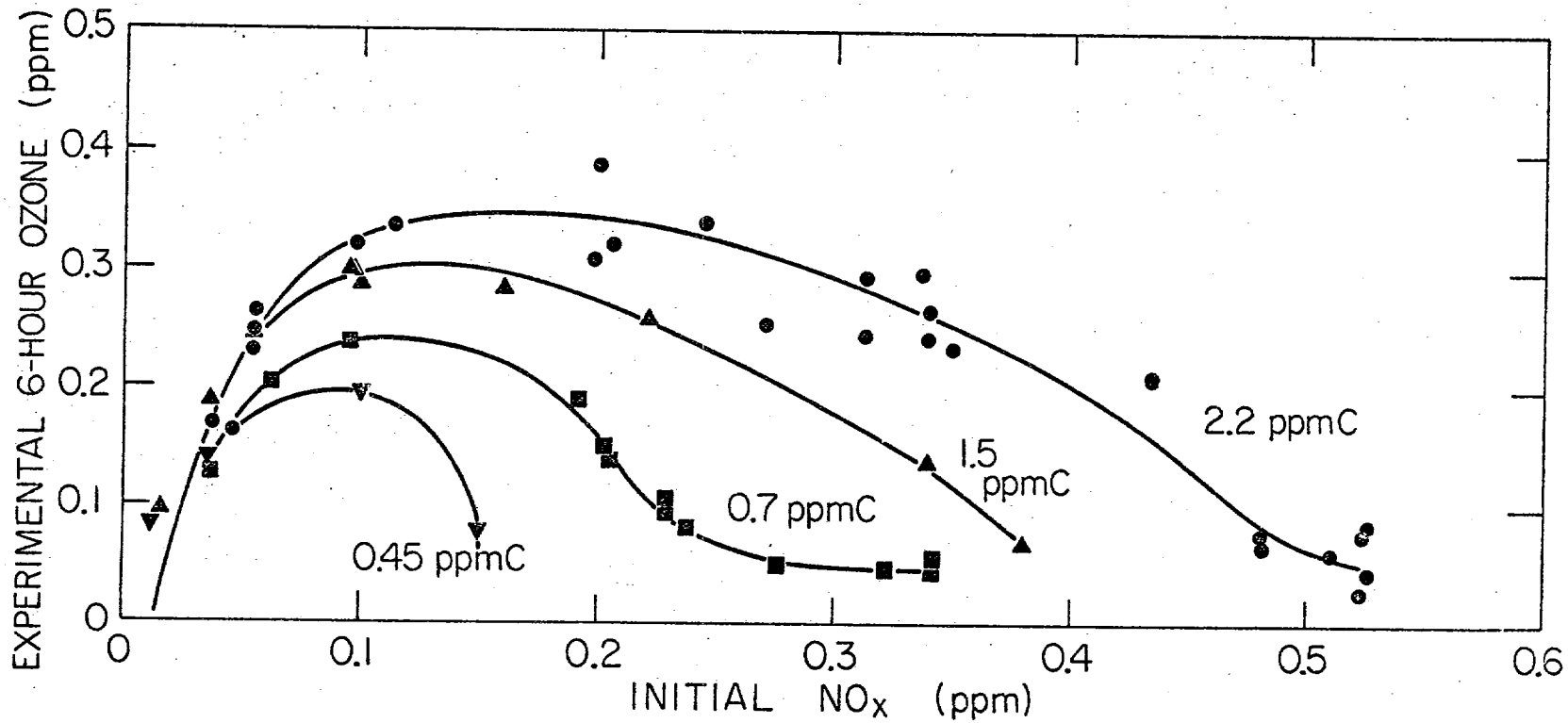

Figure 20. Experimentally Observed 6-Hour Ozone Concentrations as a Function of Initial NO_x at Various Nonmethane Hydrocarbon Levels.

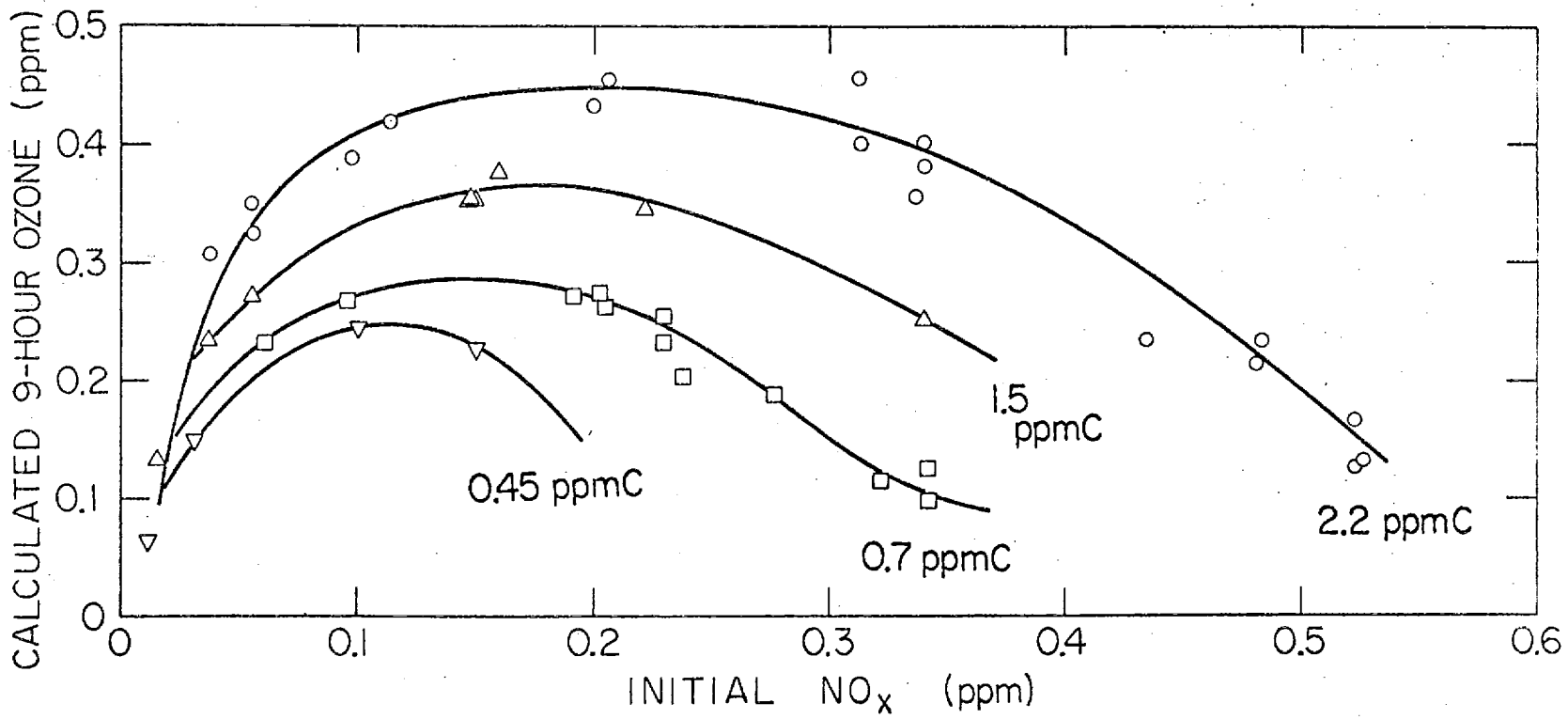

Figure 21. Nine-Hour Ozone Concentrations Calculated Using Regression Functions vs. Initial NO_x at Various Nonmethane Hydrocarbon Concentrations.

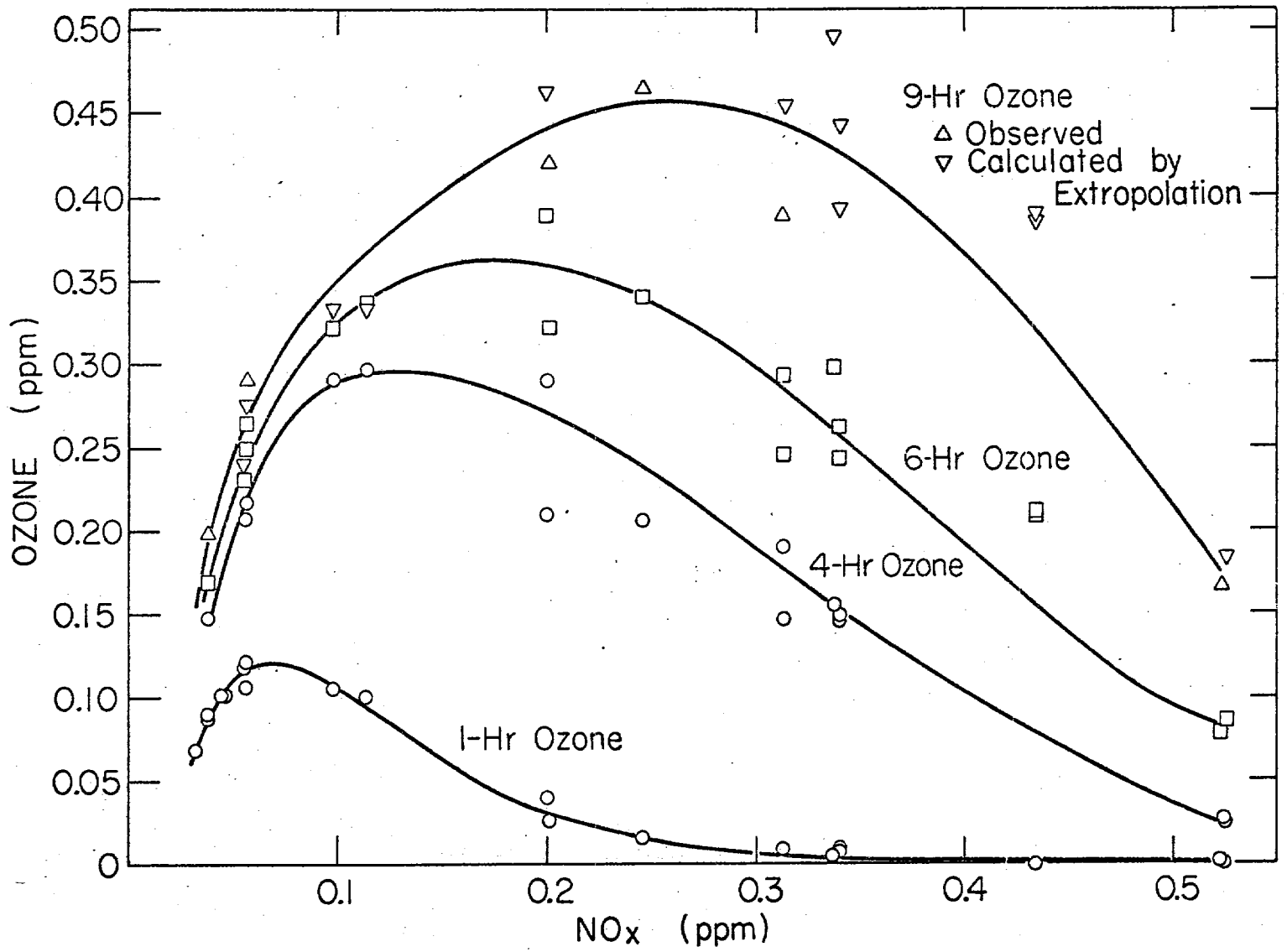

Figure 22. Maximum Ozone Observed During 1-, 4-, 6-, and 9-Hour Chamber Irradiations as a Function of Initial NO_x for Initial NMHC of 2.2 ppm.

irradiation are plotted as a function of initial NO_x for initial NMHC 2.2 ppmC. The 9-hour data include both the current experimental values as well as those calculated from previous 6-hour runs by the linear extrapolation method described above. It is apparent that at least three factors must be considered here: (a) the absolute ambient concentrations of primary pollutant NMHC and oxides of nitrogen, (b) their relative amounts, i.e., the NMHC/NO_x ratio, and (c) irradiation time. For example, inspection of Figure 12 indicates that, for any given irradiation period, the relationship of ozone formation to precursor levels may be divided into two regions: (a) at low NO_x levels and high NMHC/NO_x ratios ($\gtrsim$ 20), increasing NMHC does not appear to affect the rate of ozone formation significantly, and (b) at high NO_x levels and low NMHC/NO_x ratios ($\lesssim$ 3), increasing NO_x does not appear to increase the rate of ozone production appreciably (see 0.7 ppm HC isopleth in Figure 20). A third region is apparent from Figure 22; namely, at intermediate NO_x and NMHC levels (NMHC/NO_x ratios ~5 to ~15), the greatest ozone levels occur at an NMHC/NO_x ratio determined largely by the irradiation period.

Hydrocarbon Composition as a Function of Irradiation Time. A further aspect in considering effects resulting from longer irradiation periods concerns the changing hydrocarbon composition of an air mass as the more reactive hydrocarbons are preferentially depleted with respect to less reactive compounds. Figure 23 illustrates this effect for selected components of the surrogate mixture. After some 7 or 8 hours of irradiation, a representative alkene (propene) and aromatic (m-xylene) have been almost entirely consumed, while the less reactive n-butane and toluene remain in substantial concentrations. Thus, in the later stages of this 12-hour irradiation, the alkane and aromatic are contributing to the continued ozone production. The implications are obvious for air parcel transport in the ambient atmosphere during the season around the summer solstice, when 11-14 hours of daylight are experienced.

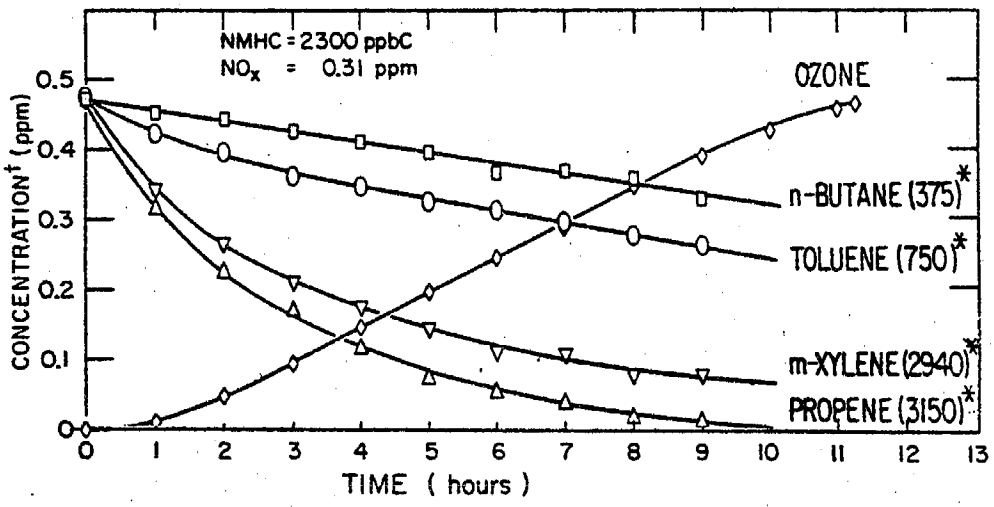

†Not corrected for dilution due to sampling.

*Reactivity relative to methane from SAPRC reactivity scale (Darnall, Lloyd, Winer, and Pitts).[50]

Figure 23. Concentration of Selected Hydrocarbons and Ozone During Long-Term Irradiation of Surrogate Mixture.

2. Added Aldehyde Experiments

Aldehydes occur in the atmosphere both as primary emissions and as the result of atmospheric photochemistry. The scientific literature prior to 1970 concerning the modes of formation, levels of occurrence in the atmosphere, effects, and methods of measurement of aldehydes has been reviewed.[51,52]

Formaldehyde (HCHO) is particularly important because its absorption spectrum extends well into the actinic ultraviolet region. The photodecomposition of HCHO can proceed by both a radical path and a molecular path[53] as shown

$$HCHO + h\nu\,(\lambda < 3700\ \text{Å}) \begin{cases} \longrightarrow H + CHO \\ \longrightarrow H_2 + CO \end{cases}$$

The relative and absolute importance of these two paths is still not definitively decided, since there have been differing reports concerning the quantum yields for these two reactions in the actinic ultraviolet region.[54,55] Nevertheless, it seems clear that HCHO photolysis in air will lead to the formation of hydroperoxy radicals (HO_2) via

$$H + O_2 + M \rightarrow HO_2 + M$$

and

$$CHO + O_2 \rightarrow HO_2 + CO$$

Aliphatic aldehydes will also photodissociate[53] to give formyl radicals (CHO) and hence are also a source of HO_2. Thus, aldehyde photolysis drives the important HO_2-OH chain mechanism by the above reactions and

$$HO_2 + NO \rightarrow OH + NO_2$$

leading to the oxidation of NO and hydrocarbons via OH attack. Demerjian, Kerr and Calvert have recently computer modeled[56] the importance of aldehyde photolysis in photochemical smog using data from experimental studies by Bufalini and Brubaker[57] (photooxidation of HCHO) and Dimitriades and Wesson[58] (reactivities of exhaust aldehydes).

As stated by Demerjian, Kerr and Calvert, the number of available rate studies for added aldehydes at low concentrations in irradiations of

$HC-NO_x$ systems under simulated atmospheric conditions is very limited. In fact, only Dimitriades and Wesson's data were suitable for their purposes.[58]

In the present study, irradiations of the standard surrogate mixture (2450 ppbC nonmethane HC, 0.33 ppm NO_x, 7.0 ppm CO, and 2.8 ppm CH_4) were carried out at several initial formaldehyde concentrations. The quantitative effects of increasing HCHO on both initial rates of reaction and on 6-hour ozone levels are summarized in Table 12. Clearly, the reactivity of the mixture is enhanced with higher initial HCHO levels as seen by the increased initial rates of NO oxidation and ozone formation, and substantially higher ozone levels at 6 hours. The 6-hour ozone concentration as a function of HCHO is shown graphically in Figure 24. An experiment carried out with acetaldehyde (CH_3CHO) instead of HCHO gave comparable results.

The effect of added HCHO on ozone levels throughout a series of 9-hour irradiations of the $HC-NO_x$ surrogate mixture is shown in Figure 25. The enhancement in ozone production is striking. The detailed initial conditions and reactivity parameter data for each of the added aldehyde experiments (Runs 140-148) are given in Appendices A and C. Such data should prove useful in further computer model validation studies of the type reported by Demerjian, Kerr, and Calvert. The experimental results obtained here and in previous studies, such as that by Dimitriades and Wesson, leave little doubt that the occurrence of aldehydes in the atmosphere, whether from emission sources or as products of chemistry in the polluted atmosphere, will lead to enhanced photochemical smog manifestations.

Table 12. Selected Reactivity Parameters for Standard Surrogate Experiments with Varying Initial Aldehyde Concentrations

Run No.	Initial HCHO (ppm)	Initial NMHC (ppbC)	Estimated Time to NO = NO_2 (min)	Time to O_3 = 0.08 ppm (min)	Maximum 1-Hour Average Ozone for 6-Hour Irradiation (ppm)
140	0	2417	80	240	-
141	0	2374	75	234	.155
143	0	2323	67	219	-
146	.004	2297	70	224	-
147	.040	2307	73	223	-
144	.038	2329	63	192	.192
149	.091	2275	47	162	.222
142	.162[a]	2796	45	131	.317
145	.185	2570	42	122	.319
148	.255	2460	27	74	.452

[a] CH_3CHO added instead of HCHO.

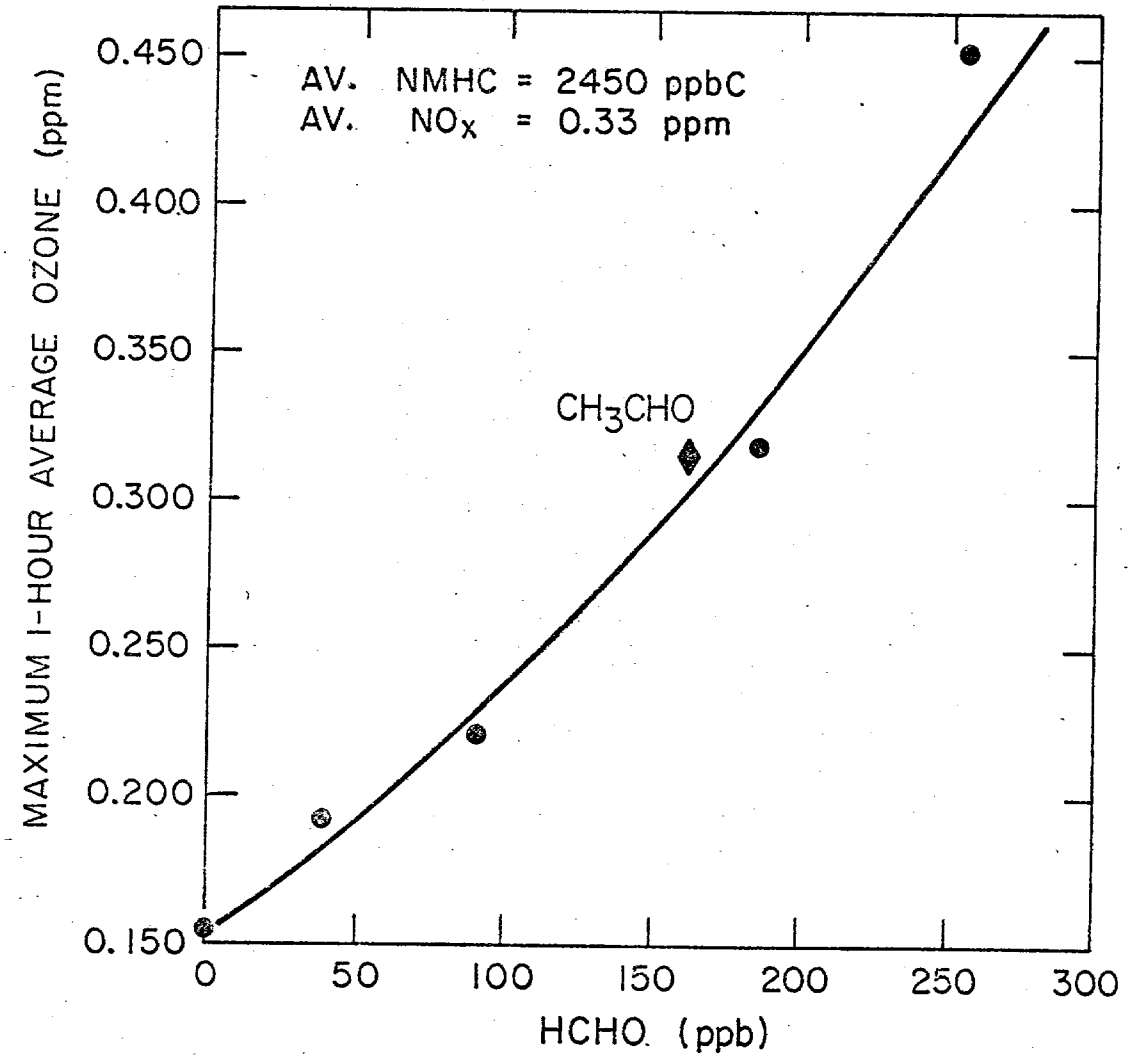

Figure 24. Effect of Added HCHO on Six-Hour Ozone Concentration During Irradiation of Surrogate Mixture

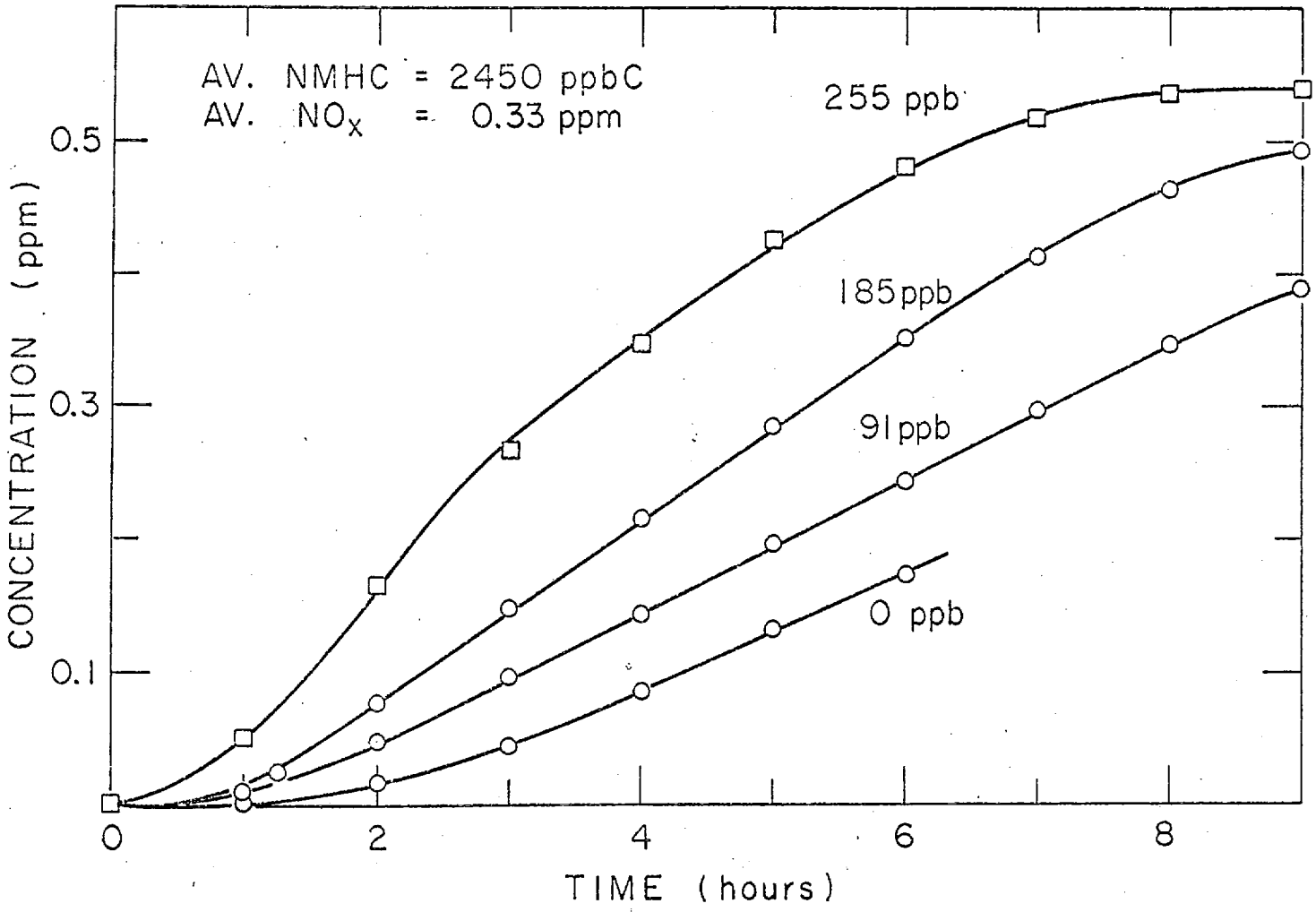

Figure 25. Effect of Added HCHO on Ozone Formation in Long-Term Irradiations of Surrogate Mixture

E. Investigation of the 2% Neutral Buffered Potassion Iodide Method for Ozone

The accurate measurement of ozone concentrations is critical to the development of any new major HC-NO_x-O_3 data base, such as the one being generated in this research program. This is true, not only for the interpretation of the oxidant-precursor relationships which may be developed in such a program, but also with respect to the application of such data to assessments of ongoing or proposed control strategies. In June 1974, at a time when a major body of data relating ozone production to initial HC and NO_x levels had already been generated in this chamber program, it was disclosed by the California Air Resources Board (ARB) and the Los Angeles Air Pollution Control District (LAAPCD) that a significant discrepancy (approximately 30%) existed between ozone concentrations measured by their respective calibration procedures. Inasmuch as the 2% neutral buffered potassium iodide (NBKI) method for determination of ozone (i.e., the ARB method) had been employed in our laboratories in the calibration of ozone monitors used in our HC-NO_x-O_3 research program, we felt that it was critical to understand the implications of this discrepancy for our data.

Having the appropriate resources, personnel, and experience, we undertook an investigation of the stoichiometry of the 2% NBKI method at ambient concentrations of ozone using long-path infrared (LPIR) spectroscopy. This investigation consisted of three subprograms. First, a determination of the absolute absorptivity of the 9.6-micron band of ozone as a function of both spectral resolution and abundance, since such data have not been previously reported and, therefore, were not available to us. Second, we have investigated the correlation between the 2% NBKI method and the infrared absorption of ozone over a concentration range from 0.1-1.2 ppm by means of an *in situ* study in the SAPRC 5800-liter evacuable environmental chamber, which had been constructed with ARB support. Finally, SAPRC staff members have analyzed the implications for the historical oxidant data base in the South Coast Air Basin of placing the data obtained by both the LAAPCD and the ARB on a common calibration basis.

In the remainder of this section, we will present the results of the experimental studies carried out in our investigation of the 2% NBKI method. The implications of correcting the South Coast Air Basin oxidant data base, on the basis of our experimental results and those of the ARB Ad Hoc Oxidant

Committee, are presented in Section III-F. Portions of the work described below were conducted as adjuncts to research being carried out for both the California Air Resources Board and the National Science Foundation--Research Applied to National Needs (NSF-RANN). Subsequently, reports of all phases of this research have been accepted for publication in refereed journals, but have not yet appeared in the literature. Thus, the following results and discussions are excerpted from the refereed reports of our work.

1. Determination of the Infrared Absorptivity of the 9.6 Micron Ozone Band as a Function of Spectral Resolution and Abundance[59]

Introduction. The absorptivity of ozone in the ultraviolet has been accurately determined by a number of workers.[60-63] However, in the infrared, we have found that the published data refer to the integrated absorption,[64,65] or statistical band model parameters.[66-68] The only published absorptivity, that of Hanst, Stephens, Scott, and Doerr [HSSD],[69] is applicable only to a limited range of conditions. We have thus found it necessary to determine the absorptivity of the ozone ν_3 R-branch maximum as a function of spectral resolution and abundance. The data presented here will be useful and accurate for a wide range of commonly encountered experimental parameters.

Experimental. Known volumes of ozone were prepared in the apparatus diagrammed in Figure 26. The design was similar to those given by Birdsall et al.[70] and HSSD.[69] The ozonizer (205-ml internal volume) was thoroughly flushed with oxygen (Liquid Carbonic, industrial grade) for several minutes before the stopcocks were closed, trapping a known volume of the gas. The silicone oil manometer was checked until no pressure change was observed for a period of several minutes. Then 17,000 volts (a.c.) were applied to the ozonizer for 90 seconds after the constant temperature bath was unplugged (to avoid grounding the high voltage through the bath). After turning off the high voltage, the amount of ozone produced by the reaction

$$3\ O_2 \rightarrow 2\ O_3 \qquad (1)$$

was determined by measuring either the pressure or the volume decrease of the gas in the ozonizer.

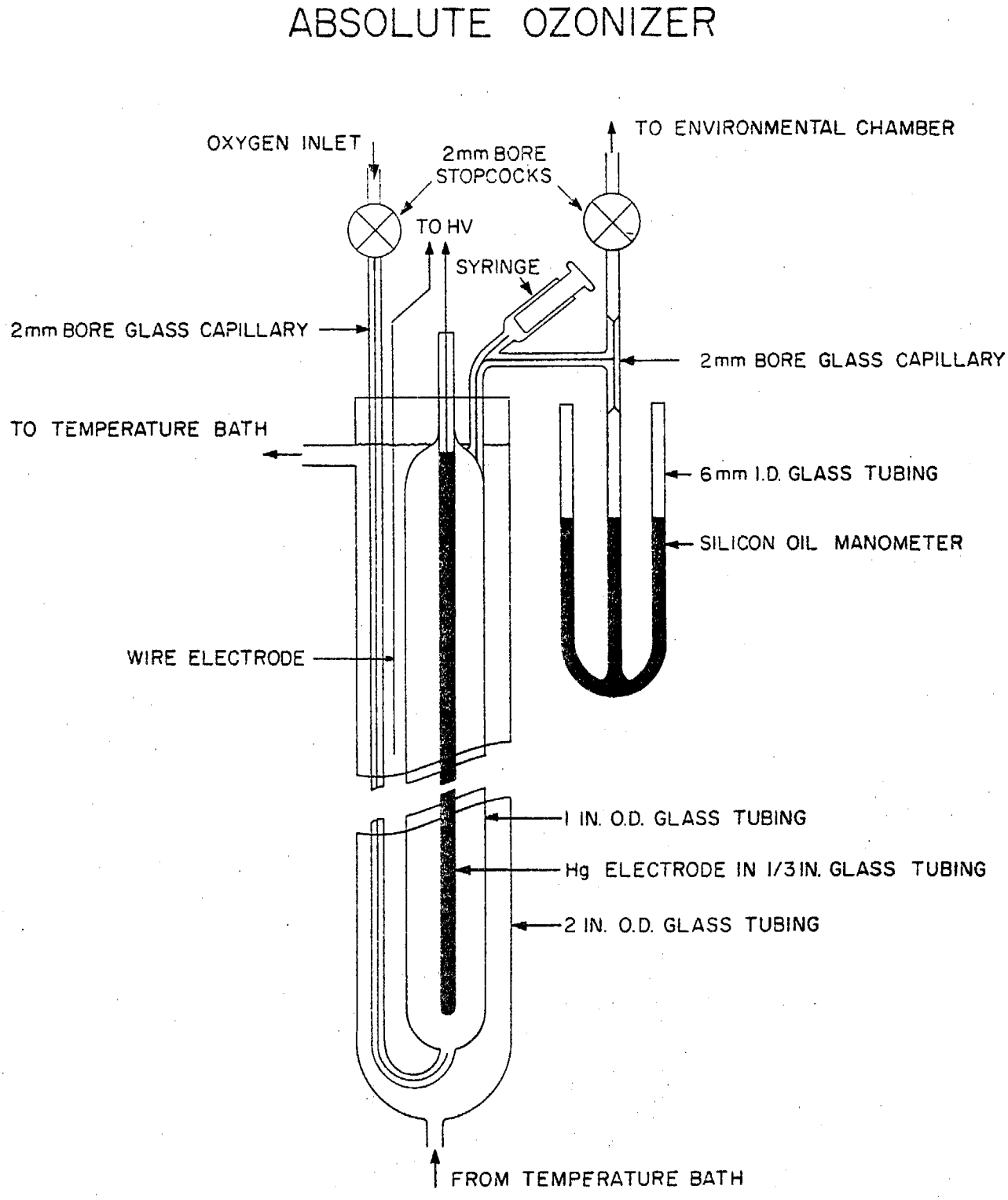

Figure 26. Diagram of the Absolute Ozonizer.

The pressure decrease was measured without a change in volume by withdrawing a glass rod from one of the legs of the silicone oil manometer so that the center column of oil remained at a constant level. The pressure difference was read between the two legs without the glass rod. Typically, the manometer deflection was about 13 cm of oil with an uncertainty of, at most, ±0.03 cm on each leg.

In the alternate method, the volume decrease was measured without a change in pressure by adjusting the 5-ml gas syringe shown in Figure 26, such that the manometer was kept at zero pressure difference. The typical volume decrease was about 2.6 ml, read to an uncertainty of about ±0.05 ml. Therefore, we consider the pressure-change measurement to be the most accurate and thus have used the volume-change method only as a confirmatory check on the results. In all cases, thermal equilibrium in the sample was established within 30 to 40 minutes after ozonization.

The ozone-oxygen mixture was introduced into the SAPRC 5800-liter evacuable environmental chamber[24] by flushing the ozonizer with oxygen at a flow of 1 ℓ min^{-1} for 5 minutes. The mixing of the ozone with the dry chamber air was monitored at each end of the chamber by commercial UV ozone analyzers (Dasibi). Approximately one hour was required for complete mixing of the ozone. Since, during this period, the ozone was continually being destroyed at a measurable rate by contact with the chamber walls, the decay of each sample was also monitored by these ozone analyzers. From these data, a decay constant (half-life) was determined for each sample over a period of several hours, both during and after recording infrared spectra. Half-lives between 15 and 22 hours were observed; the slower decays occurred in the later experiments due to conditioning of the chamber walls. The ozone concentration in the chamber at the time of the recording of each spectrum was determined by applying the first-order decay law to the amount of ozone initially measured in the ozonizer at the time of the sample introduction. Typically, spectra were taken during the interval between 1 and 2 hours after the ozone was flushed into the chamber.

Infrared spectra of the 9.48-micron absorption maximum were obtained by using a 1.33-meter baselength White cell incorporated into the environmental chamber. The spectrometer consisted of a Nernst glower source, a one-meter scanning monochromator (Interactive Technology, Inc. CT103)

employing a 75 gr/mm grating blazed at 8.0 microns, and a mercury-cadmium-telluride detector (Santa Barbara Research Center, 2 mm X 0.5 mm, D^* = 7.4 X 10^9) operated at liquid nitrogen temperature [the spectrometer is described more fully below].

All spectra of the ozonizer samples admitted to the chamber were taken at a path of 69.17 meters with the monochromator entrance and exit slits set at 0.75 and 1.75 mm, respectively. The spectral region from 8.80 and 9.70 microns was scanned at 0.2 microns min^{-1} with a time constant of 1.0 second and a 6 dB/octave roll-off. These conditions give about 3.5 time constants per resolution element, which are quite sufficient for good photometric accuracy. A sample spectrum and background are given in Figure 27. All spectra were normalized on the chart recorder at the spectrally clear wavelength of 8.822 microns, thus assuring the applicability of the background (I_0) to all of the ozone spectra (I) without ordinate correction. The signal-to-noise ratio for all spectra was approximately 1000. The completely detailed procedure used for measuring and reducing the infrared data is given below (Section III-F-2).

The effect of spectral resolution on the ozone absorbance at 9.48 microns was determined by an extensive series of measurements at torr pressures of ozone in dry air in a 6-cm path-length cell. A Perkin-Elmer Model 621 spectrophotometer was used to obtain data with a slit width ranging from 200 to 2500 microns [spectral slit from 0.9 to 9.9 cm^{-1}][71] and fractional absorptions from 0.09 to 0.48. The decay of the ozone in the cell was monitored by repeated measurements at a given set of experimental conditions throughout the experiment.

Since the study of resolution vs. absorbance was performed on an instrument that could only be set with equal slits (i.e., triangular slit function), we felt it necessary to verify the theoretical contention that, for a given spectral slit (i.e., entrance slit X exit slit = constant), the measured absorption is independent of slit shape. For entrance slits ranging from 0.750 to 2.128 mm and exit slits from 0.750 to 1.285 mm, the standard deviation of the absorbance for a given sample was only 1.2% at 0.48 microns. Therefore, the extrapolation of the data from triangular to trapezoidal slit function is certainly valid for the conditions of this study.

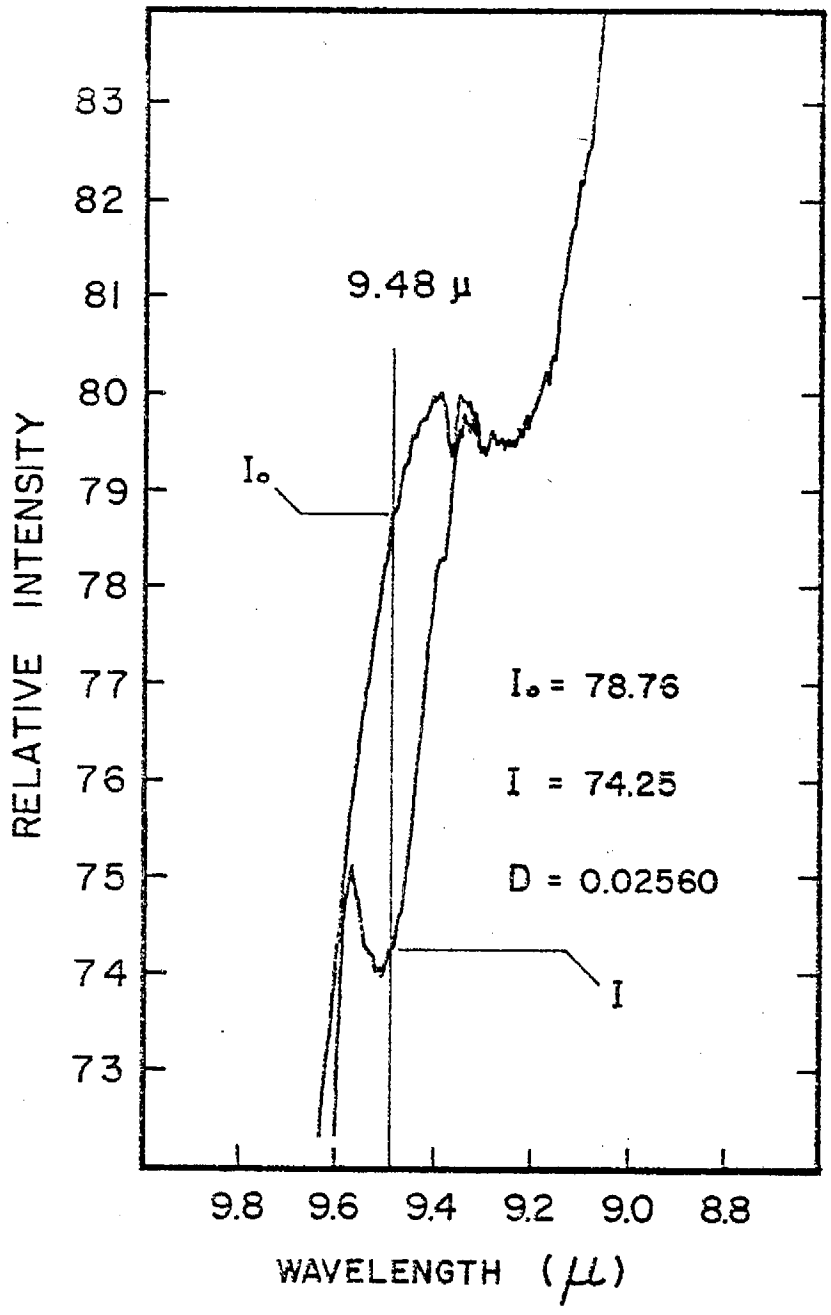

Figure 27. Typical Spectrum at the ν_3 R-Branch of Ozone. The actual Absorption Peak (Indicated by the Vertical Line at 9.48 Microns) Is Not Coincident with the Apparent Peak Due to the Slope of the I_o Line.

The validity of the Beer-Lambert absorption law to the R-branch maximum was tested by using a "high" (4.7 ppm) concentration of ozone in the chamber, and recording spectra as a function of optical path-length. Care was taken to include the small range of absorbances measured for the ozonizer samples.

Results and Discussion. The absorptivities determined from the spectra of the ozonizer samples are listed in Table 13. The absorptivities are given in both $ppm^{-1}\ m^{-1}$ RTP (735 torr, 25°C) and cm^{-1} STP units. The mean and standard deviation for all of the data are $(4.23 \pm 0.04) \times 10^{-4}$ $ppm^{-1}\ m^{-1}$ RTP and $4.61 \pm 0.04\ cm^{-1}$ STP. Since this value is approximately 13% greater than that of HSSD (3.74×10^{-4} $ppm^{-1}\ m^{-1}$), we endeavored to determine the experimental parameters that would cause such a disagreement.

It is well known that the measured absorbance of a given spectral feature at specified conditions at a single frequency is dependent on the spectral resolution.[72] However, quantitative determinations of this effect have been limited mainly to single lines.[73] The magnitude of this effect over several lines is related to the density and distribution of the unresolved fine structure and to the portion of the gross spectral feature encompassed in a resolution element. In comparing the result[69] of HSSD to the present work, we can ignore the effect of the fine structure, since the absorbing species is the same. Since HSSD used a prism spectrometer to obtain their data and we have used a grating monochromator, there is good reason to believe the respective spectral resolutions were quite different, hence different fractions of the R-branch were included. In searching for a way to estimate spectral resolution, we discovered a linear relationship between the ratio of the absorbance minimum between the R and Q branches of the 9.6-micron ozone band (D_{valley}) to the absorbance of the R-branch maximum (D_{peak}). This ratio is designated $R_{v/p}$ and is defined as

$$R_{v/p} = \frac{\log_{10}(I_0/I)_{valley}}{\log_{10}(I_0/I)_{peak}} = \frac{D_{valley}}{D_{peak}} \qquad (2)$$

Figure 28 shows a plot of $R_{v/p}$ vs. spectral slit ($\Delta\nu$). The values for the spectral slit were calculated from the mechanical slit widths.[71] A least squares fit of the data in Figure 28 gives

Table 13. Absorptivity of ν_3 R-Branch Maximum for $R_{v/p} = 0.086$[a]

O_3(ppm v/v)[b]	Time(hr)[c]	Absorptivity $ppm^{-1}\ m^{-1} \times 10^4$ RTP	Absorptivity cm^{-1} STP
0.863	1.083	4.22	4.61
	1.500	4.35	4.74
	1.750	4.30	4.69
	2.083	4.35	4.75
0.916	1.333	4.16	4.54
	1.517	4.17	4.56
	1.683	4.12	4.50
	1.917	4.06	4.43
0.889	1.300	4.20	4.58
	1.433	4.23	4.62
	1.617	4.28	4.67
	1.833	4.27	4.66
0.907[d]	1.367	4.21	4.59
	1.667	4.22	4.61
	1.883	4.26	4.65
	Mean[e] =	4.23 ± 0.04	4.61 ± 0.04

[a] All spectra recorded at 69.17 meters in 735 torr of dry (RH <4%) air at 25°C.

[b] At t = 0.

[c] After introduction of ozone into chamber.

[d] Based on measurement of volume change in ozonizer by use of the gas syringe (see text).

[e] Uncertainty is the standard deviation of the mean. Standard deviation of an individual measurement is ±0.13.

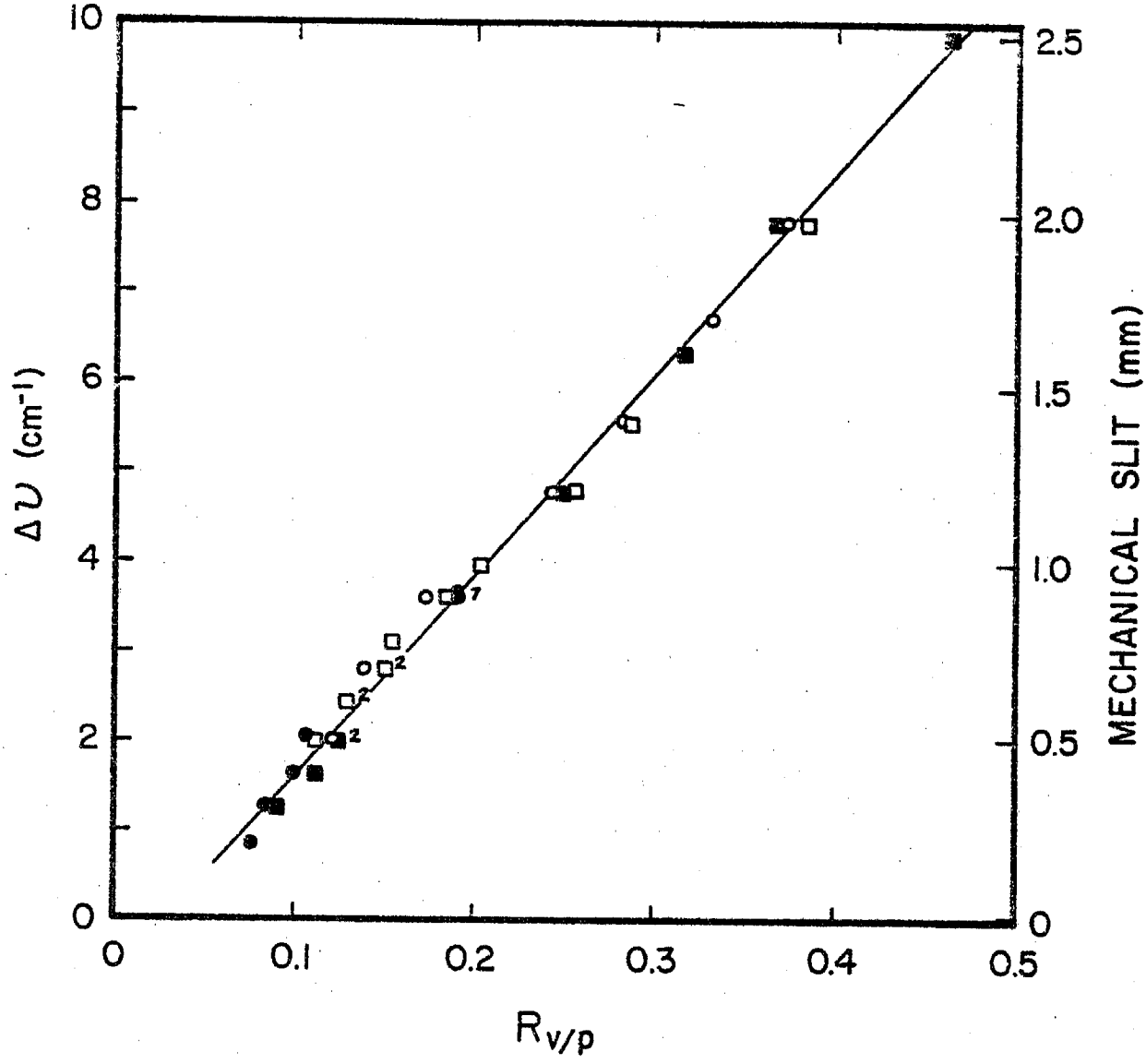

Figure 28. $R_{v/p}$ vs. Spectral Resolution for the 9.48-Micron Ozone Absorption.

$$\Delta\nu(cm^{-1}) = 22.3\ R_{v/p} - 0.58 \qquad (3)$$

As can be seen from the figure, this relation is independent of absorption intensity up to 0.48 fractional absorption. We do not expect equation (3) to hold outside the indicated ranges of $R_{v/p}$ and $\Delta\nu$, since better resolutions ($R_{v/p} \leq 0.07$) bring out the fine structure of the bank making $R_{v/p}$ undefined, and lower resolution ($R_{v/p} \gtrsim 0.5$) destroys the P-, Q-, R-shape of the band.

The advantage of using $R_{v/p}$ as a measure of resolution, rather than $\Delta\nu$, which is tenuous and difficult to determine, is obvious. One need only measure a given spectrum to determine $R_{v/p}$, whereas an estimate of $\Delta\nu$ requires assumptions (sometimes unwarranted) about the performance of a given instrument and is therefore, at best, approximate.

The results of the series of infrared measurements at torr pressures of ozone are given in Figure 29. All of the data were corrected for decay of the sample during the measurement period. The absorptivity scale was determined by normalization of the data to HSSD's value of 3.74×10^{-4} $ppm^{-1}\ m^{-1}$ for $R_{v/p} = 0.334$, as measured from their published spectrum.[69] The excellent agreement of the absolute absorptivity determined from this work [at $R_{v/p} = 0.086$, see Section III-F-2] with the value determined from the curve in Figure 29 demonstrates the consistency of the two determinations. The portion of the curve at low values of $R_{v/p}$ rises steeply due to the fact that the rotational structure of the band is resolved at $\Delta\nu \leq 0.8\ cm^{-1}$.

2. Determination of the Stoichiometry of the 2% NBKI Method by LPIR Spectroscopy[26]

Introduction. To our knowledge, physical measurement methods such as UV or IR spectroscopy had not been applied to investigations of the 2% unbuffered KI (LAAPCD) or 2% buffered KI (ARB) methods prior to the discovery of the discrepancy between these methods. In contrast, the 1% neutral buffered KI method specified[74] by the EPA as the calibration procedure for instruments measuring oxidant or ozone had been extensively investigated. These investigations followed a report by Boyd and co-workers[75] that at high (>100 ppm O_3 in O_2) concentrations they obtained (from UV photometric measurements) a ratio of 1.5 moles of iodine released per mole of

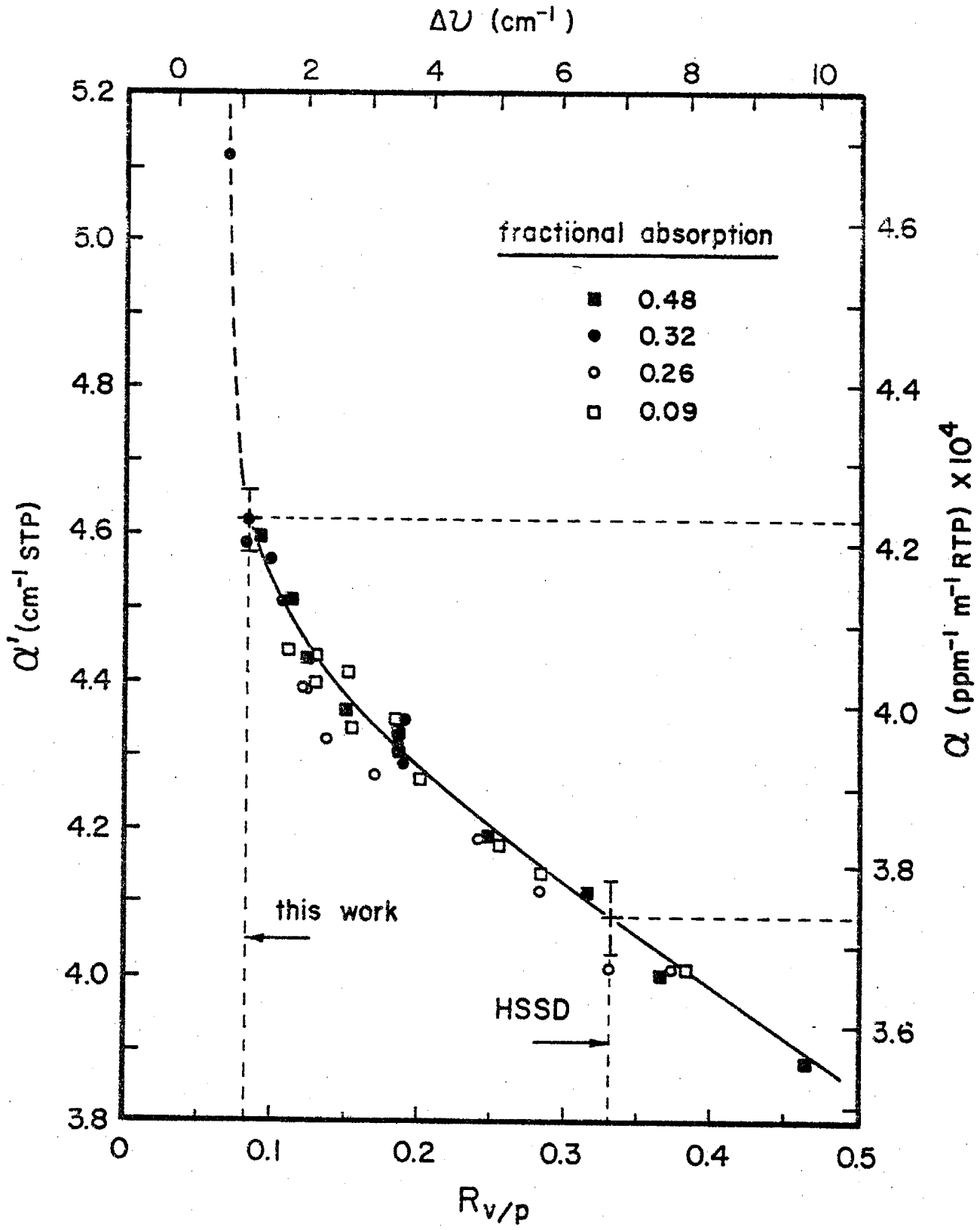

Figure 29. $R_{v/p}$ vs. Absorptivity (α) for the 9.48-Micron Ozone Absorption.

ozone absorbed in 1% neutral buffered reagent, thus calling into question the 1:1 stoichiometry previously assumed for this method. However, in subsequent investigations by Kopczynski and Bufalini[76] (using infrared absorption spectroscopy), by Hodgeson et al.[77] (using gas phase titration of ozone with nitric oxide in air), and by Behl[78] (using a Kruger-type ozone photometer), all reported a 1:1 stoichiometry for the 1% neutral buffered method within their experimental uncertainties.

In view of the ramifications of the reported discrepancy between the buffered and unbuffered 2% KI methods, as well as our use of the 2% neutral buffered method in calibrating the various ozone analyzers employed in our laboratories and air monitoring sites, we began an investigation of the stoichiometry of the 2% neutral buffered KI method at ambient concentrations using long-path infrared (LPIR) spectroscopy. Although our infrared study of the ARB reference method was similar in principle to that of Kopczynski and Bufalini[76] (for the 1% NBKI method), it differed significantly in two important respects. First, the majority of our data were obtained for ozone concentrations below 1 ppm (i.e., at ambient levels), whereas their lowest determination was for 2 ppm of ozone. Secondly, the absorptivity we employed was determined for absolute ozone samples under the precise spectroscopic conditions used in our KI study, whereas Kopczynski and Bufalini employed an absorptivity determined (by Hanst, et al.[69]) for spectroscopic conditions, which could have differed from those used in their KI study. We report here the results of our investigation and our conclusions concerning the validity of the 2% neutral buffered KI method for the measurement of ozone in air monitoring applications.

Infrared Measurements. For sensitivity in the fractional parts per million (ppm) range an in-situ multiple reflection cell (based on the design of White[79] and of Horn and Pimentel[80]) was employed in a 5800-liter evacuable environmental chamber, which has been described in detail elsewhere.[23] The gold-coated, multiple-reflection optics were coupled to a spectrometer consisting of a Nernst glower source, a one-meter scanning monochromator (Interactive Technology, Inc., Model CT103) employing a 75-line/mm grating blazed at 0.8 μ, and a Santa Barbara Research Center mercury-cadmium-telluride detector (2 mm X 0.5 mm, $D^* = 7.4 \times 10^{+9}$)

operated at 77 K. The infrared beam was chopped at 1100 Hz, and the pre-amplifier (Princeton Applied Research Model 118) output was carried to a PAR Model 126 lock-in amplifier operating at a 3 KHz bandpass. Figure 30 shows a schematic of the environmental chamber with its in-situ long-path cell and the infrared spectrometer.

All spectra were obtained at a path length of 69.2 meters and a spectral slit width of approximately 1.3 cm^{-1}. In this work, spectral slit width was defined as follows: For spectra obtained with a Perkin-Elmer Model 621 spectrophotometer (see below), spectral slit width was calculated from the mechanical slit width using data provided by Perkin-Elmer,[81] while for spectra obtained with the Interactive Technology monochromator, spectral slit width was calculated by comparison to the Perkin-Elmer 621 spectra, using the ratio of "valley" to "peak" absorbances as discussed above.

The spectral region from 8.80 to 10.40 microns was scanned in 8.0 minutes, using time constants of either 1.0 or 0.3 seconds. Thus, the scan rate was equivalent to 5 or 15 time constants per resolution element, more than sufficient in either case for good photometric accuracy. The spectral region scanned included wavelengths about 0.3 microns to both the long and short wavelength sides of the 9.6-micron ozone band. A sample spectrum recorded for an ozone concentration of 6 ppm is shown in Figure 31. The well-resolved 9.48-micron R-branch was used to derive quantitative data.

Background (I_o) spectra were taken both before the introduction of ozone into the chamber and after a complete flushing at the end of the runs. No changes occurred in these spectra over the course of the run. All spectra were normalized at the spectrally clear wavelength of 8.822 microns, thus assuring the applicability of the I_o spectra to all of the ozone spectra without ordinate correction in either sample or background spectra.

Ordinate scale expansions of X5 and X10 were used when measuring absorptions less than, or equal to, about 5%. The results from several scale-expanded spectra were compared with nonexpanded spectra taken as soon as possible before and after the scale expansion. The ozone concentrations deduced from these replicate measurements at concentrations between 2 and 0.6 ppm differed by 1 to 5%, depending on the concentration. We attribute much of this small difference to the inability to measure

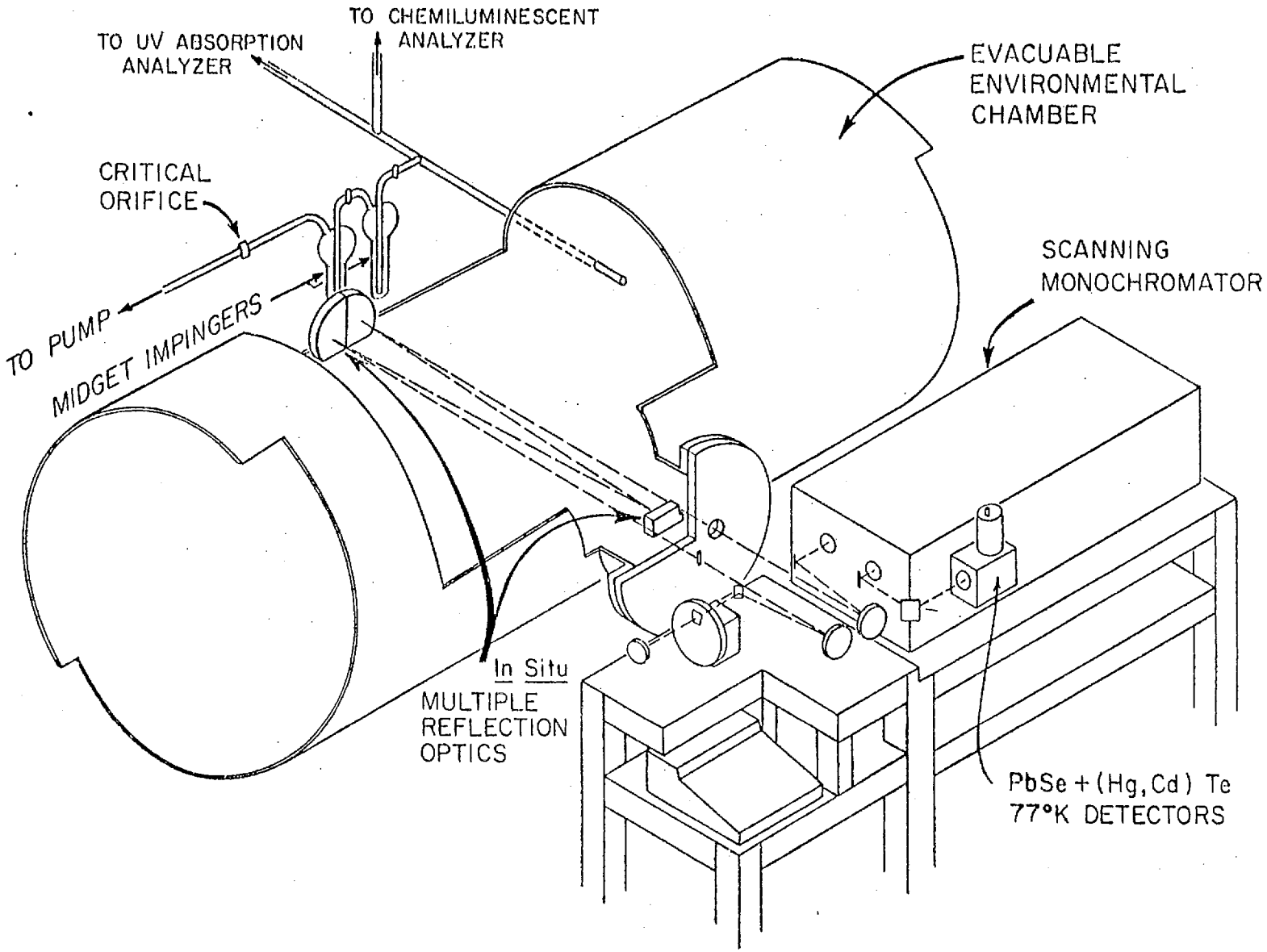

Figure 30. Schematic of Environmental Chamber and Infrared Spectrometer with In-Situ Long-Path Optical System.

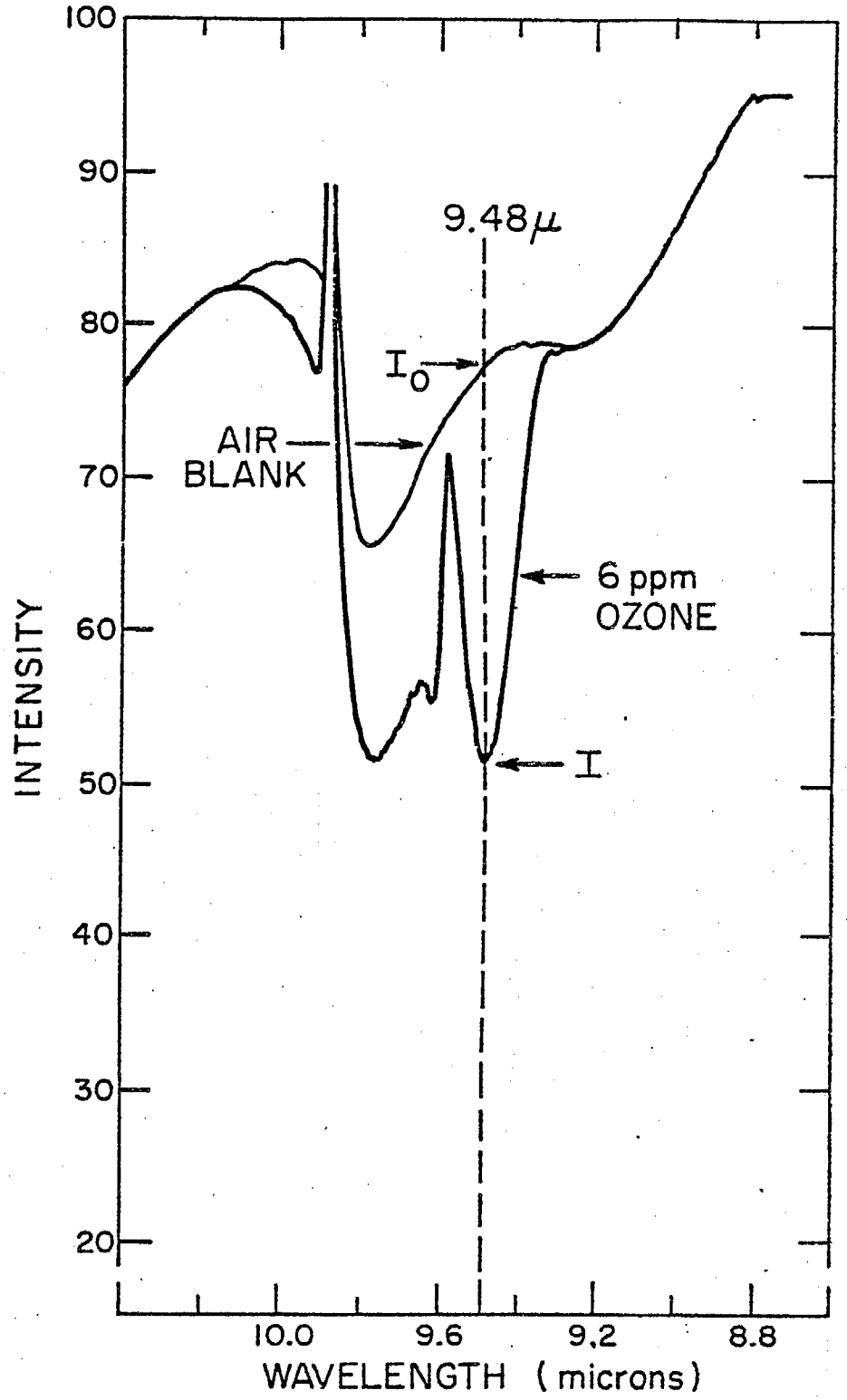

Figure 31. Ozone Absorption Band Centered at 9.6 Microns Showing R-Branch at 9.48 Microns Used to Determine Ozone Concentrations.

the nonexpanded spectra of these weak absorptions to better than about 2 or 3% in ozone concentrations.

The photometric accuracy of the scale expansion was checked before and after each expanded spectrum by recording at least two transmission values in both the expanded transmission region and the normal scale. In general, the expanded transmission scale was accurate to 0.05%, with a correctable I_o offset of no more than 0.2%. (I_o-I) was not sensitive to this correction and was known to at least ±0.1%.

Matching the background to the ozone spectra on the wavelength axis was accomplished by using 8 weak, isolated water absorption lines in the region 8.8 to 9.4 microns. The transmission scale was matched as explained above by single wavelength normalization before taking spectra. This resulted in excellent intensity match between the background and ozone spectra for all spectrally clear regions on both sides of the ozone absorption.

The 9.48-micron peak in the ozone band was reproducibly found by counting interference fringes present due to the 7.47-micron blocking filter used with the monochromator. As shown in Figure 32, obtained for an ozone concentration of 0.36 ppm, these fringes are just resolved in both background and ozone spectra, thus insuring accurate wavelength determination for the intensity (I and I_o) measurements. The large slope observed in Figure 32 results from multiplication of the changing HgCdTe detector response in this wavelength region by the X10 scale expansion. However, even for the lowest ozone concentrations and hence weakest absorptions, identification of the 9.48-micron wavelength was made unambiguously by counting the interference fringes.

The absorptivity of the 9.48-micron band appropriate to these studies was determined as described in Section III-F-1, and all ozone concentrations from infrared measurements reported here were calculated by using an absorptivity of 4.23×10^{-4} ppm^{-1} m^{-1} RTP.

Preparation of Ozone Samples. In the initial experiment, a 5.4-liter bulb was filled to 1 atm pressure with an ~1% ozone-in-oxygen stream from a Welsbach ozonizer. The contents of the bulb were then flushed with nitrogen into the environmental chamber, which had already been filled to

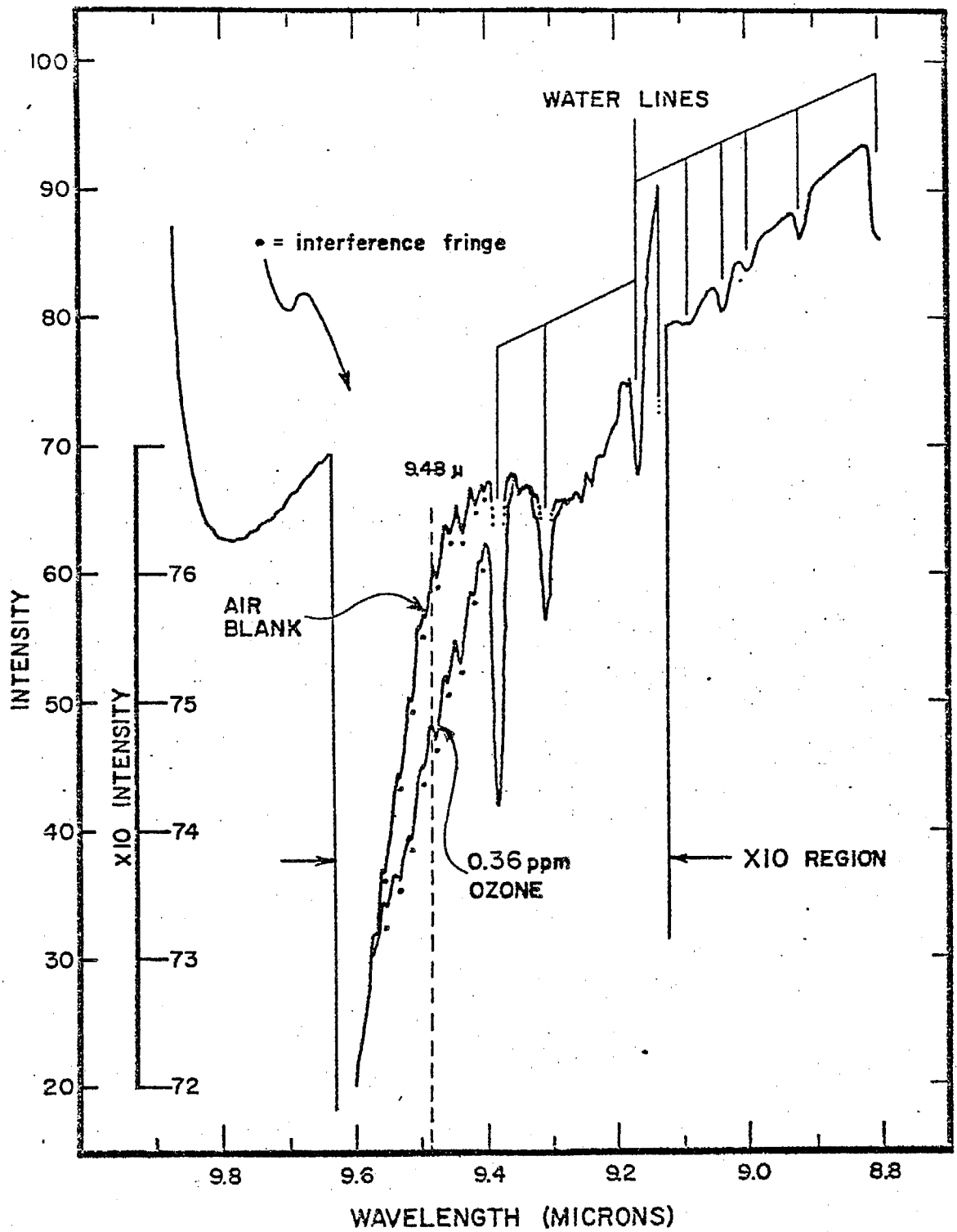

Figure 32. Scale-Expanded Spectrum for 0.36 ppm Ozone Exhibiting Water Absorptions and Interference Fringes from Which Precise Wavelengths Were Determined. Steep Baseline Slope in 9.48-μ Region Is Due to Multiplication of Changing HgCdTe Detector Response by the X10 Scale Expansion.

1 atm pressure (733 torr) with purified air[35] at 298.5 K. The resulting ozone concentration in the chamber was approximately 10 ppm, which was usually immediately reduced to ~2-5 ppm by flushing the chamber with pure air. The strong absorption at 9.6 microns from this high ozone concentration was used to optimize the infrared scanning parameters and other experimental conditions. To study successively lower concentrations below 2 ppm, the chamber was flushed for specified lengths of time with additional pure air. After each flush, the chamber contents were allowed to equilibrate as shown by constant ozone concentrations measured by both UV absorption (Dasibi) and chemiluminescent (Monitor Laboratories) ozone analyzers, which were employed as convenient monitors of relative ozone levels during the experiment. Data obtained with these instruments also permitted calculation of the average ozone decay rate due to decomposition at the chamber walls and sampling losses. This rate ($k = 9.0 \times 10^{-4}$ min^{-1}) was used to make small corrections necessary to normalize the KI and LPIR ozone determinations to the same point in time as discussed below.

In succeeding experiments, the ozone sample was made up in a 0.5-liter bulb and flushed into the chamber to produce an ozone concentration of 1.0 ppm. This sample was then successively diluted as before to study lower concentrations.

2% Neutral Buffered Potassium Iodide Measurements. Two percent KI absorbing reagent buffered at pH 6.89 was supplied by the ARB. Solutions were kept cool and in dark containers and were not more than four weeks old when used. To obtain an ozone measurement, 20 ml of this reagent were pipetted into each of two all-glass impingers, which were connected in sequence via ungreased ball joints to a carbon vane pump at one end and a sample probe in the evacuable chamber at the other (see Figure 30). A critical orifice was used to insure a constant sample flow rate of approximately 1 liter per minute, and the precise rate was accurately calibrated against a bubble meter. Knowing the flow rate, sample times (5, 10, or 24 minutes) were measured on a stopwatch to obtain exact sample volumes. For the studies carried out at 3% and 50% RH, sampling periods were either 5 or 10 minutes, and 10 ml of reagent were used in the impingers. For the study conducted at ~18%, sample periods were 24 minutes and 20 ml of reagent were employed.

No dependence of measured ozone concentration on sampling period was observed in this investigation. In all but one study the impinger samples were read after 3-5 minutes. Data obtained in a study in which the samples were allowed to develop for 30-50 minutes were subsequently corrected to 4 minutes after establishing the dependence of absorbance on time over a period of one hour.

The samples were read on a Bausch and Lomb Spectronic 20 spectrophotometer at 350 nm. Two matched cells were used for the sample and a blank consisting of unreacted absorbant solution. The absorbances were converted to ozone concentrations, using a calibration function supplied by the ARB. The resulting ppm (at 760 torr and 298 K) concentrations were corrected to the respective pressures and temperatures of the experiments described below. For concentrations of ozone above 0.55 ppm, samples were diluted[82] by pipette in the ratio 1 to 3 or 1 to 2, so that all absorbances were less than 0.5 and the corresponding ozone concentrations could be interpolated directly from the calibration function.

To obtain an independent calibration function for the particular Spectronic 20 spectrophotometer being employed in this study, an approximately 0.1 N sodium thiosulfate (Mallinckrodt No. 8100 Analytical Reagent Grade) solution was prepared and standardized[83] by titrating accurately weighed amounts of primary standard grade potassium dichromate (Mallinckrodt No. 6772). The standard sodium thiosulfate (0.095 N) was then used to standardize[83] an iodine solution prepared from U.S.P. Grade KI (Mallinckrodt No. 1112) and analytical reagent grade iodine crystals (Mallinckrodt No. 1008). An aliquot of the standardized iodine solution (0.049 N) was diluted with ARB 2% NBKI to arrive at a working standard whose concentration was equivalent to 1 μℓ of O_3 per ml.[25] A series of aliquots of the working standard were further diluted with ARB 2% NBKI and their absorbances read on the Spectronic 20 at 350 nm. The data obtained were in excellent agreement with those furnished by the ARB.

Results and Discussion. Quantitative infrared data obtained in two separate experiments in an initial study are summarized in Table 14. The ozone concentrations were calculated from the experimentally determined absorbances ($\log_{10} I_o/I$) and from the absorptivity 4.23×10^{-4} ppm^{-1} m^{-1} RTP.

Table 14. Ozone Concentrations Measured Simultaneously by Long-path Infrared Spectroscopy and 2% Neutral Buffered Potassium Iodide at Ambient Conditions of Temperature, Pressure, and Concentration[a]

IR Time[b]	I_o (arbitrary units)	I (arbitrary units)	Absorbance	Ozone from LPIR[c] (ppm)	KI Time[d]	Corrected Ozone from LPIR[e] (ppm)	Average Ozone from LPIR (ppm)	Ozone from 2% Neutral Buffered Potassium Iodide (ppm)
Experiment A								
15:16	76.2	71.2	0.0295	1.00		0.99		
15:28	76.31	71.02	0.0312	1.06	15:32	1.06	1.02	1.18
15:41	75.75	70.83	0.0292	0.99		1.00		
16.35	75.50	71.87	0.0214	0.728	16:24	0.734	0.734	0.829
17:01	76.48	73.49	0.0173	0.589	17:11	0.584	0.596	0.620
17:20	76.38	73.30	0.0178	0.604		0.608		
17:54	76.38	74.46	0.0111	0.376		0.372		
18:05	76.49	74.55	0.0112	0.379	18:05	0.379	0.380	0.431
18:18	76.40	74.43	0.0113	0.385		0.390		
19:08	76.12	75.19	0.00534	0.181		0.179		
19:22	76.06	75.28	0.00448	0.152	19:26	0.151	0.165	0.168
Experiment B								
12:37	76.0	73.2	0.0163	0.554	12:53	0.547	0.544	0.595
12:48	76.0	73.26	0.0159	0.542		0.540		
13:16	75.74	73.12	0.0153	0.520	13:24	0.516	0.502	0.546
13:28	75.80	73.35	0.0143	0.485		0.487		
14:03	76.40	74.40	0.0115	0.392		0.388	0.386	0.444
14:17	76.46	74.50	0.0113	0.384	14:15	0.385		
15:26	75.77	74.47	0.00752	0.256	15:08	0.259	0.259	0.299

Table 14. (continued)

IR Time[b]	I_o (arbitrary units)	I (arbitrary units)	Absorbance	Ozone from LPIR[c] (ppm)	KI Time[d]	Corrected Ozone from LPIR[e] (ppm)	Average Ozone from LPIR (ppm)	Ozone from 2% Neutral Buffered Potassium Iodide (ppm)
15:39	76.16	75.00	0.00667	0.226	15:38	0.226	0.226	0.284
16:13	75.99	74.79	0.00691	0.235	16:14	0.235	0.235	0.282
17:06	75.85	75.39	0.00264	0.090	16:59	0.091	0.091	0.108

[a] During these measurements, the temperature of the samples ranged from 23.2 to 25.5°C, the pressure ranged from 732.6 to 733.4 torr, and the relative humidity ranged from 23% to 6%.

[b] Time at which scan reached 9.48 μ.

[c] Based on absorptivity of 4.23×10^{-4} ppm^{-1} m^{-1} RTP from Reference 59, and pathlength of 69.2 m.

[d] Time halfway through 2% neutral buffered KI impinger sample.

[e] $(O_3)_{t_{KI}} = (O_3)_{t_{IR}} e^{-k(t_{KI}-t_{IR})}$; $k = 8.0 \times 10^{-4}$ min^{-1}. Under these conditions, the difference between the average concentration for a 24-minute sample and the ozone concentration 12 minutes into the sample period (i.e., at t_{KI}) was 1 part in 10^5 of the ozone concentration, hence the average concentration from an impinger sample was taken to be identical to the ozone concentration at t_{KI}.

In order to (a) take advantage of the fact that several infrared spectra could be recorded during the time required to obtain the KI impinger samples, and (b) directly compare IR and KI determinations, the IR ozone concentrations (Column 5, Table 14) were corrected to the time halfway through the corresponding KI sample. The corrections were made according to the first order function

$$[O_3]_{t_{KI}} = [O_3]_{t_{IR}} e^{-k(t_{KI}-t_{IR})} \quad (4)$$

where t_{KI} was the time halfway through the impinger sample, t_{IR} was the time at which an infrared scan reached 9.48 μ, and k(= 8.0 X 10^{-4} min^{-1}) was the average first-order rate of loss of ozone (due to sampling and wall decomposition) observed during eight different sample periods using a continuous ozone analyzer (Dasibi Model 1003). The normalization of the IR ozone concentrations to the impinger halftime involved corrections of less than 8 ppb of ozone, except for the highest concentration (1.2 ppm), for which the correction was 10 ppb.

The normalized IR ozone concentrations for each impinger sample were averaged, and the final two columns of Table 14 are compared to the corresponding KI ozone concentrations. The latter were obtained from measured absorbances for impinger samples and a linear regression fit to the ARB calibration data

$$\text{Ozone} = 1.0095\ (\text{absorbance}) - 0.0015 \quad (5)$$

Calibration data obtained in our laboratory, using U.S.P. Grade KI, yielded a function (ozone = 0.987 absorbance + 0.0014), which was in excellent agreement (2%) with the ARB data. Earlier calibration data obtained in our laboratory using reagent grade KI yielded ozone concentrations lower by approximately 5%. We subsequently learned[84,85] that reagent grade KI often contains a reducing agent to prevent the oxidation of iodide to iodine during shelf life, whereas KI meeting U.S.P. specifications usually contains little or no reducing agent.

The KI and IR data from Table 14 are plotted in Figure 33. The linear regression equation for these data for an unrestricted intercept is

$$[O_3]^{KI} = 1.12\ [O_3]^{IR} + 0.001 \quad (6)$$

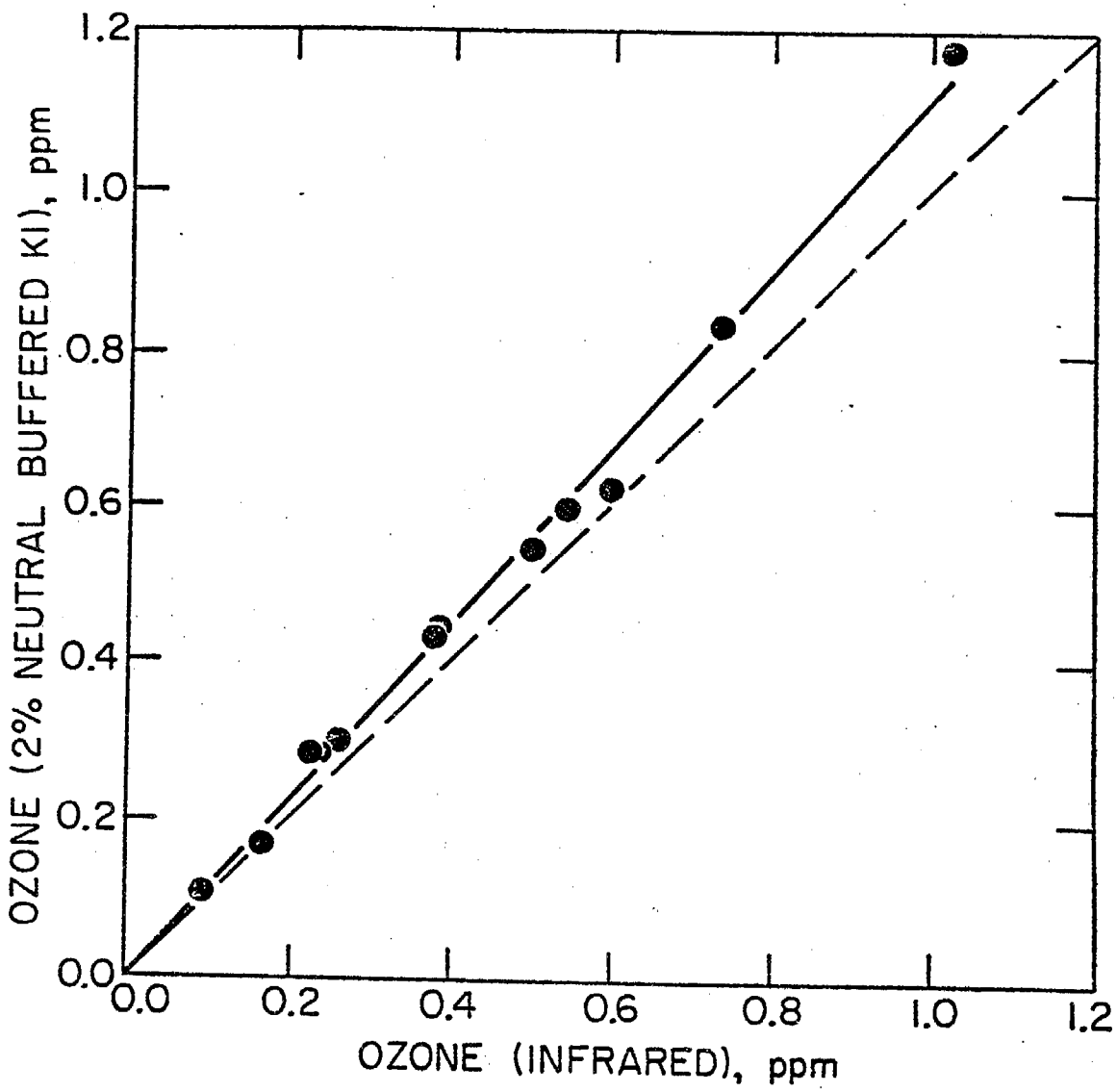

Figure 33. Linear Regression Fit of Ozone Concentrations Measured by LPIR and 2% NBKI Methods at an Average Relative Humidity of 18%; Slope = 1.12 ± 0.03, Intercept = 0.001 ± 0.014.

where ozone concentrations are in parts per million, and the standard deviation for the slope and intercept are ±0.03 and ±0.014, respectively. Thus, results from this experiment suggested that the ARB 2% NBKI method yielded ozone concentrations some 12% higher than concentrations obtained from absolute infrared measurements.

Humidity Effect. During the course of these experiments, the humidity ranged from ~20% down to ~10% as the ozone sample was diluted by flushing the chamber with essentially dry air. (It was not believed important at the time of these experiments to hold the RH rigorously constant.) However, a commercial UV analyzer (Dasibi Model 1003) was being used as a convenient, continuous "real time" monitor of the relative ozone concentration in the chamber, and it was observed that, whereas the ratio of KI to IR concentrations was ~1.1, the ratio of Dasibi to IR concentrations was approximately 1.2, although the Dasibi itself was calibrated by the ARB 2% NBKI method and therefore should have yielded concentrations in the same ratio to the IR measurements.

It was first demonstrated that the difference observed between the Dasibi and 2% NBKI measurements was not due to the fact that the chamber experiments represented a static sampling condition, whereas the normal 2% NBKI calibration procedure is conducted using a dynamic flow system. The only other obvious difference in procedure appeared to be the fact that the ARB calibration procedure is normally conducted at ambient relative humidities (which typically might range from 40-60%), whereas the chamber experiment was carried out at an average relative humidity of approximately 18%. To investigate the possible dependence of the 2% NBKI method on relative humidity, a comparison of ozone concentrations measured simultaneously by IR and 2% NBKI was made as described above, but with the relative humidity in the chamber held at 50% throughout the experiment. Data obtained in this experiment were not corrected for the very slow ozone decay in the chamber or for the small sampling losses, since from the previous analysis it was clear that these corrections (typically less than 5 ppb) were negligible compared to random variations in the KI bubbler measurements (see Table 14).

The data obtained are shown in Table 15 and are plotted in Figure 34. Linear regression analyses of these data yielded the functions

$$[O_3]^{NBKI} = (1.23 \pm 0.06)[O_3]^{IR} + (0.001 \pm 0.034) \quad (7)$$

$$[O_3]^{DSBI} = (1.22 \pm 0.05)[O_3]^{IR} - (0.030 \pm 0.027) \quad (8)$$

$$[O_3]^{DSBI} = (0.99 \pm 0.04)[O_3]^{NBKI} - (0.028 \pm 0.027) \quad (9)$$

Thus, for 50% relative humidity, the Dasibi (DSBI) and 2% NBKI data are in good agreement as expected, but both are some 23% higher than the concentrations measured by the infrared method. These results strongly suggest that the response obtained by the 2% NBKI method is dependent upon the relative humidity of the ozone sample stream, although we are unaware of any obvious chemical interpretation for this effect, since the reaction that is presumed to hold[25]

$$2\ KI + O_3 + H_2O \rightarrow I_2 + O_2 + 2\ KOH \quad (10)$$

takes place in an aqueous solution. Following completion of the present study, an extensive joint investigation of humidity effects by the LAAPCD, ARB, and EPA (Region IX) yielded data for the 2% NBKI method and Dasibi ozone analyzers, which are consistent with the data reported here.[86]

Comparison with Ultraviolet Measurements. An additional significant study in this investigation was a collaborative effort with W. B. DeMore,[87] who participated in an experiment similar to those described above. In this study, conducted for ozone samples in dry matrix air (RH ~3%) in the evacuable chamber, DeMore recorded data with a Dasibi ozone analyzer which he had previously calibrated against a 1-meter UV photometer. Simultaneously, ozone concentrations were also measured using the in-situ long-path infrared spectrophotometer, 2% NBKI impingers, and two Statewide Air Pollution Research Center (SAPRC) Dasibi instruments previously calibrated against the 2% NBKI method at ambient relative humidity. The data obtained in this study are summarized in Table 16, and appropriate linear regression equations for the various sets of measurements are as follows:

$$[O_3]^{UV} = (0.99 \pm 0.02)[O_3]^{IR} + (0.016 \pm 0.011) \quad (11)$$

$$[O_3]^{NBKI} = (1.14 \pm 0.04)[O_3]^{IR} + (0.013 \pm 0.023) \quad (12)$$

Table 15. Ozone Concentrations Measured Simultaneously at 50% Relative Humidity by Long-Path Infrared Spectroscopy, 2% Neutral Buffered Potassium Iodide, and a Dasibi UV Ozone Analyzer Calibrated Against 2% NBKI[a]

Ozone from LPIR[b] (ppm)	Ozone from 2% NBKI (ppm)	Ozone from Dasibi Calibrated Against 2% NBKI[c] (ppm)
0.655	0.792	0.787
0.648	0.834	0.772
0.651	0.790	0.751
0.509	0.623	0.595
0.524	0.638	0.585
0.348	0.463	0.422
0.241	0.279	0.252

[a] Sample temperature and pressure were 24.3°C and 736 torr, respectively.

[b] Based on absorptivity of 4.23×10^{-4} ppm^{-1} m^{-1} RTP from Reference 59, and pathlength of 69.2 m.

[c] Calibrated at ambient relative humidity.

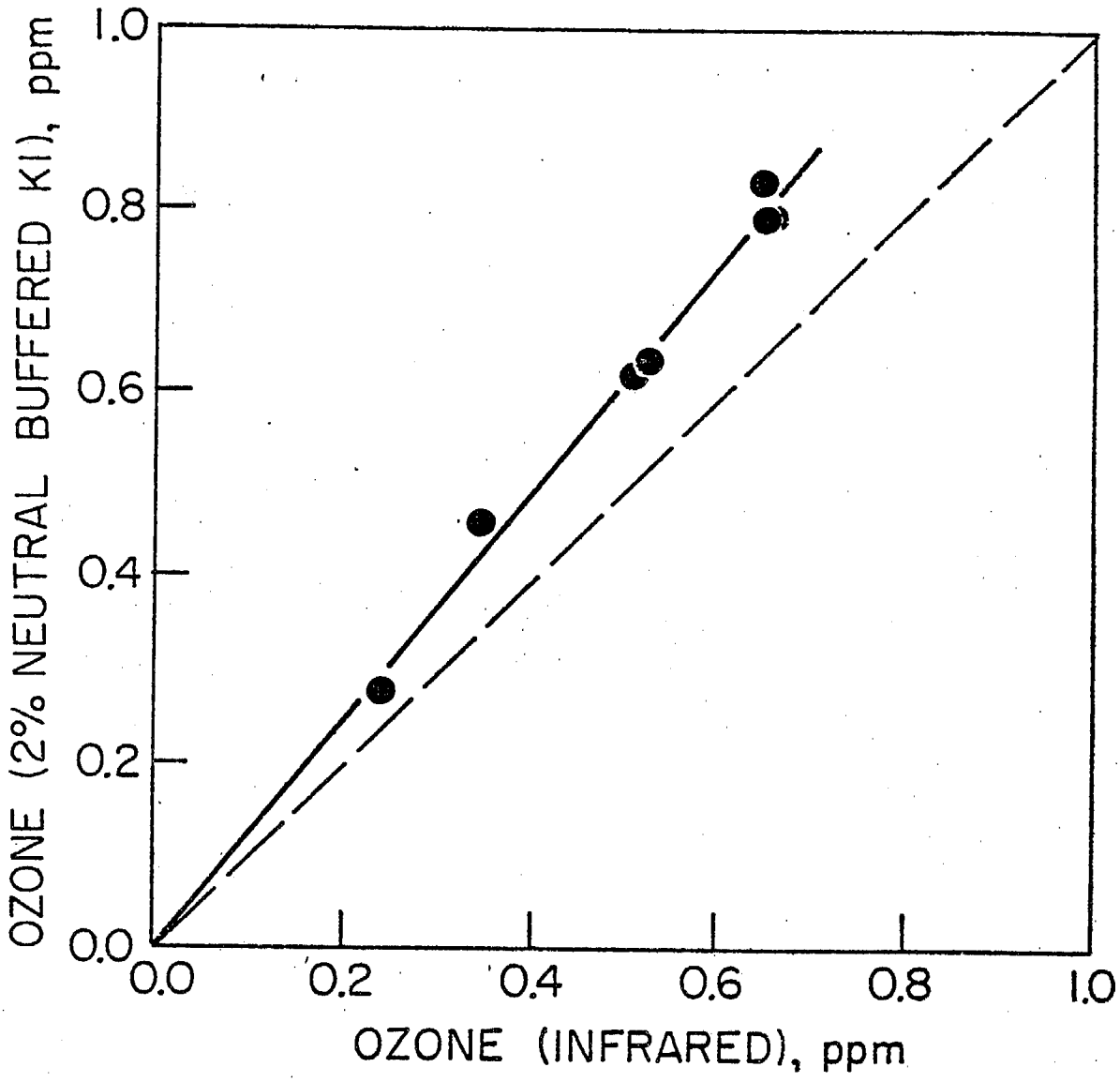

Figure 34. Linear Regression Fit of Ozone Concentrations Measured by LPIR and 2% NBKI Methods at a Relative Humidity of ~50%; Slope = 1.23 ± 0.06, Intercept = 0.001 ± 0.034.

Table 16. Ozone Concentrations Measured Simultaneously at ~3% Relative Humidity by LPIR, 2% NBKI and Dasibi Ozone Analyzers Calibrated by UV Photometry and 2% NBKI, Respectively.[a]

Ozone from LPIR[b] (ppm)	Ozone from Dasibi Calibrated Against UV Photometry[c] (ppm)	Ozone from 2% NBKI (ppm)	Ozone from Dasibis Calibrated Against 2% NBKI[d] (ppm)	
			Dasibi #1	Dasibi #2
0.780	0.776	0.884	0.973	0.961
0.627	0.638	0.736	0.798	0.796
0.450	0.468	0.551	0.588	0.580
0.328	0.347	0.391	0.432	0.420
0.161	0.164	0.178	0.196	0.193

[a] Sample temperature and pressure were 23.9°C and 735 torr, respectively.

[b] Based on absorptivity of 4.23×10^{-4} ppm^{-1} m^{-1} RTP from Reference 59, and pathlength of 69.2 m.

[c] Instrument calibrated and employed by W. B. DeMore.

[d] Calibrated at ambient relative humidity.

$$[O_3]^{NBKI} = (1.16 \pm 0.02)[O_3]^{UV} - (0.007 \pm 0.012) \quad (13)$$

$$[O_3]^{DSBI\ \#1} = (1.25 \pm 0.03)[O_3]^{IR} + (0.012 \pm 0.017) \quad (14)$$

$$[O_3]^{DSBI\ \#2} = (1.24 \pm 0.03)[O_3]^{IR} + (0.007 \pm 0.017) \quad (15)$$

Equation 11 shows that the UV measurements made by DeMore, using a Dasibi instrument as a transfer standard and based on an ultraviolet absorptivity of 135 cm^{-1} atm^{-1} at 253.7 nm, were in excellent agreement with simultaneous in-situ long-path infrared measurements based on an infrared absorptivity of 4.23 X 10^{-4} ppm^{-1} m^{-1} RTP. Thus, the two spectroscopic methods gave comparable results (as shown in Equations 12 and 13), for comparison with the 2% NBKI measurements. Specifically, for the dry sample stream provided in this experiment, the ARB 2% NBKI method yielded ozone values from 14-16% higher than either the UV or IR measurements.

However, as seen from Equations 14 and 15, the two SAPRC Dasibi instruments which had been previously calibrated by the ARB 2% NBKI method at ambient relative humidities, and which have been shown[86] to respond essentially independently of the RH of ozone sample streams, gave ozone values some 25% higher than those obtained by the IR (or UV) measurements. The independence of the Dasibi data, with respect to the relative humidity of the sample stream, is illustrated by the agreement between Equations 14 and 8 obtained for relative humidities of 3% and 50%, respectively.

Comparison with a Previous Infrared Study. In the only previously published report[76] of an investigation of the neutral buffered potassium iodide method by long-path infrared spectroscopy, Kopczynski and Bufalini describe a study of the 1% NBKI method over a range of ozone concentrations from 2-20 ppm, apparently for dry air. For an unrestricted intercept they obtained regression Equation 16

$$[O_3]^{NBKI} = 0.947[O_3]^{IR} - 0.22 \quad (16)$$

with a standard error estimate, Sy, of ±0.28 ppm. When the intercept was restricted to zero their data fit Equation 17

$$[O_3]^{NBKI} = 0.929[O_3]^{IR} \quad (17)$$

with a standard error, Sy, of ±0.32 ppm.

The slopes of 0.95 and 0.93 in these equations may be contrasted with those of 1.14 and 1.23, observed in the present study for the 2% NBKI method for 3% and 50% RH, respectively. Kopczynski and Bufalini concluded from their results that 1:1 stoichiometry is valid for the 1% NBKI method within their experimental error. However, in view of the recently demonstrated effects on KI measurements due to humidity, the nature of potassium iodide reagent employed, etc., and since Kopczynski and Bufalini worked at ozone concentrations from 2-20 ppm with a resulting large intercept for extrapolation of their data to the ambient concentration range, the 10-25% deviation from unit stoichiometry observed in this and other recent investigations could well have been masked in their earlier study. Thus, although different conclusions were reached in the previous[76] and present infrared studies concerning the stoichiometry of the NBKI methods, there is no inherent conflict in the data obtained in these investigations.

Conclusions. Results obtained in this study indicate that rather than being unity, as had been thought prior to 1974, the stoichiometry of the 2% NBKI ozone (or oxidant) analyzer calibration procedure employed by the California Air Resources Board from 1960 until June 1, 1975, ranges from ~1.12 to ~1.25, depending upon whether the relative humidity of the sample stream is low or high, respectively. The results obtained at low humidities may also be relevant to the 1% NBKI calibration procedure specified in the Federal Register,[74] in view of the near equivalence (to within ~5%) of the ARB 2% NBKI method and EPA 1% NBKI method demonstrated by most,[27,88-90] although not all,[91] previous comparisons of the two methods. Further investigation of the 1% NBKI Federal Register method and development of a replacement for this calibration procedure are currently being carried out by the EPA.[92] Effective June 1, 1975, the California calibration procedure for oxidant (ozone) was changed from the 2% neutral buffered potassium iodide method to an ultraviolet photometry method employing a 1-meter UV photometer as a primary standard and a Dasibi UV ozone analyzer as a portable secondary standard for field calibrations.[93]

Within experimental uncertainties encountered in the use of the potassium iodide methods by different laboratories, the data obtained for comparison with long-path infrared measurements are consistent with data

obtained for comparison of the NBKI methods with UV photometry (in our laboratory, as reported here, and in other more extensive studies[27,90,94,95]) and with recent data reported for comparison with gas-phase titration (GPT) measurements.[94] It thus appears that IR, UV, and GPT measurement methods for ozone have been reconciled and, when carefully carried out, that each can be relied upon to provide absolute ozone concentrations against which ambient air analyzers can be calibrated, either directly or by means of "transfer" standards. Uniform adoption of one or more of these methods by local, state, and federal agencies--and abandonment of the wet chemical potassium iodide methods--seems necessary and desirable if an accurate, reliable, and common data base of ozone measurements is to be achieved.

F. Conclusions and Implications of Corrected South Coast Air Basin Oxidant Data[96]

Introduction. The Federal Air Quality Standard for oxidant,[97] many health alert levels and control programs for oxidant, and models of oxidant formation and transport are based substantially on air monitoring data from the Los Angeles Basin, which is the most densely populated portion of the California South Coast Air Basin. Figure 35 shows that portion of the South Coast Air Basin which surrounds metropolitan Los Angeles and lies below the 1500-foot contour of the mountains that define the Los Angeles Basin. Currently, some 10 million people live in this air basin.

As discussed above, in June 1974, the ARB and the LAAPCD announced jointly that different methods of calibration of oxidant monitoring instruments cause oxidant measurements made by the LAAPCD to be "one-quarter to one-third" lower than ARB measurements made at the same time and place.[98] This significant measurement disparity was first observed more than a year earlier, during the late spring and early summer of 1973, when the ARB operated a mobile air monitoring van--first, near the Pomona air monitoring station of the LAAPCD and, second, adjacent to the LAAPCD station in Azusa. Oxidant measurements recorded in the ARB van were found to be 20 to 40% above those recorded by the Pomona LAAPCD station and about 30% higher than those recorded by the Azusa LAAPCD station.[99] Since the sampling techniques and instruments used were similar, it was suspected that the measurement discrepancy resulted from differences in the methods used to calibrate the analyzers. Accordingly, the California Air and Industrial Hygiene Laboratory (AIHL) and the ARB performed a laboratory study using ozone, which showed that the methods used by the ARB and the Environmental Protection Agency (EPA) to calibrate their oxidant analyzers were equivalent within experimental error under the conditions of the study, but that the method used by the LAAPCD to calibrate its oxidant analyzers yielded readings 69 to 73% as high as those obtained by the ARB calibration method.[88,99]

Until June 1, 1975, all three agencies (ARB, EPA, and LAAPCD) used the oxidation by ozone of aqueous iodide ion to molecular iodine as the basis of their calibration methods. The ARB[75] used a 2% neutral buffered potassium iodide absorbing solution and determined the released molecular iodine spectrophotometrically. The spectrophotometer was calibrated against iodine

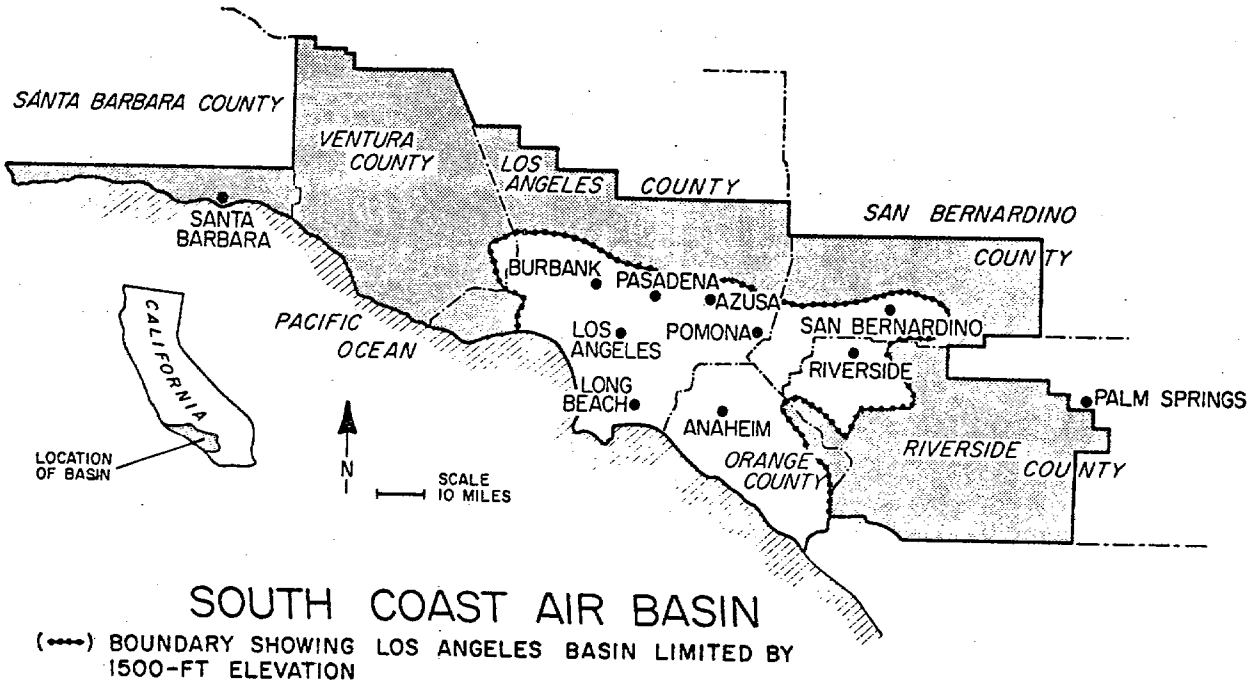

Figure 35. Map of the South Coast Air Basin (Outer Limits Shaded Gray) Showing the Extent of the Los Angeles Basin (White Region), as Defined by the 1500-foot Contour of the Surrounding Mountains. The Locations of the Nine Air Monitoring Stations in the Los Angeles Basin from Which Data are Used in this Paper Are Indicated on the Map.

solutions which had been standardized by titration with $Na_2S_2O_3(aq)$. The $Na_2S_2O_3(aq)$ was standardized against primary grade $KH(IO_3)_2$. The EPA calibration procedure[74] was similar to that formerly used by the ARB, except that essentially dry air and 1% neutral buffered KI were used, and the spectrophotometer was calibrated using I_2 solutions standardized against primary grade As_2O_3. The LAAPCD[100] used 2% neutral unbuffered KI, and the released I_2 was titrated, using 0.002 N $Na_2S_2O_3(aq)$ which had been standardized against $K_2Cr_2O_7$.

Because the LAAPCD calibration method is difficult to perform,[88] to confirm the AIHL/ARB results

> "...a joint ARB-LAAPCD study was conducted at the laboratories of the LAAPCD. Two colorimetric oxidant analyzers, one provided by the ARB and one by the LAAPCD, were used to sample simultaneously from a common manifold. The ozone concentration in the manifold was determined by the three [EPA, ARB, LAAPCD] calibration methods. Again it was demonstrated that the EPA and ARB procedures were approximately equivalent, while, on the average, concentrations by the LAAPCD method were approximately 70% of those by the ARB method."[99]

Because of the discrepancy between LAAPCD oxidant measurements and non-Los Angeles County oxidant measurements, on August 15, 1974, the ARB appointed an ad hoc committee to evaluate oxidant calibration methods. The ad hoc committee[27] used a UV photometer ($[O_3]^{UV}_{absolute}$) to calibrate the response to ozone of a Dasibi ozone monitor ($[O_3]_{Dasibi}$). The Dasibi was then used to determine the response of the LAAPCD, ARB, and EPA iodimetric calibration methods ($[O_3]_{LAAPCD}$, $[O_3]_{ARB}$, $[O_3]_{EPA}$). The latter measurements were made simultaneously at about 50% relative humidity. Analysis of the resulting data yielded the following regression lines:[27]

$$[O_3]^{UV}_{absolute} = 1.054[O_3]_{Dasibi} + 0.028 \quad (18)$$

$$[O_3]_{ARB} = 1.29[O_3]_{Dasibi} - 0.005 \quad (19)$$

$$[O_3]_{LAAPCD} = 0.96[O_3]_{Dasibi} - 0.032 \quad (20)$$

$$[O_3]_{EPA} = 1.24[O_3]_{Dasibi} - 0.035 \quad (21)$$

However, the responses of all the iodimetric methods are humidity-dependent,[86] whereas the response to ozone of Dasibi ozone monitors are not dependent on humidity. This humidity effect was studied by a joint ARB-LAAPCD-EPA team.[86,101] It should be realized that the EPA calibration

procedure[74] employs essentially dry air. The response of the various iodimetric methods was determined at 0, 20, 40, and 60% relative humidity (RH), compared to that of a Dasibi which had been calibrated by the ARB 2% neutral buffered KI method. Because field ozone monitors are calibrated by spanning them against iodimetric measurements, the study team concluded in their draft report[101] that regression lines forced through zero best approximated actual calibration procedures for field instruments. The slopes of the regression lines forced through zero given in the final report of the ARB-LAAPCD-EPA humidity study,[86] may be used to formulate an equation which gives the variation with relative humidity of the relative response of the ARB and LAAPCD iodimetric calibration methods:

$$[O_3]_{ARB}/[O_3]_{LAAPCD} = 3.56 \times 10^{-3} \text{ RH} + 1.28 \qquad (22)$$

At 50% RH, this equation gives a value of $[O_3]_{ARB}/[O_3]_{LAAPCD} = 1.46$. Significantly, if the data of the ad hoc committee[27] are also forced to zero, then at RH ~50% a value of $[O_3]_{ARB}/[O_3]_{LAAPCD} = 1.43$ is obtained. Previous studies of ozonized room air obtained the following values for this ratio: 1.37, 1.43, and 1.46 by Tang, Jeung, and Imada;[88] 1.34 by Crowe;[102] and 1.33 and 1.39 by Holland.[103] A value of 1.37 was obtained by Dickinson[104] for the ratio of the LAAPCD iodimetric calibration procedure when run with and without buffering at pH 7. The average of these values is $[O_3]_{ARB}/[O_3]_{LAAPCD} = 1.40 \pm 0.05$. Significantly, after an independent assessment of the available data,[101] the ARB also concluded that $[O_3]_{ARB}/[O_3]_{LAAPCD} = 1.4$.

As described above (Section III-E-2), the SAPRC investigation of the validity of the ARB calibration technique showed that at 50% RH, $[O_3]^{IR}_{absolute}/[O_3]_{ARB} = 0.81$, which is in good agreement with the value of $[O_3]^{UV}_{absolute}/[O_3]_{ARB} = 0.78$ obtained by the ad hoc committee using UV photometry. Taken together, these two values suggest that ambient oxidant data referenced to the ARB 2% neutral buffered KI method be corrected using the following equation:

$$[O_3]_{absolute} = 0.8\ [O_3]_{ARB} \qquad (23)$$

Again, this conclusion is in exact agreement with a previous ARB recommendation.[105] Further, if $[O_3]_{ARB}/[O_3]_{LAAPCD} = 1.4$, then the following

equation should be used to correct ambient oxidant data referenced to the LAAPCD 2% neutral unbuffered method:

$$[O_3]_{absolute} = 1.1\ [O_3]_{LAAPCD} \qquad (24)$$

Calculations. We have used Equations 23 and 24 and a computer (IBM 360/50) to generate an internally consistent set of ambient oxidant data for 18 air monitoring stations located in the South Coast Air Basin. Hourly average oxidant data, stored on magnetic tapes, were obtained from the ARB and the LAAPCD for the years 1955 through 1974. Hourly average oxidant data from air monitoring stations in Los Angeles County are available on tapes from the LAAPCD. Under contract to the ARB, hourly average oxidant measurements are made by non-Los Angeles stations. These measurements comprise the data base stored on tapes by the ARB.

The computer program used surveyed the data available one day at a time, dropping days for which three or more consecutive daytime hours of data were lacking. When one or two consecutive hours of data were lacking, a four-point Lagrangian interpolation was used to estimate the missing data points. The resulting set of internally consistent (hereinafter termed "corrected") oxidant data is probably accurate to about ± 10%.

Results. For the full 19-year period from 1955 through 1974, complete data are not available for any of the 18 stations surveyed. When data are available for a specified station and year, they are not available for all 365 days of that year. Further, because the days for which data are lacking are not distributed throughout the year in a strictly random fashion, no normalization to 365 days was possible. Therefore, all yearly totals reported here (Tables 17-19) are minimum values. Conversely, because the missing days are not bunched either during the smog season or during the winter, the data also do not contain any significant intrinsic biases.

Because the South Coast Air Basin oxidant data are voluminous, we have chosen to present here only data for the years 1973 and 1974 and for the following nine air monitoring stations: Long Beach, Los Angeles Downtown, Burbank, Pasadena, Azusa, and Pomona (all in Los Angeles County); Anaheim (Orange County); Riverside (Riverside County); and San Bernardino (San Bernardino County). Figure 35 shows the locations of the nine air

monitoring stations from which the data used in this study were taken. As was stated above, the Los Angeles County stations used oxidant analyzers calibrated by the LAAPCD method,[100] while the non-Los Angeles County stations used analyzers calibrated by the ARB method.[25] Data from other stations and for other years will be published as an SAPRC report.[106]

To facilitate discussion of the implications of the corrected data presented in Tables 17-19, we have summarized the corrected hourly average values of oxidant in terms of the number of days per year, the number of hours per year, and the yearly dosage (hours X concentration) for which the following levels of oxidant were equaled or exceeded: 0.08, 0.20, and 0.35 ppm. These levels were chosen because 0.08 ppm for 1 hour is the Federal Air Quality Standard for oxidant, and 0.20 and 0.35 ppm for 1 hour are the California first-and second-episode criteria levels for oxidant.[107] Reference will also be made to the California third-state episode criteria level (0.50 ppm for 1 hour and predicted to persist for an additional hour) for oxidant and to the Federal "significant harm" level (0.60 ppm) for oxidant.[108]

On May 15, 1975, the California Air Resources Board adopted UV photometric measurement of ozone as the state reference method for the calibration of oxidant monitors.[93] On the same day, the ARB changed the state's second- and third-episode criteria levels for oxidant from 0.40 and 0.60 ppm to 0.35 and 0.50 ppm.[107] Changes were made because "the [old] stage 2 and stage 3 levels...[were] based predominantly on experimental exposures of human subjects to ozone, calibrated using neutral buffered potassium iodide reagent."[109] Accordingly, since the neutral buffered potassium iodide calibration procedure for ozone yields readings high by about 25%, the ARB chose to reduce the old stage 2 and stage 3 episode criteria levels so that they will be in better conformity with ambient oxidant measurements referenced to UV photometric measurements of ozone.

Oxidant Transport. For many years, the air monitoring data--as reported by the LAAPCD and the APCD's of Riverside, San Bernardino, and Orange counties--have shown that the highest oxidant levels in the South Coast Air Basin occur at cities such as Riverside and San Bernardino, which lie in the less-populated eastern portion of the basin. The conventional

explanation[110,111] of this seeming anomaly has generally been the following: Large amounts of hydrocarbons and oxides of nitrogen are emitted during the morning traffic rush hour, principally in the more densely populated western regions of the basin. While being transported toward the eastern portion of the basin by the prevailing onshore sea breezes, the oxides of nitrogen promote the photooxidation of the hydrocarbon pollutants. Ozone, the principal component of oxidant, is a major product of this complicated process.[112-116] Because it is consumed rapidly by NO to produce NO_2 and O_2, ozone does not begin to accumulate until almost all of the NO has been converted to NO_2. Because ozone formation is delayed, downwind transport causes oxidant levels in eastern cities of the basin, such as Riverside and San Bernardino, to exceed those of the more densely populated regions to their west.

This conventional view was reiterated in a recent National Academy of Sciences-National Academy of Engineering (NAS-NAE) report,[117] which stated:

> "Thus, over a period of hours the mass of smog-laden air from downtown Los Angeles experiences a growth in ozone concentration as it travels eastward so that a shift in maximum ozone concentrations eastward should be expected, and has been confirmed by measurements. The shift in ozone concentrations to the east also has been enhanced by the growth in urbanization in that region, which causes increases in local hydrocarbon and NO_x emissions."

One can examine the two parts of this statement separately. First, is there a downwind transport of oxidant, and, second, does oxidant buildup occur during downwind transport?

On the basis of published data, the evidence for downwind transport of pollutants is convincing. For example, Figure 36 presents the diurnal variation of oxidant levels on July 25, 1973, at four air monitoring stations--Los Angeles Downtown, Pomona, Riverside, and Palm Springs--which lie on a west-east axis across the South Coast Air Basin. The second late-afternoon peak in the oxidant profiles at Pomona, Riverside, and Palm Springs is a common occurrence, which is best explained by windborne transport of pollutants to the inland cities from regions nearer the coast. This long-held view of pollutant transport is supported by two recent studies. The first, a fluorescent tracer study, showed that some coastal air parcels do reach inland cities, such as Riverside and San Bernardino,[118] in the span of one day. The second, analyses of observational data of

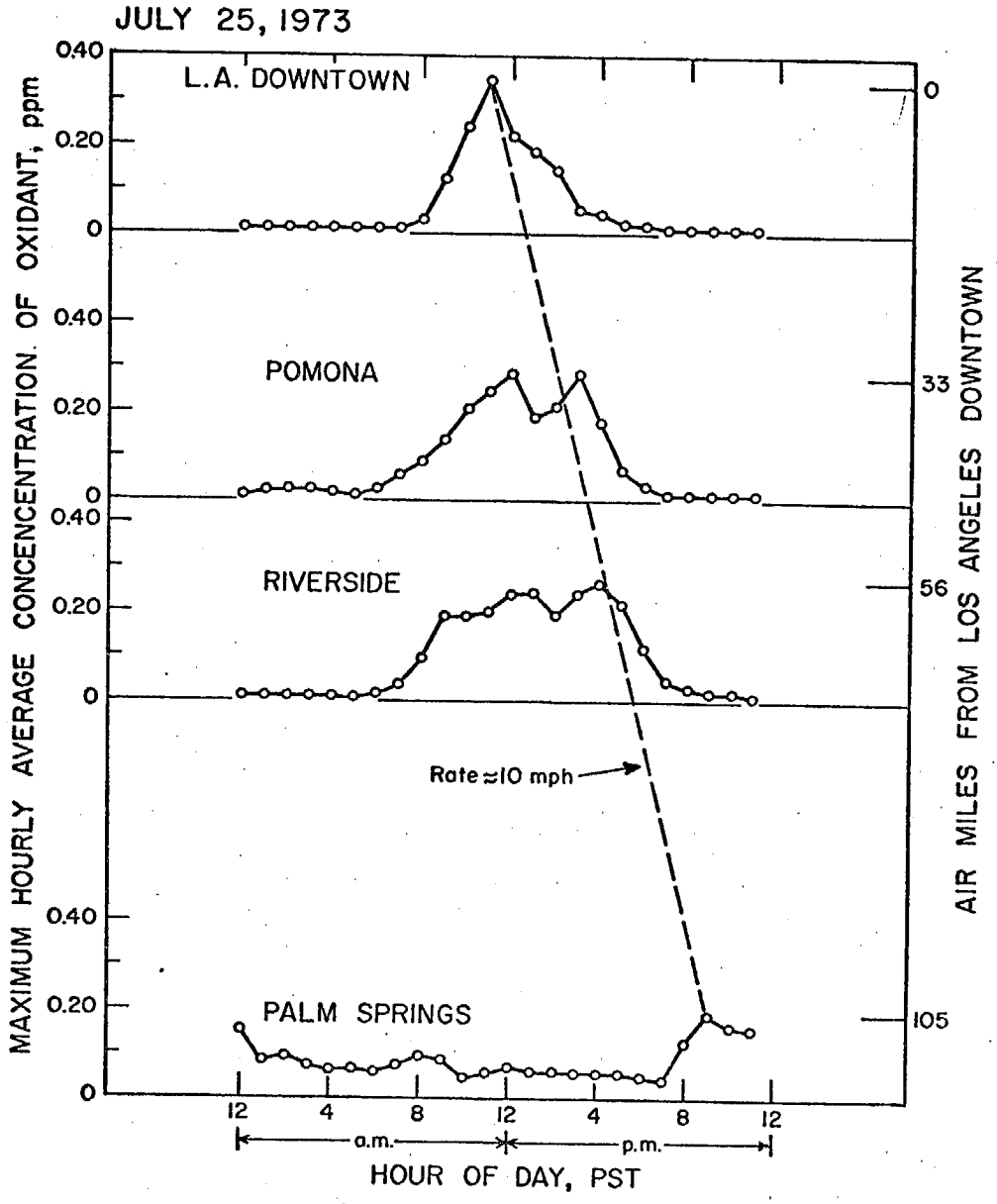

Figure 36. Diurnal Variation July 25, 1973, of Oxidant Concentrations at Air Monitoring Stations at Los Angeles Downtown, Pomona, Riverside, and Palm Springs, California. Values are Corrected Data: Los Angeles Downtown and Pomona X 1.1, and Riverside and Palm Springs X 0.8.

air pollutants from an airborne sampling system, indicated that ozone and/or its precursors in an episode were transported in the Los Angeles basin from the metropolitan area to the eastern portion of the basin.[119]

It is interesting that if the oxidant maxima in Figure 36 are spaced proportionately to the distances between the four cities, as has been done in the figure, the second oxidant maxima fall on the same connecting line.[120] This result suggests that the average wind speed in the basin on July 25, 1973, was about 10 mph in an easterly direction. In fact, the average ground wind speed on that day actually was approximately 8 mph in an east-northeasterly direction.

The evidence for the NAS-NAE statement "...a shift in maximum ozone concentrations eastward should be expected, and has been confirmed by measurements"[117] is typified in Figure 37(a). This shows the number of days in 1973 on which the reported average hourly oxidant readings equaled or exceeded 0.20 ppm at six South Coast Air Basin air monitoring stations. Clearly, the data as reported do indeed suggest an inland buildup of oxidant. However, when all the air monitoring data are placed on a consistent scale, no matter what scale is used, the corrected data [Figure 37(b) through (e)] show that, in 1973, cities such as Pasadena, Azusa, and Pomona actually had significantly higher oxidant levels than did Riverside and San Bernardino. Tables 17 and 18 show that this conclusion also holds for 1974. It is also true for all other years for which data are available (1963-1970). Clearly, oxidant levels do not increase along a west-to-east axis across the basin. However, data from other stations indicate that they do increase along a southwest-to-northeast axis across the basin, which roughly matches the orientation of the prevailing onshore sea breezes. Thus, buildup of oxidant during downwind transport may explain the fact that cities such as Pasadena, Azusa, and Pomona usually have higher oxidant levels than do locations which lie upwind of them, such as downtown Los Angeles.

Oxidant Levels. Table 17 shows that when LAAPCD data are appropriately corrected, the number of days on which the hourly oxidant concentration equals or exceeds 0.08 ppm is increased by at least 5% at the six Los Angeles County stations, and that the average increase is almost 20%. Table 18 shows that at these same six Los Angeles County stations, the

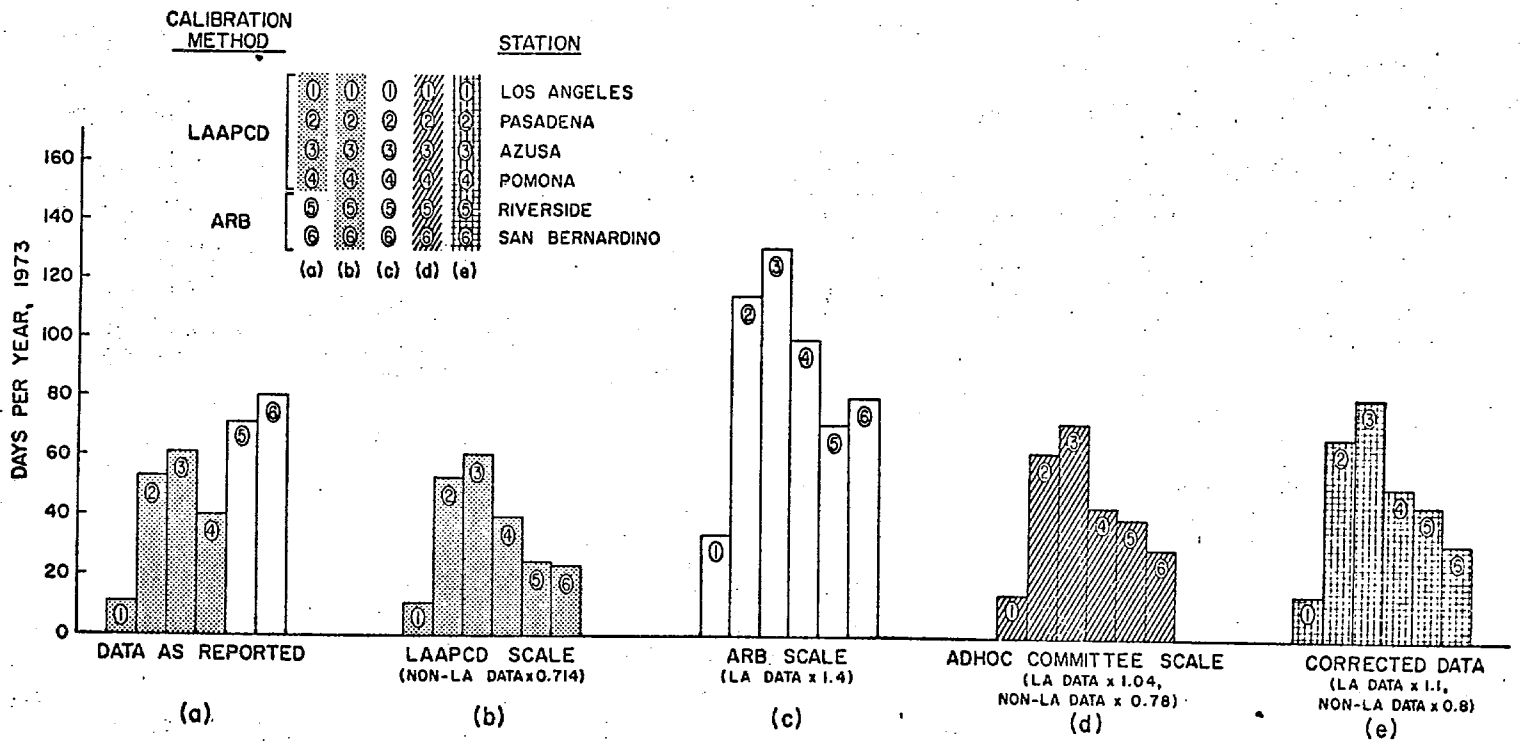

Figure 37. Number of Days in 1973 in Which Hourly Average Oxidant Concentration Equaled or Exceeded 0.20 ppm at Six Air Monitoring Stations in the South Coast Air Basin; (a) Data as Reported; (b) LAAPCD Scale--Non-LAAPCD Data (Riverside and San Bernardino X 0.714); (c) ARB Scale--LAAPCD Data (Los Angeles, Pasadena, Azusa, Pomona) X 1.4; (d) Ad Hoc Committee Scale--LAAPCD Data X 1.04, Non-LAAPCD Data X 0.78; (e) Corrected Data--LAAPCD Data X 1.1, Non-LAAPCD Data X 0.8.

Table 17. Days for which Oxidant ≥ 0.08, 0.20, and 0.35 ppm[a,b,c]

1973

Station	LB	LADT	Bur	Pas	Azu	Pom	SB	Riv	Ana
Total Days	347	349	353	350	346	351	322	355	344
				≥0.08 ppm					
AS REPORTED	17	134	159	183	184	174	169	195	105
CORRECTED	34	160	171	194	194	189	154	172	72
RATIO	2.0	1.2	1.1	1.1	1.1	1.1	0.91	0.88	0.69
				≥0.20 ppm					
AS REPORTED	2	11	12	53	61	40	80	71	15
CORRECTED	2	15	19	68	82	52	33	46	7
RATIO	1.0	1.4	1.6	1.3	1.3	1.3	0.41	0.65	0.47
				≥0.35 ppm					
AS REPORTED	0	1	0	4	6	0	5	4	0
CORRECTED	0	2	0	6	9	2	0	0	0

1974

Station	LB	LADT	Bur	Pas	Azu	Pom	SB	Riv	Ana
Total Days	350	333	360	351	360	360	360	356	335
				≥0.08 ppm					
AS REPORTED	27	156	190	228	220	178	195	208	101
CORRECTED	37	175	207	243	233	194	172	184	60
RATIO	1.4	1.1	1.1	1.1	1.1	1.1	0.88	0.89	0.59
				≥0.20 ppm					
AS REPORTED	0	14	30	52	80	49	95	94	4
CORRECTED	0	30	48	80	99	72	73	65	2
RATIO	-	2.1	1.6	1.5	1.2	1.5	0.77	0.69	0.50
				≥0.35 ppm					
AS REPORTED	0	0	1	0	2	0	25	8	0
CORRECTED	0	0	1	2	6	0	1	0	0

a) LB = Long Beach, LADT = Los Angeles Downtown, Bur = Burbank, Pas = Pasadena, Azu = Azusa, Pom = Pomona, SB = San Bernardino, Riv = Riverside, and Ana = Anaheim

b) Corrected data means LAAPCD Data x 1.1 and ARB Data x 0.8

c) RATIO = CORRECTED/AS REPORTED

Table 18. Hours for which oxidant ≥ 0.08, 0.20, and 0.35 ppm [a,b,c]

1973

Station	LB	LADT	Bur	Pas	Azu	Pom	SB	Riv	Ana
Total Days	347	349	353	350	346	351	322	355	344
				≥0.08 ppm					
AS REPORTED	46	615	745	1122	1129	936	1182	1363	389
CORRECTED	85	777	894	1282	1267	1088	962	1101	213
RATIO	1.8	1.3	1.2	1.1	1.1	1.2	0.81	0.81	0.55
				≥0.20 ppm					
AS REPORTED	2	38	25	147	189	105	244	264	31
CORRECTED	4	51	46	217	264	150	88	109	13
RATIO	2.0	1.3	1.8	1.5	1.4	1.4	0.36	0.41	0.42
				≥0.35 ppm					
AS REPORTED	0	5	0	7	10	0	5	7	0
CORRECTED	0	6	0	11	15	2	0	0	0

1974

Station	LB	LADT	Bur	PAS	Azu	Pom	SB	Riv	Ana
Total Days	350	333	360	351	360	360	360	356	335
				≥0.08 ppm					
AS REPORTED	53	773	995	1246	1280	963	1414	1504	372
CORRECTED	83	983	1186	1446	1490	1136	1150	1205	214
RATIO	1.6	1.3	1.2	1.2	1.2	1.2	0.81	0.80	0.58
				≥0.20 ppm					
AS REPORTED	0	25	72	131	222	120	401	333	11
CORRECTED	0	59	115	210	306	197	217	171	5
RATIO	-	2.4	1.6	1.6	1.4	1.6	0.54	0.51	0.45
				≥0.35 ppm					
AS REPORTED	0	0	1	0	3	0	36	9	0
CORRECTED	0	0	2	3	8	0	1	0	0

a) LB = Long Beach, LADT = Los Angeles Downtown, Bur = Burbank, Pas = Pasadena, Azu = Azusa, Pom = Pomona, SB = San Bernardino, Riv = Riverside, and Ana = Anaheim.

b) Corrected data means LAAPCD Data x 1.1 and ARB Data x 0.8.

c) RATIO = CORRECTED/AS REPORTED.

number of hours ≥ 0.08 ppm is increased by at least 12%, with the average increase being almost 30%. For Los Angeles County stations, the increases observed relative to the first-stage episode criteria level of 0.20 ppm are substantially larger, though more variable. Thus, the number of days ≥ 0.20 ppm increase by 20 to 130%, with the average increase being 50%, and the number of hours increase by 40 to 140%, with the average increase being 60%.

Tables 17 and 18 also show that, if the data from the San Bernardino, Riverside, and Anaheim stations, which are referenced to the ARB 2% neutral buffered KI method, are appropriately corrected, then days ≥ 0.08 ppm decrease by an average of 20%, and hours ≥ 0.08 ppm decrease by an average of 30%, while days and hours ≥ 0.20 ppm decrease by 23 to 70% and 46 to 80%, respectively.

Examination of the data in Tables 17 and 18 shows that, once the data have been appropriately corrected, the new second-stage episode criteria level of 0.35 ppm (formerly 0.40 ppm) has been exceeded more frequently at Pasadena, Azusa, and Pomona than it has at San Bernardino and Riverside, while the data as reported suggest that the converse is true. Also, the corrected data show that from 1971 through 1974 the new third-stage episode criteria level of 0.50 ppm (formerly 0.60 ppm) was exceeded only on eight days, once at Los Angeles Downtown, once at Pasadena, on four days at Azusa, and twice at Upland. Using data as reported, no third stage-levels were recorded at any of the LAAPCD stations, although the San Bernardino APCD reported two third-stage episodes at Upland.

Oxidant Dosages. It is widely recognized that reliable assessment of the health effects of any pollutant should not be based simply on peak exposure levels, which are frequently brief in duration, but on cumulative dosage above some specified exposure level, where dosage is defined as the integral of the concentration of the pollutant over the time of exposure. This concept is illustrated in Figure 38, which presents the diurnal variation of oxidant levels (both as reported and corrected) at Upland on July 25, 1973. The shaded portion of the figure is the uncorrected Upland dosage above the old California 0.40 ppm second-stage episode level for oxidant. This area can be defined mathematically as follows:

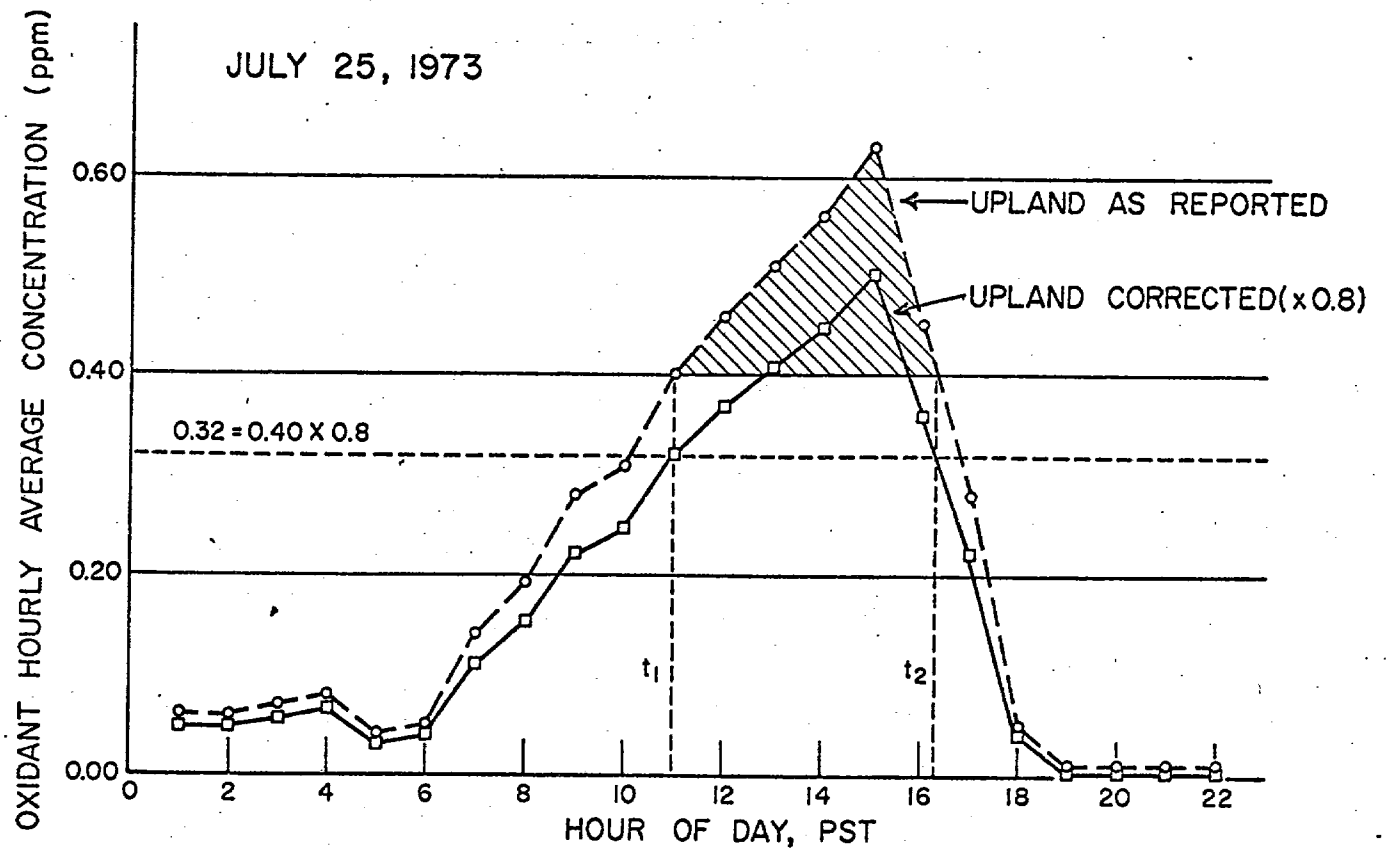

Figure 38. Diurnal Variation of Oxidant Concentration (Data as Reported; Corrected Values--Data X 0.8) at the Upland Air Monitoring Station on July 25, 1973. Upland Station is in the San Bernardino Air Pollution Control District, Which Used the ARB Oxidant Measurement Calibration Method.

$$\text{Dosage } (\geq\delta) = \int_{t_1}^{t_2} [f(t)-\delta]\, dt \qquad (25)$$

where f(t) is the dashed curve, which gives the diurnal variation of the uncorrected oxidant concentrations {[Ox] = f(t)}, δ is the specified exposure level (0.40 ppm), and t_1 and t_2 (11:00 a.m. and 4:20 p.m.) are the times between which the oxidant concentration exceeded the exposure level δ.

Figure 39 contrasts the uncorrected and corrected Upland oxidant dosages for July 25, 1973, to those of Pasadena. With correction, the Pasadena dosages are almost as high as those in Upland.

The geographical extent of the elevated noontime oxidant dosages of July 25, 1973, can best be seen by constructing an oxidant contour map of that portion of the basin surrounded by a 1500-foot elevation barrier.[121-123] Figures 40 and 41 present such maps, using data as reported and corrected data from 20 stations in the South Coast Air Basin. Comparison of the two maps shows that the data as reported significantly overestimate the extent of the regions of high dosage, especially near the City of Upland. It also shows that at noon on July 25, 1973, the regions of high oxidant in the South Coast Air Basin lay just below the San Gabriel Mountains (Pasadena and Azusa) directly downwind from major population centers.

Figure 42 presents 1973 yearly oxidant dosages $\geq$ 0.20 ppm for six air monitoring stations in the South Coast Air Basin. As before, correction of the data produces significant shifts in relative dosages with the result that highest dosages occur at Pasadena and Azusa and not at Riverside and San Bernardino. Table 19 shows that this result is true for other levels and stations and for 1974. Specifically, when the data are appropriately corrected, LAAPCD dosages $\geq$ 0.08 ppm increase by an average of 30%, and those $\geq$ 0.20 ppm increase by 40 to 200%. The decreases in the dosages experienced at non-LAAPCD stations are also pronounced. Dosages $\geq$ 0.08 ppm decrease on the average by 40%, while dosages $\geq$ 0.20 ppm decrease by 60 to 90%.

It is often assumed that, if a set of oxidant data and the air quality standards and health-warning episode levels based on those data both are scaled by the same factor, then the oxidant exposure above the scaled

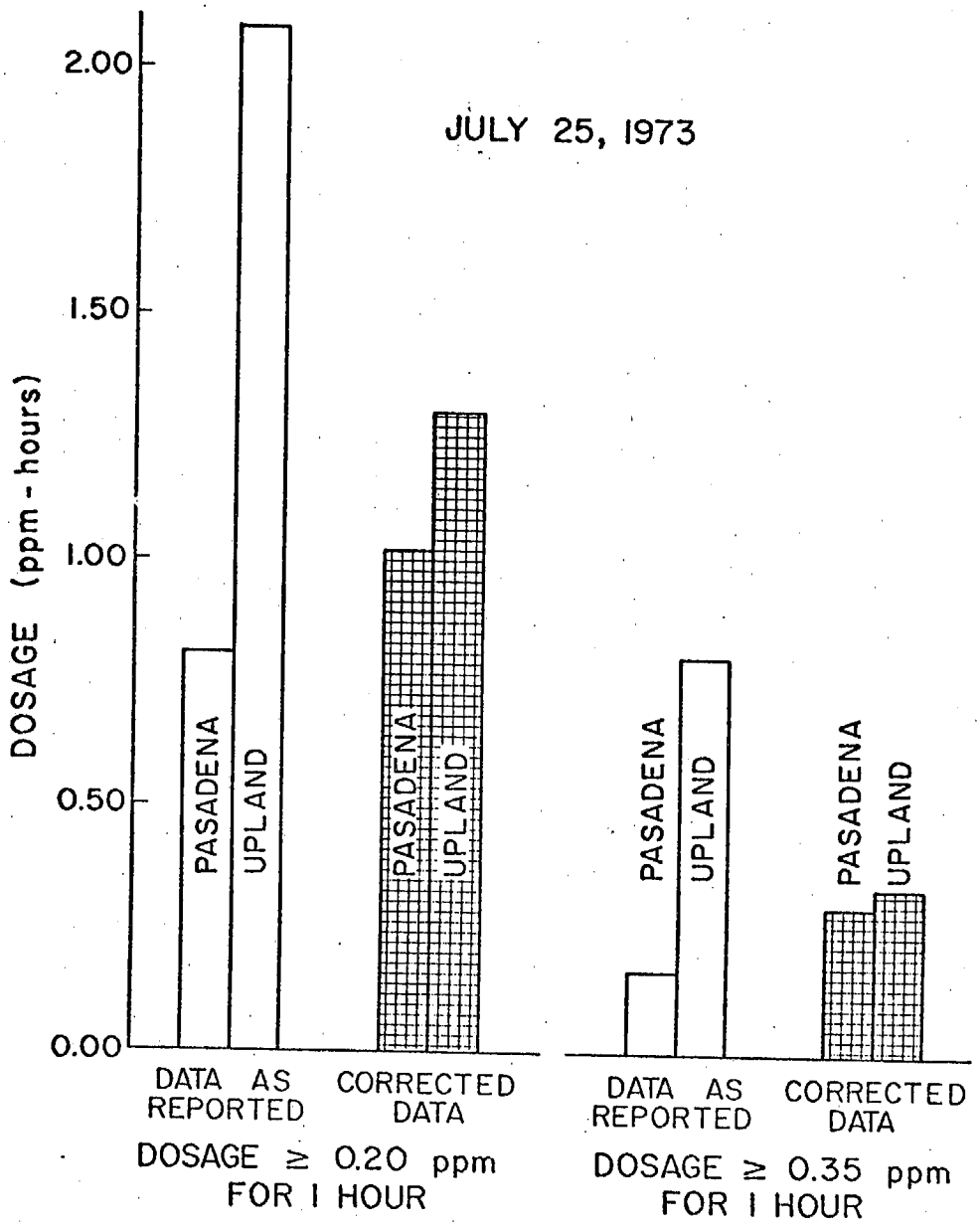

Figure 39. July 25, 1973, Oxidant Dosages Greater than or Equal to 0.20 and 0.35 ppm at the Pasadena and Upland Air Monitoring Stations (Corrected Data--Pasadena Values X 1.1 and Upland Values X 0.8).

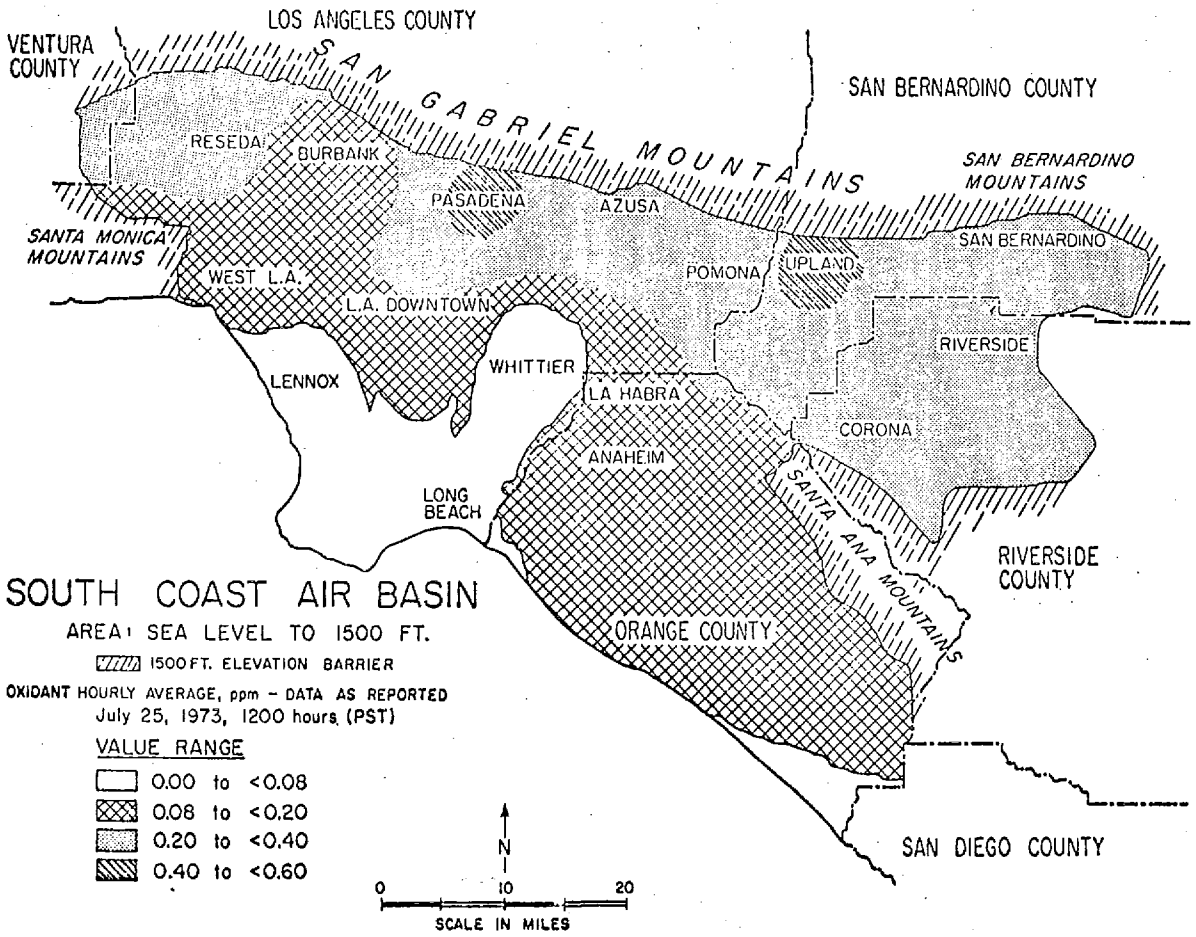

Figure 40. Uncorrected Oxidant Contour Map, Data as Reported, of the South Coast Air Basin Between Sea Level and 1500 Feet, 12 Noon, July 25, 1973.

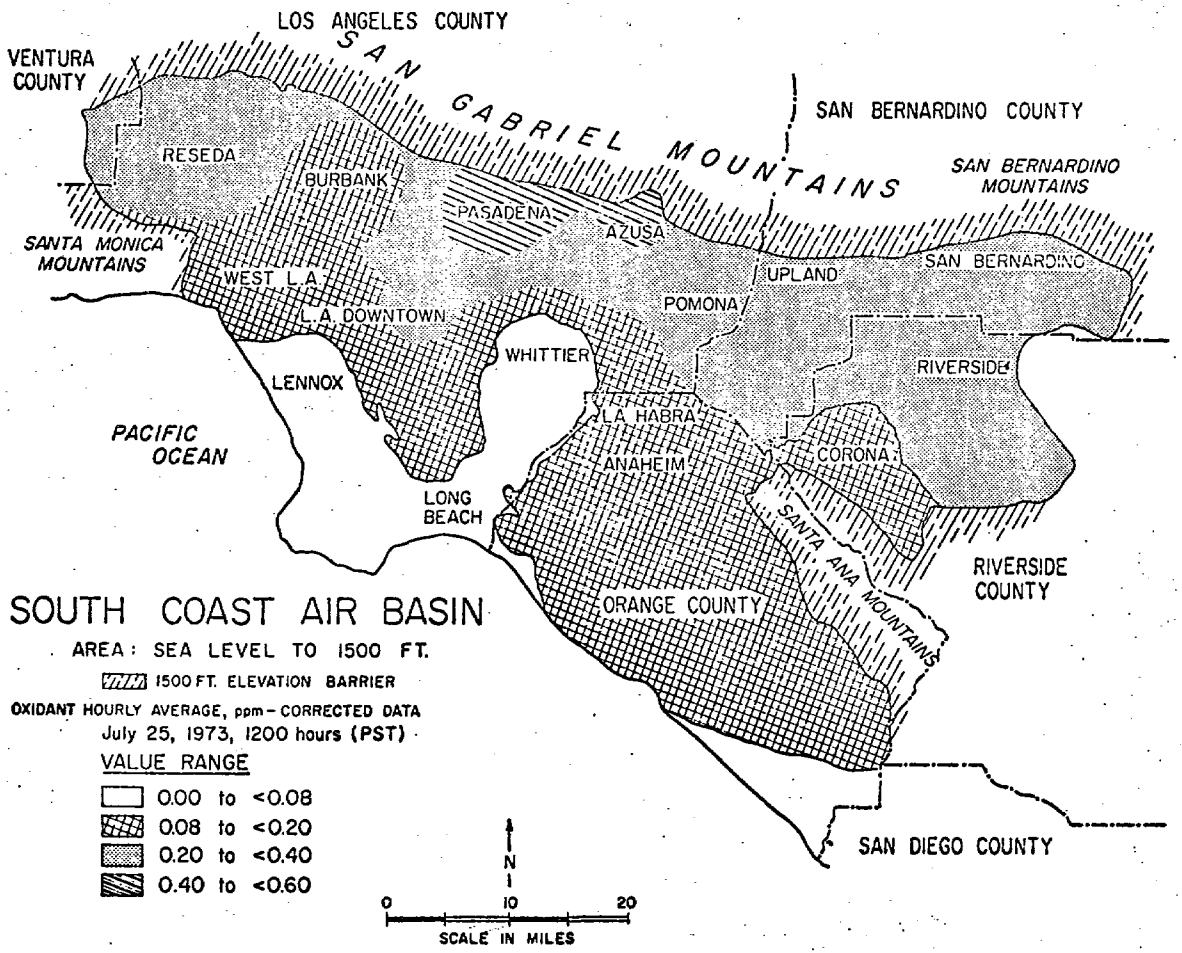

Figure 41. Corrected Oxidant Contour Map (LAAPCD Data X 1.1, Non-LAAPCD Data X 0.8) of the South Coast Air Basin Between Sea Level and 1500 Feet, 12 Noon, July 25, 1973.

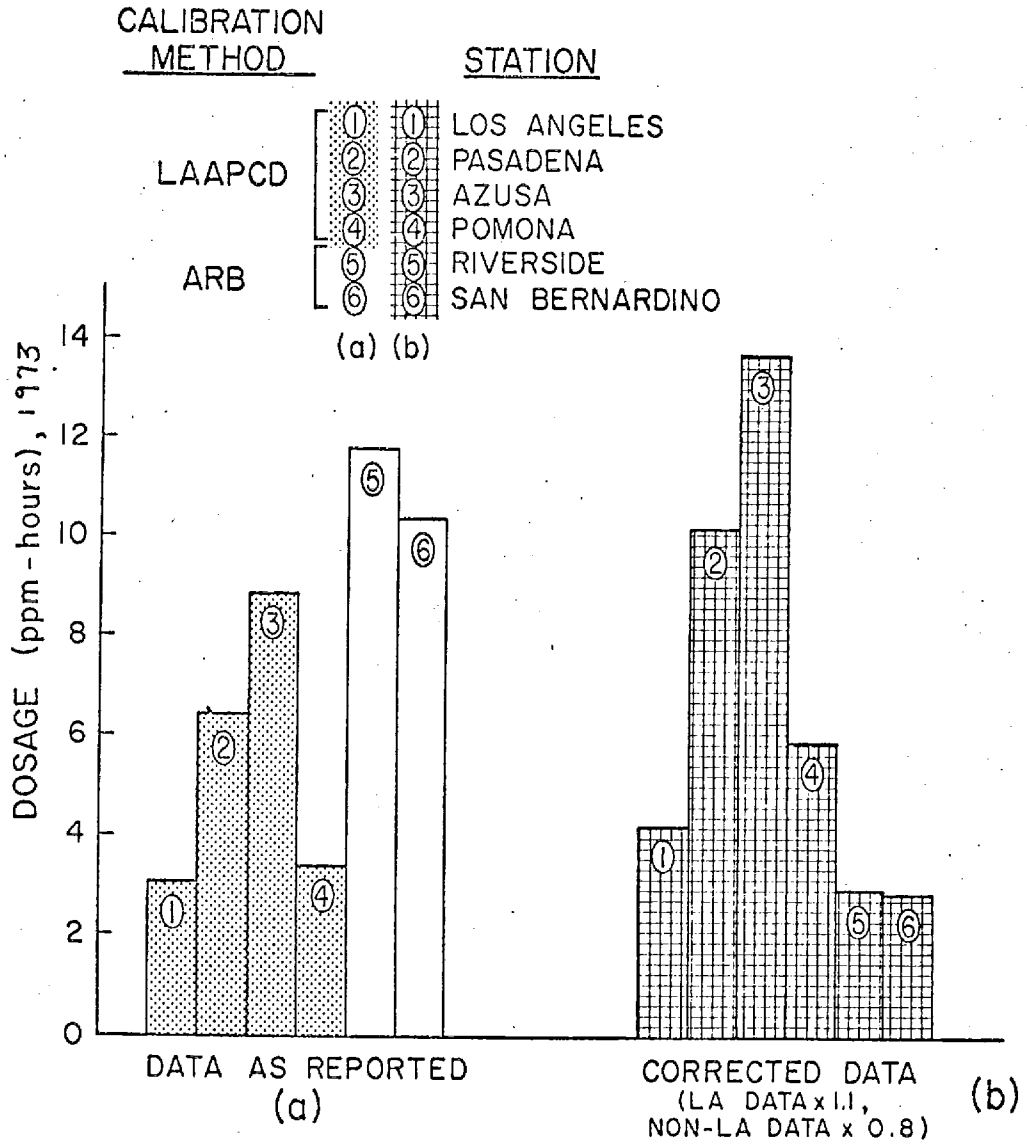

Figure 42. 1973 Oxidant Dosage Greater than or Equal to 0.20 ppm at Six Air Monitoring Stations in the South Coast Air Basin; (a) Data as Reported; (b) Corrected Data--LAAPCD Data X 1.1, Non-LAAPCD Data X 0.8.

Table 19. Oxidant Dosage (ppm X hr) $\geq$ 0.08, 0.20, and 0.35 ppm[a,b,c]

Station	LB	LADT	Bur	Pas	Azu	Pom	SB	Riv	Ana
1973									
Total Days	347	349	353	350	346	351	322	355	344
≥0.08 ppm									
AS REPORTED	1.32	22.0	27.1	62.0	70.5	47.1	84.7	92.5	14.5
CORRECTED	1.84	29.2	35.5	76.8	86.1	58.9	51.2	55.7	7.62
RATIO	1.4	1.3	1.3	1.2	1.2	1.3	0.60	0.60	0.53
≥0.20 ppm									
AS REPORTED	0	3.02	0.61	6.39	8.85	3.38	10.3	11.7	1.27
CORRECTED	0.04	4.15	1.26	10.2	13.6	5.91	2.81	2.91	0.22
RATIO	-	1.4	2.1	1.6	1.5	1.7	0.27	0.25	0.17
≥0.35 ppm									
AS REPORTED	0	0.54	0	0.34	0.38	0	0.12	0.12	0
CORRECTED	0	0.77	0	0.64	0.82	0	0	0	0
1974									
Total Days	350	333	360	351	360	360	360	356	335
≥0.08 ppm									
AS REPORTED	1.24	28.7	44.7	61.8	78.4	52.1	119	109	12.1
CORRECTED	1.79	37.5	56.8	77.6	96.0	64.8	75.9	67.1	5.92
RATIO	1.4	1.3	1.3	1.3	1.2	1.2	0.64	.62	0.49
≥0.20 ppm									
AS REPORTED	0	0.31	1.88	4.04	7.78	3.83	24.3	17.8	0.44
CORRECTED	0	0.99	3.48	7.22	13.2	6.81	8.20	5.24	0.12
RATIO	-	3.2	1.9	1.8	1.7	1.8	0.34	0.29	0.27
≥0.35 ppm									
AS REPORTED	0	0	0	0	.04	0	0.76	0.14	0
CORRECTED	0	0	0.04	0.03	0.18	0	0.02	0	0

a) LB = Long Beach, LADT = Los Angeles Downtown, Bur = Burbank, Pas = Pasadena, Azu = Azusa, Pom = Pomona, SB = San Bernardino, Riv = Riverside, and Ana = Anaheim.

b) Corrected data means LAAPCD Data x 1.1 and ARB Data x 0.8

c) RATIO = CORRECTED/AS REPORTED

standard, calculated by using the scaled data, will equal the oxidant exposure calculated using the old standard and the uncorrected data. For example, had the state's former second- and third-stage episode criteria levels, 0.40 and 0.60 ppm, respectively, been scaled down by a factor of exactly 0.8 to 0.32 and 0.48, respectively, then one might expect that the dosage above those corrected criteria levels, calculated by using the scale data, would equal the old dosage above the former standards, calculated by using unscaled data.

This is not the case. For example, had the California second-stage episode criteria level (0.40 ppm) been lowered by a factor of exactly 0.8, then the new corrected dosages above the new corrected episode criteria level (0.32 ppm) would not have equaled the old uncorrected dosages. Instead, they would be lower than the old uncorrected dosages by 20%, that is, decreased by a factor of 0.8. This results from the fact that scaling both oxidant readings and standards by 0.8 is equivalent to multiplying Equation 8 by a constant, k = 0.8. Because this does not change the limits of integration (see Figure 38), the corrected dosage above the scaled standard equals the uncorrected dosage above the existing standard multiplied by the factor k = 0.8.

$$\text{Corrected Dosage } (\geq k\delta) = \int_{t_1}^{t_2} [kf(t) - k\delta]\, dt$$

$$= k \int_{t_1}^{t_2} [f(t) - \delta]\, dt = k \times \begin{matrix}\text{uncorrected} \\ \text{dosage } (\geq \delta)\end{matrix} \qquad (26)$$

Control Strategies. Uncorrected data show that the maximum hourly average oxidant level (0.63 ppm), recently measured in the South Coast Air Basin, occurred at Upland on both July 25, 1973, and June 27, 1974. When corrected, this level becomes 0.50 ppm, a 20% reduction from the data as reported. Because this reduction is substantial, it is likely that in the South Coast Air Basin, attainment of the Federal Air Quality Standard for oxidant of 0.08 ppm for 1 hour may be significantly less difficult than was first thought

in 1973, when the EPA originally published its strategy[124] for the linear rollback of emissions of reactive hydrocarbons in the South Coast Air Basin. However, only a thorough reevaluation of South Coast Air Basin oxidant control programs[125] can determine whether the hydrocarbon control measures necessary to reduce the true peak hourly oxidant levels of ~0.5 ppm, not 0.6 ppm, to 0.08 ppm will be significantly less severe--technically and economically--than those previously proposed.

Socioeconomic Effects. Regulatory actions taken by local APCD's, when oxidant levels reach the California episode criteria levels of 0.20, 0.35 and 0.59 ppm for one hour, significantly affect the activities of private citizens, schools, organizations, businesses, and industries. For example, when oxidant levels reach 0.20 ppm (health advisory alert), APCD's advise that school children and health-sensitive individuals refrain from strenuous physical exercise; at 0.35 ppm (warning), traffic reductions and curtailment of industrial emissions are required; and at 0.50 ppm (emergency), businesses may be closed to reduce traffic, and industrial activities which release significant emissions, may be directed to cease operations.[126]

Figure 43 compares the maximum hourly average oxidant readings reported[127] on July 25, 1973 by 16 South Coast Air Basin air monitoring stations to the true readings which would have been reported had consistent ozone calibration methods been in use at that time. Figure 43 shows that the use of nonconsistent oxidant data caused two Orange County air monitoring stations, Anaheim and La Habra, to report first-stage oxidant episodes which did not exist, while the West Los Angeles station in Los Angeles County failed to report a first-stage episode which did exist. Figure 43 also shows that, while a third-stage alert requiring emergency action was declared for Upland on July 25, 1973, one should also have been called for Pasadena, which also experienced an oxidant level of 0.50 ppm for one hour.

Formation of a four-county Southern California Air Pollution Control District including Los Angeles, Orange, Riverside, and San Bernardino Counties on July 1, 1975,[128] as well as the continued possibility of a state legislatively mandated basinwide APCD,[129] should ensure that oxidant episodes are reported throughout the region based upon measurements which are self-consistent.

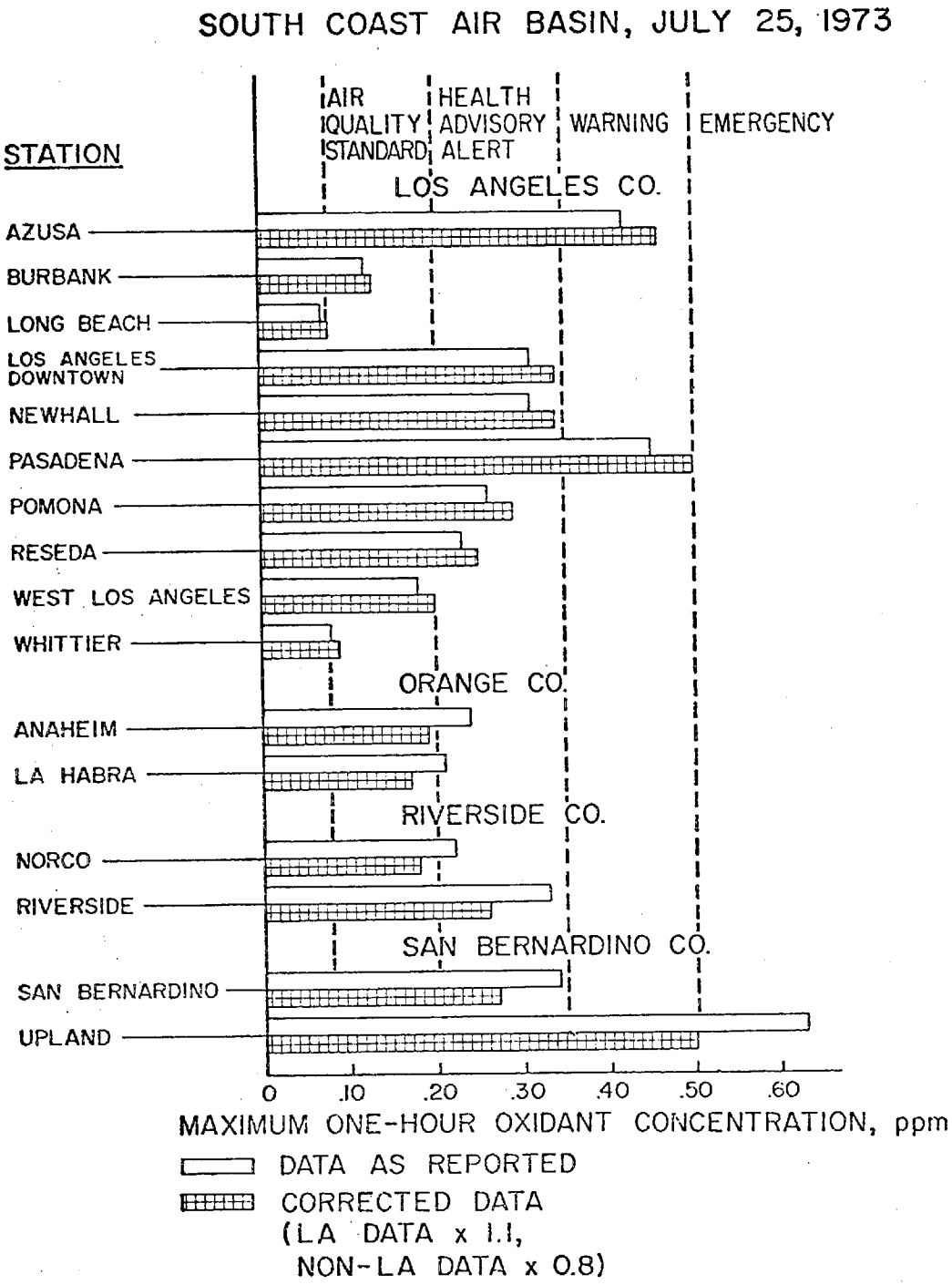

Figure 43. Maximum One-Hour Oxidant Concentrations on July 25, 1973, at Selected Air Monitoring Stations in Four South Coast Air Basin Counties, Showing Data as Reported and as Corrected (LAAPCD Data X 1.1, Non-LAAPCD Data X 0.8).

Scientific Implications. Observations made in this paper are offered with the viewpoint that scientific investigators using the published data and interpreting the oxidant data across the South Coast Air Basin will wish to make appropriate changes in their data. For example, computer simulations of photochemical smog formation and transport in the Los Angeles Basin should be reexamined. Specifically, models based partly on LAAPCD oxidant data and partly on non-LAAPCD data[130] have been validated against an inconsistent data base.

Finally, it is of considerable concern to both the scientific community and the public that air quality data and standards be credible. The credibility of air quality data and standards based on those data has already been strained by the NO_2 measurement controversy resulting from the Chattanooga Study.[131] The present oxidant measurement controversy has not helped matters. It is essential that air pollution standards and control programs be based on consistent data obtained by valid experimental methods, mutually agreed upon by control agencies and research scientists.

Conclusions. The corrected South Coast Air Basin oxidant data clearly show that cities located below the southern slopes of the San Gabriel Mountains (Pasadena and Azusa) have significantly higher oxidant levels than cities located in the eastern portion of the basin (Riverside and San Bernardino) and that non-Los Angeles County oxidant dosages have been substantially lower than has been believed. These two conclusions significantly alter current views of the oxidant problem in the South Coast Air Basin and have important ramifications for the understanding and control of photochemical oxidant.

IV. REFERENCES

1. Environmental Protection Agency Smog Chamber Conference, Research Triangle Park, North Carolina, October 24-25, 1974.

2. "Technical Bases for Control Strategies of Photochemical Oxidant: Current Status and Priorities in Research," UC-ARB Conference, University of California, Riverside, CA, December 16-17, 1974.

3. Conference on "Strategies for Air Pollution Control in the South Coast Air Basin," Environmental Quality Laboratory, California Institute of Technology, Pasadena, CA, December 2-3, 1975.

4. California Air Resources Board Grant No. 5-067-1.

5. California Air Resources Board Contract No. 2-377.

6. J. N. Pitts, Jr., A. M. Winer, K. R. Darnall, G. J. Doyle, and J. M. McAfee, "Chemical Consequences of Air Quality Standards and of Control Implementation Programs: Roles of Hydrocarbons, Oxides of Nitrogen, and Aged Smog in the Production of Photochemical Oxidant," Final Report, California Air Resources Board Contract No. 3-017, July 1975.

7. A. P. Altshuller, S. L. Kopczynski, W. A. Lonneman, F. D. Sutterfield, and D. L. Wilson, "Photochemical Reactivities of Aromatic Hydrocarbon-Nitrogen Oxide and Related Systems," Environ. Sci. Technol., 4, 44 (1970) and references therein.

8. W. A. Glasson and C. S. Tuesday, "Hydrocarbon Reactivity and the Kinetics of the Atmospheric Photooxidation of Nitric Oxide," J. Air Pollut. Contr. Assoc., 20, 239 (1970).

9. W. A. Glasson and C. S. Tuesday, "Inhibition of Atmospheric Photooxidation of Hydrocarbons by Nitric Oxide," Environ. Sci. Technol., 4, 37 (1970).

10. A. Levy and S. E. Miller, "Final Technical Report on The Role of Solvents in Photochemical Smog Formation," National Paint, Varnish and Lacquer Association, Report No. 799, April 1970.

11. J. M. Heuss, W. A. Glasson, "Hydrocarbon Reactivity and Eye Irritation," Environ. Sci. Technol., 2, 1109 (1968).

12. J. C. Romanovsky, R. M. Ingels, and R. J. Gordon, "Estimation of Smog Effects in the Hydrocarbon-Nitric Oxide System," J. Air Pollut. Contr. Assoc., 17, 454 (1967).

13. M. W. Korth, A. H. Rose, Jr., and R. C. Stahman, "Effects of Hydrocarbon to Oxides of Nitrogen Ratios on Irradiated Auto Exhaust, Part 1," J. Air Pollut. Contr. Assoc., 14, 168 (1964).

14. S. W. Nicksic, J. Harkins, and L. J. Painter, "Statistical Survey of Data Relating to Hydrocarbon and Oxides of Nitrogen Relationships in Photochemical Smog," Intern. J. Air Water Poll., 10, 15 (1966).

15. W. J. Hamming and J. E. Dickinson, "Control of Photochemical Smog by Alteration of Initial Reactant Ratios," J. Air Pollut. Contr. Assoc., 16, 317 (1966).

16. B. Dimitriades, "On the Function of Hydrocarbon and Nitrogen Oxides in Photochemical Smog Formation," USDI Report 7433, Bureau of Mines, 1970.

17. B. Dimitriades, "Effects of Hydrocarbon and Nitrogen Oxides on Photochemical Smog Formation," Environ. Sci. Technol., 6, 253 (1972).

18. "A Critique of the 1975-6 Federal Automobile Emission Standards for Hydrocarbons and Oxides of Nitrogen," Committee on Motor Vehicle Emissions, National Academy of Sciences, May 22, 1973; NTIS No. PB 244 863.

19. S. D. Reynolds and J. H. Seinfeld, "Interim Evaluation of Strategies for Ambient Air Quality Standard for Photochemical Oxidant," Environ. Sci. Technol., 9, 433 (1975).

20. "Control of Photochemical Oxidants - Technical Basis and Implications of Recent Findings," U. S. Environmental Protection Agency, Office of Air Quality Planning and Standards, Research Triangle Park, North Carolina 27711, July 15, 1975.

21. J. N. Pitts, Jr., A. M. Winer, P. J. Bekowies, G. J. Doyle, J. M. McAfee, and P. H. Wendschuh, "A Study of the Chemical Consequences of Air Quality Standards and of Control Implementation Programs," Final Report, California ARB Contract No. 2-377, September, 1976.

22. J. N. Pitts, Jr., P. J. Bekowies, A. M. Winer, G. J. Doyle, J. M. McAfee, and K. W. Wilson, "The Design and Construction of an Environmental Chamber Facility for the Study of Photochemical Air Pollution," Final Report, California ARB Grant No. 5-067-1, in draft.

23. J. N. Pitts, Jr., A. M. Winer, K. R. Darnall, G. J. Doyle, J. M. McAfee, P. J. Bekowies, and W. D. Long, "A Smog Chamber Study of the Role of Hydrocarbons, Oxides of Nitrogen and Aged Smog in the Production of Photochemical Oxidants. I. Facilities, Methodology, and Results for Six-Hour Irradiations," in preparation (1976).

24. J. N. Pitts, Jr., P. J. Bekowies, A. M. Winer, J. M. McAfee, and G. J. Doyle, "An Evacuable Chamber-Solar Simulator Facility for the Study of Atmospheric Photochemistry," Environ. Sci. Technol., to be submitted (1976).

25. "Analysis for Total Oxidant Content of the Atmosphere (2% Potassium Iodide Method)," Recommended Method No. 2A, Air and Industrial Hygiene Laboratory, California State Department of Public Health, Berkeley, California, January 1969.

26. J. N. Pitts, Jr., J. M. McAfee, W. D. Long, and A. M. Winer, "Long-Path Infrared Spectroscopic Investigation at Ambient Concentrations of the 2% Neutral Buffered Potassium Iodide Method for Determination of Ozone," Environ. Sci. Technol., 10, 787 (1976).

27. State of California Air Resources Board, Sacramento, California, "Comparison of Oxidant Calibration Procedures," Final Report of the Ad Hoc Committee, February 3, 1975.

28. A. M. Winer, J. W. Peters, J. P. Smith, and J. N. Pitts, Jr., "Response of Commercial Chemiluminescent NO-NO_2 Analyzers to Other Nitrogen-Containing Compounds," Environ. Sci. Technol., 8, 1118 (1974).

29. C. W. Spicer and D. F. Miller, "Nitrogen Balance in Smog Chamber Studies," presented at the 67th Annual Meeting of the Air Pollution Control Association, Denver, Colorado, June 1974; J. Air Pollut. Contr. Assoc., 26, 45 (1976).

30. E. F. Darley, K. A. Kettner, and E. R. Stephens, "Analysis of Peroxyacyl Nitrates by Gas Chromatography with Electron Capture Detection," Anal. Chem., 35, 589 (1963).

31. E. R. Stephens and M. A. Price, "Analysis of an Important Air Pollutant: Peroxyacetyl Nitrate," J. Chem. Educ., 50, 351 (1973).

32. R. G. Smith, R. J. Bryan, M. Feldstein, B. Levadie, F. A. Miller, E. R. Stephens, and N. G. White, "Tentative Method of Analysis for Formaldehyde Content of the Atmosphere (Colorimetric Method)," H.L.S., 7, (1) Supplement, 87 (1970).

33. E. R. Stephens and F. R. Burleson, "Distribution of Light Hydrocarbons in Ambient Air," J. Air Pollut. Contr. Assoc., 19, 929 (1969).

34. E. R. Stephens, "Hydrocarbons in Polluted Air," Summary Report, Coordinating Research Council, Project CAPA-5-68, June 1973; NTIS No. PB 230 993/AS.

35. G. J. Doyle, P. J. Bekowies, A. M. Winer, and J. N. Pitts, Jr., "A Charcoal Adsorption Air Purification System for Chamber Studies Investigating Atmospheric Photochemistry," Environ. Sci. Technol., submitted for publication.

36. J. R. Holmes, R. J. O'Brien, J. H. Crabtree, T. A. Hecht, and J. H. Seinfeld, "Measurement of Ultraviolet Radiation Intensity in Photochemical Smog Studies," Environ. Sci. Technol., 7, 519 (1973).

37. K. R. Darnall, A. M. Winer, and J. N. Pitts, Jr., "Effects of Incremental Reductions in HC and NO_x Ambient Concentrations on Ozone Production in Photochemical Smog," in preparation (1975).

38. California State Senate Bill No. 2471 amending Section 39177.1 of the Health and Safety Code, September 5, 1974.

39. D. L. Blumenthal, W. H. White, R. L. Peace, and T. B. Smith, Meteorology Research Inc., "Determination of the Feasibility of the Long-Range Transport of Ozone or Ozone Precursors," EPA Report No. 450/3-74-061, November, 1974.

40. L. M. Vaughan, A. R. Stankunas, Metronics Assoc., Inc., Palo Alto, Calif., "Field Study of Air Pollution Transport in the South Coast Air Basin," Tech. Rept. No. 197, July, 1974.

41. W. Kuby, A. C. Lloyd, and J. N. Pitts, Jr., "Pollutant Transport in the South Coast Air Basin," in preparation (1975).

42. No corrections have been made for NO_2 and SO_2 to convert oxidant readings from LAAPCD Stations to ozone. In general such corrections are quite small if not negligible.

43. J. Holmes and F. Bonamassa, Air Resources Board, El Monte, Private communication, 1975.

44. Attachment to Memorandum from W. Simmons to D. Benedict, "NO_x Retrofit Program for 1966-70 Light-Duty Vehicles," Air Resources Board, January 30, 1975.

45. Reference 44 states a 5.6% overall reduction in HC, however a recalculation based on the emissions given indicates the correct reduction to be 3.7%.

46. California Air Resources Board Report to Governor Edmund G. Brown, Jr., April 23, 1975.

47. J. R. Holmes and F. Bonamassa, "Summary of the Calculation of the Effects of the Mandatory Phase of the NO_x Retrofit Program on Oxidant Levels in the South Coast Air Basin," Draft Report, California Air Resources Board, May 24, 1975.

48. A. Q. Eschenroeder and J. R. Martinez, "Concepts and Applications of Photochemical Smog Models," in Advances in Chemistry, Series 113, American Chemical Society, 1972.

49. P. J. W. Roberts, P. M. Roth, and C. L. Nelson, "Contaminant Emissions in the Los Angeles Basin--Their Sources, Rates, and Distribution," Appendix A of Development of a Simulation Model for Estimating Ground Level Concentrations of Photochemical Pollutants, Systems Applications, Inc., Report No. 71SAI-6, March, 1971.

50. K. R. Darnall, A. C. Lloyd, A. M. Winer, and J. N. Pitts, Jr., "Reactivity Scale for Atmospheric Hydrocarbons Based on Reaction with Hydroxyl Radical," Environ. Sci. Technol., 10, 692 (1976).

51. Q. R. Stahl, "Preliminary Air Pollution Survey of Aldehydes," Contract No. PH 22-68-25, U. S. Dept. of Health, Education and Welfare, October, 1969.

52. A. P. Altshuller and J. J. Bufalini, "Photochemical Aspects of Air Pollution: A Review," Photochem. and Photobiol., 4, 97 (1965) and references therein; A. P. Altshuller and J. J. Bufalini, "Photochemical Aspects of Air Pollution: A Review," Environ. Sci. Technol. 5, 39 (1971) and references therein.

53. J. G. Calvert and J. N. Pitts, Jr., Photochemistry, John Wiley and Sons, N. Y., 1966.

54. H. P. Sperling and S. Toby, "The Photochemical Decomposition of Gaseous Formaldehyde," Can. J. Chem., 51, 471 (1973).

55. R. D. McQuigg and J. G. Calvert, "The Photodecomposition of CH_2O-CD_2O, CHDO, and CH_2O-CD_2O Mixtures at Xenon Flash Lamp Intensities," J. Am. Chem. Soc. 91, 1590 (1969).

56. K. L. Demerjian, J. A. Kerr and J. G. Calvert, "The Mechanism of Photochemical Smog Formation," Adv. Environ. Sci. Technol. 4, 1 (1974).

57. J. J. Bufalini and K. L. Brubaker, "The Photooxidation of Formaldehyde at Low Partial Pressures," in Chemical Reactions in Urban Atmospheres, C. S. Tuesday (editor), American Elsevier Publishing Co., New York, pg. 225 (1971).

58. B. Dimitriades and T. C. Wesson, "Reactivities of Exhaust Aldehydes," J. Air. Pollut. Control Assoc., 22, 33 (1972).

59. J. M. McAfee, E. R. Stephens, D. Fitz, and J. N. Pitts, Jr., "Infrared Absorptivity of the 9.6 Micron Ozone Band as a Function of Spectral Resolution and Abundance," J. Quant. Spectrosc. and Radiat. Transfer, 16, 829 (1976).

60. A. G. Hearn, "The Absorption of Ozone in the Ultra-Violet and Visible Regions of the Spectrum," Proc. Phys. Soc., 78, 932 (1961).

61. E. C. Y. Inn and Y. Tanaka, "Absorption Coefficient of Ozone in the Ultraviolet and Visible Regions," J. Opt. Soc. Amer., 43, 870 (1953).

62. W. B. DeMore and O. Raper, "Hartley Band Extinction Coefficients of Ozone in the Gas Phase and in Liquid Nitrogen, Carbon Monoxide, and Argon," J. Phys. Chem., 68, 412 (1964).

63. M. Griggs, "Absorption Coefficients of Ozone in the Ultraviolet and Visible Regions," J. Chem. Phys., 49, 857 (1968).

64. C. D. Walshaw, "Integrated Absorption by the 9.6 μ Band of Ozone," Quart. J. Roy. Meteorol. Soc., 83, 315 (1957).

65. D. J. McCaa and J. H. Shaw, "The Infrared Spectrum of Ozone," J. Mol. Spectrosc., 25, 374 (1968).

66. A. Goldman and T. G. Kyle, "A Comparison Between Statistical Model and Line by Line Calculation with Application to the 9.6-μ Ozone and the 2.7-μ Water Vapor Bands," Appl. Opt., 7, 1167 (1968).

67. A. Goldman, T. G. Kyle, D. G. Murcray, F. H. Murcray, and W. J. Williams, "Long Path Atmospheric Ozone Absorption in the 9-10 μ Region Observed from a Balloon-Borne Spectrometer," Appl. Opt., 9, 565 (1970).

68. A Goldman, "Statistical Band Model Parameters for Long Path Atmospheric Ozone in the 9-10 μ Region," Appl. Opt., 9, 2600 (1970).

69. P. L. Hanst, E. R. Stephens, W. E. Scott, and R. C. Doerr, "Absorptivities for the Infrared Determination of Trace Amounts of Ozone," Anal. Chem., 33, 1113 (1961).

70. C. M. Birdsall, A. C. Jenkins, and E. Spadinger, "Iodometric Determination of Ozone, Anal. Chem., 24, 662 (1952).

71. Spectral resolution was determined from the mechanical slit width by using the data provided in the 621 instruction manual. Spectral resolution, $\Delta\nu$, at 9.48 microns is given by $\Delta\nu(cm^{-1}) = 0.090 + 0.0039$ W, where W is the slit width in microns.

72. S. S. Penner, Quantitative Molecular Spectroscopy and Gas Emissivities, Chapter 5, Addison-Wesley, Reading, Mass. (1959).
In their investigation of the stoichiometry of the NBKI wet chemical method of ozone determination, Kopczynski and Bufalini [Anal. Chem., 43, 1126 (1971)] reported no change in absorbance of the ν_3 R-branch maximum by varying their spectrometer slits from 750 to 500 microns. They also reported an absorbance reduction of 3% at slits of 400 microns. These data are inconsistent with the present work. However, having done our resolution study on the same type of spectrometer (Perkin-Elmer 621), our experience has shown that for slits of less than about 600 microns the slowest scan rate available on the PE-621 is not slow enough for the time constant required to achieve adequate signal-to-noise. Therefore, narrowing the slits does not necessarily improve resolution and can actually degrade it to a significant extent (evidenced by the 3% reduction in absorbance mentioned above). We were able to avoid this problem by manual step-wise scanning over the R-Q valley and R-branch peak, making certain the recorder pen had come to equilibrium before making the next scan step.

73. D. A. Ramsay, "Intensities and Shapes of Infrared Absorption Bands of Substances in the Liquid Phase," J. Amer. Chem. Soc., 74, 72 (1952); A. Cabana and C. Sandorfy, "Calculation of Infra-red Intensities by Direct Integration--An Improvement to Ramsay's Method," Spectrochim. Acta, 16, 335 (1960); J. Deltour, "Tables for the Calculation of Absolute Infrared Intensities with a Triangular Slit Function," Infrared Phys., 10, 207 (1970).

74. "Reference Method for the Measurement of Photochemical Oxidants," Federal Register, 36, No. 228, page 22392, November 25, 1971.

75. A. W. Boyd, C. Willis, and R. Cyr, "New Determination of Stoichiometry of the Iodometric Method for Ozone Analysis at pH 7.0," Anal. Chem., 42, 670 (1970).

76. S. L. Kopczynski and J. J. Bufalini, "Some Observations on Stoichiometry of Iodometric Analyses of Ozone at pH 7.0" Anal. Chem., 43, 1126 (1971).

77. J. A. Hodgeson, R. E. Baumgardner, B. E. Martin, and K. A. Rehme, "Stoichiometry in the Neutral Iodometric Procedure for Ozone by Gas Phase Titration with Nitric Oxide," Anal. Chem., 43, 1123 (1971).

78. B. A. Behl, "Absolute Continuous Atmospheric Ozone Determination by Differential Ultraviolet Absorption," Air Pollution Control Association 65th Meeting, Miami Beach, Florida, June 1972.

79. J. U. White, "Long Optical Paths of Large Aperture," J. Opt. Soc. Amer., 32, 285 (1942).

80. D. Horn and G. C. Pimentel, "2.5-km Low-Temperature Multiple Reflection Cell," Applied Optics, 10, 1892 (1972).

81. Operating Instructions, Model 621 Spectrophotometer, Perkin-Elmer, Norwalk, CT, April 1973, p. 5-6.

82. "Selected Methods for the Measurement of Air Pollutants," USDHEW Public Health Service Publication No. 999-AP-11, page D-1, May 1965.

83. D. A. Skoog and D. M. West, Analytical Chemistry, Holt, Rinehart and Winston, Inc., New York, 1965.

84. P. K. Mueller, Y. Tokiwa, E. R. deVera, W. J. Wehrmeister, T. Belsky, S. Twiss, and M. Imada, "A Guide for the Evaluation of Atmospheric Analyzers," Air and Industrial Hygiene Laboratory Report No. 168, California State Department of Public Health, Berkeley, California, June 1973.

85. J. B. Clements, "Summary Report: Workshop on Ozone Measurement by the Potassium Iodide Method," EPA Report No. 650/4-75-007, February 1975.

86. "A Study of the Effect of Atmospheric Humidity on Analytical Oxidant Measurement Methods," California Air Resources Board Report, July 9, 1975.

87. California Institute of Technology, Jet Propulsion Lab, Pasadena, California 91103; Chairman of the ARB Ad Hoc Measurement Committee.

88. J. Tang, E. Jeung, and M. R. Imada, Air and Industrial Hygiene Laboratory, California State Department of Public Health, Berkeley, California, "Collaborative Study of Manual Ozone Methods," AIHL Report No. 158, November 1973.

89. "Oxidant Calibration Study" memorandum from K. Rehme, R. Paur, W. A. McClenny, R. K. Stevens to A. P. Altshuller, Environmental Protection Agency, Research Triangle Park, NC, November 11, 1974.

90. J. A. Hodgeson, "Evaluation of the Neutral Buffered Potassium Iodide and Ultraviolet Photometric Methods for Ozone Calibration," presented at the ASTM/EPA/NBS Symposium on Calibration in Air Monitoring, Boulder, Colorado, August 4-7, 1975.

91. Results obtained by R. Paur and R. K. Stevens, private communication from J. J. Bufalini.

92. R. Strelow, "Errors in Ozone/Oxidant Monitoring System," memorandum to EPA regional administrators from Office of Air and Waste Management, U.S. Environmental Protection Agency, December 18, 1975.

93. W. Simmons, filing sheet amending Section 70200, "Table of Standards Applicable Statewide," of Title 17 of the California Administrative Code, May 15, 1975.

94. R. Paur, "Comparison of UV Photometry and Gas Phase Titration as Candidate Methods for Absolute Calibration of Ozone Generator Output in the Sub-Part-Per-Million Range," presented at the ASTM/EPA/NBS Symposium on Calibration in Air Monitoring, Boulder, Colorado, August 4-7, 1975.

95. W. B. DeMore, "Interagency Comparison of Iodimetric Methods for Ozone Determination," presented at the ASTM/EPA/NBS Symposium on Calibration in Air Monitoring, Boulder, Colorado, August 4-7, 1975.

96. J. N. Pitts, Jr., J. L. Sprung, M. Poe, M. C. Carpelan, and A. C. Lloyd, "Corrected South Coast Air Basin Oxidant Data: Some Conclusions and Implications," Environ. Sci. Technol., 10, 794 (1976).

97. USDHEW, National Air Pollution Control Administration, Washington, DC, AP-63, "Air Quality Criteria for Photochemical Oxidants," p. 2-3, 1970.

98. State of California Air Resources Board Bulletin, 5, No. 5, June 1974.

99. State of California Air Resources Board, Sacramento, California. "Oxidant Measurements and Emergency Plan Episode Criteria Levels," Staff Report No. 74-16-6, August 15, 1974.

100. Air Pollution Control District, County of Los Angeles, Laboratory Methods, APCD 14-56, 1958. (Subsequently revised as "Ozone Calibration Procedure.")

101. State of California Air Resources Board Draft Report, "Tentative Results of the Oxidant Measurement Study," May 14, 1975.

102. D. C. Crowe, Memo to K. Nishikawa, "Report of Joint Ozone Measurement Study," State of California Air Resources Board, August 26, 1974.

103. W. D. Holland, "Joint Los Angeles County Air Pollution Control District-California Air Resources Board Ozone Calibration Project," Los Angeles County Air Pollution Control District, Los Angeles, California, July 1973.

104. J. E. Dickinson, "Construction and Calibration Ozonator," APCD test No. 691, Progress Report, December 1, 1952.

105. State of California Air Resources Board Bulletin, 6, No. 3, p. 5, March-April 1975.

106. J. N. Pitts, Jr., J. L. Sprung, M. C. Carpelan, M. Poe, and A. C. Lloyd, "Corrected South Coast Air Basin Oxidant Data," Statewide Air Pollution Research Center Report 76-03, May 1976.

107. State of California Air Resources Board, "California Air Pollution Emergency Plan," Revised May 15, 1975.

108. "Requirements for Preparation, Adoption, and Submittal of Implementation Plans. Significant Harm and Emergency Levels for Photochemical Oxidants (Smog)," Federal Register, 39 (50), 9672, March 13, 1974.

109. State of California, Department of Health, Air Quality Advisory Committee, "Episode Criteria Levels for Oxidants," presented to the Air Resources Board, January 31, 1975.

110. USDHEW, National Air Pollution Control Administration, Washington, DC, AP-63, "Air Quality Criteria for Photochemical Oxidants," p. 3-15, 1970.

111. National Academy of Sciences, Committee on Motor Vehicle Emissions, "A Critique of the 1975-1976 Federal Automobile Emission Standards for Hydrocarbons and Oxides of Nitrogen," PB-224-863, 2-7, May 22, 1973.

112. P. A. Leighton, "Photochemistry of Air Pollution," Academic Press, New York, 1961.

113. A. P. Altshuller and J. J. Bufalini, "Photochemical Aspects of Air Pollution: A Review," Environ. Sci. Technol., 5, 39 (1971).

114. J. N. Pitts, Jr., A. C. Lloyd, and J. L. Sprung, "Chemical Reactions in Urban Atmospheres and Their Application to Air Pollution Control Strategies," Proceedings of the International Symposium on Environmental Measurements, Geneva, Switzerland, October 2-4, 1973, p. 27 (1974).

115. K. L. Demerjian, J. A. Kerr, and J. G. Calvert, "The Mechanism of Photochemical Smog Formation," in Advances in Environmental Science and Technology, Vol. 4, J. N. Pitts, Jr. and R. L. Metcalf, Eds., Wiley-Interscience, New York, pp. 1-262, 1974.

116. J. N. Pitts, Jr., and B. J. Finlayson, "Mechanisms of Photochemical Air Pollution," Angew. Chem. Int. Edit., 14, 1 (1975).

117. National Academy of Sciences and National Academy of Engineering, a Report by the Coordinating Committee on Air Quality Studies prepared for the Committee on Public Works, U. S. Senate, Washington, DC, "Air Quality and Automobile Emission Control, Vol. 3, "The Relationship of Emissions to Ambient Air Quality," p. 76, 87, September 1974.

118. L. M. Vaughan and A. R. Stankunas, Metronics Assoc., Inc., Palo Alto, CA, "Field Study of Air Pollution Transport in the South Coast Air Basin," Techn. Rept. No. 197, July 1974.

119. D. L. Blumenthal, W. H. White, R. L. Peace, and T. B. Smith, Meteorology Research, Inc., Altadena, Calif., "Determination of the Feasibility of the Long-Range Transport of Ozone or Ozone Precursors," EPA-450/3-74-061, Research Triangle Park, North Carolina, November 1974.

120. This idea for treating the data was suggested to us by Dr. Jack Suder, California Air Resources Board, and we acknowledge his suggestion.

121. Environmental Systems Research Institute, Redlands, Calif., "Automap II User Manual," 1972.

122. J. V. Behar, Proceedings of the Sixth Berkeley Symposium on Mathematical Statistics and Probability. VI. Effects of Pollution on Health, University of California Press, Berkeley, p. 29, 1972.

123. J. V. Behar, University of California Project Clean Air Resource Reports, 4, S-14, September, 1970.

124. Environmental Protection Agency, Region IX, "Technical Support Document for the Metropolitan Los Angeles Intrastate Air Quality Control Region," January 15, 1973.

125. "Approval and Promulgation of Implementation Plans," Federal Register, 38 (14), 2194, January 22, 1973.

126. Air Pollution Control Districts of Orange, Riverside, and San Bernardino Counties, Regulation VII - Rules 150-164, 1974.

127. State of California Air Resources Board, "Air Pollution in California," Annual Report, 1973, January 1974.

128. B. Craven, "New air district to pick director," Riverside Daily Enterprise, June 26, 1975.

129. B. Craven, "Lewis defends APCD bill despite county action," Riverside Daily Enterprise, July 11, 1975.

130. S. D. Reynolds, M-K. Liu, T. A. Hecht, P. M. Roth, and J. H. Seinfeld, "Mathematical Modeling of Photochemical Air Pollution - III. Evaluation of the Model," Atmos. Environ., 8, 563 (1974).

131. T. R. Hauser and C. M. Shy, "Position Paper: NO_x Measurement," Environ. Sci. Technol., 6, 890 (1972).

V. LIST OF PUBLICATIONS FROM SAPRC-ARB CHAMBER PROGRAM

"A Novel 20 KW Solar Simulator Designed for Air Pollution Research," J. H. Beauchene, P. J. Bekowies, J. M. McAfee, A. M. Winer, L. Zafonte, and J. N. Pitts, Jr., Proceedings of Seventh Conference on Space Simulation (NASA) Special Publication 336, Los Angeles, California, November 12-14, 1973, Paper No. 66, pp. 811-825.

"Response of Commercial Chemiluminescent NO-NO_2 Analyzers to other Nitrogen Containing Compounds," A. M. Winer, J. W. Peters, J. P. Smith, and J. N. Pitts, Jr., Environ. Sci. Technol., 8, 1118 (1974).

"Experimentally Validated Mechanisms, Models and Control Strategies for Photochemical Air Pollution," J. N. Pitts, Jr., W. P. Carter, K. R. Darnall, G. J. Doyle, W. Kuby, A. C. Lloyd, J. M. McAfee, C. Pate, J. P. Smith, J. L. Sprung, and A. M. Winer, Proceedings of the Second Annual NSF-RANN Trace Contaminants Conference, Asilomar, California, August 29-31, 1974, LBL-3217, pp. 50-53.

"A Gas Phase Kinetic Study of the Relative Rates of Reaction of Selected Aromatic Compounds, with Hydroxyl Radicals in an Environmental Chamber," G. J. Doyle, A. C. Lloyd, K. R. Darnall, A. M. Winer, and J. N. Pitts, Jr., Environ. Sci. Technol., 9, 237 (1975).

"A Long-Path Infrared Spectroscopic Investigation at Ambient Concentrations of the 2% Neutral Buffered Potassium Iodide Method for Determination of Ozone," J. N. Pitts, Jr., J. M. McAfee, W. D. Long and A. M. Winer, Environ. Sci. Technol., 10, 787 (1976).

"Infrared Absorptivity of the 9.6 Micron Ozone Band as a Function of Spectral Resolution and Abundance," J. M. McAfee, E. R. Stephens, D. R. Fitz, and J. N. Pitts, Jr., J. Quant, Spectrosc. Radiat. Transfer, 16, 829 (1976).

"A Charcoal-Adsorption Air Purification System for Chamber Studies Investigating Atmospheric Photochemistry," G. J. Doyle, P. J. Bekowies, A. M. Winer, and J. N. Pitts, Jr., Environ. Sci. Technol., 11, 45 (1977).